Neuronal Network Dynamics Underlying the Formation of Anesthesia-Resistant Memory in *Drosophila* Olfactory Learning

Inaugural-Dissertation

to obtain the academic degree

Doctor rerum naturalium (Dr. rer. nat.) submitted to the

Department of Biology, Chemistry and Pharmacy

of Freie Universität Berlin

by

Emmanuel Antwi-Adjei

August 2018

1. Reviewer: Dr. Martin Schwärzel

   Freie Universität Berlin, Institut für Biologie-Neurobiologie

2. Reviewer: Prof. Dr. Peter Robin Hiesinger

   Freie Universität Berlin, Institut für Biologie-Neurobiologie

Disputationstermin: 22-10-2018

I. Table of Contents

II. List of Figures

III. List of Tables

IV. List of Abbreviations

AC	Adenylyl cyclase
Ach	Acetylcholine
AD	Activation domain
AKAPs	A-kinase anchoring proteins
AL	Antennal lobe
APL	Anterior paired lateral neuron
ARM	Anesthesia-resistant memory
ASM	Anesthesia-sensitive memory
AZ	Active zone
BRP	Bruchpilot
CA	Calyx
cAMP	cyclic AMP
CAST	Cytomatrix at the active zone structural protein
cDNA	Complementary DNA
CRE	Crepine
CR	Conditioned response
CREB	Cyclic AMP response element binding
CS	Conditioned stimulus
DA	Dopamine
DANs	Dopaminergic neurons
DBD	DNA-binding domain
DPM	Dorsal paired medial neuron
dsRNA	double-stranded RNA
GABA	γ-aminobutyric acid
IPSP	Inhibitory postsynaptic potential
KCs	Kenyon cells
LFP	Local field potential
LH	Lateral horn
LNs	Local interneurons

9

LTM	Long-term memory
MAB	monoclonal antibody
MB	Mushroom body
MBONs	Mushroom body output neurons
mRNA	Messenger RNA
MTM	Middle-term memory
NMDAR	N-methyl-D-aspartate receptors
NMJ	Neuromuscular Junction
OA	Octopamine
OAMB	Octopamine receptor in the mushroom body
ORNs	Olfactory receptor neurons
PACAP	Pituitary adenylate cyclase-activating peptide
PAM	Protocerebral anterior medial
PKA	Protein kinase A
PNs	Projection neurons
PPL1	Protocerebral posterior lateral 1 cluster
PPL 2ab	Protocerebral posterior lateral 2ab
RNAi	RNA interference
RIM-BP	RIM-binding protein
rut	rutabaga
SIP	Superior intermediate protocerebrum
SLP	Superior lateral protocerebrum
SMP	Superior medial protocerebrum
ssRNAs	Single stranded RNAs
siRNAs	Small interfering RNAs
STM	Short-term memory
RISC	RNA-induced silencing complex
US	Unconditioned stimulus
UR	Unconditioned response
UAS	Upstream activation sequence
VGCC	Voltage- gated calcium Channels

Chapter One

1 Introduction

1.1 Learning and Memory

Learning and memory are correlated to the strengthening of existing responses or formation of newly learned behaviors to existing stimuli. However, in order to perform the strengthening of existing responses or form learned behaviors, the reaction to the existing stimuli should be encoded, stored and later retrieved in order to execute a certain behavior. Indeed, learning and memory can be divided into declarative or explicit and non-declarative or implicit. Explicit or declarative refers to knowledge or facts – which is the recognition of places, things and other species by an animal. A non-declarative or implicit type of learning and memory refers to the information that aid an animal to perform a certain behavior. However, the implicit type of memory is divided into non–associative and associative. The habituation and sensitization form the two types of non–associative memory. Habituation is the decrease in response to a harmless stimulus when it is represented repeatedly. Sensitization, on the other hand, is the enhancement of a certain response to many different stimuli.

Moreover, for associative learning, two stimuli are associated with each other or that a response is associated with a given event. The associative type of learning is divided into classical conditioning and operant conditioning. Classical conditioning was well experimented by Ivan Pavlov, and in his paradigm; he presented meat powder (US) to a dog, causing it to salivate (UR). He repeated the presentation and each time the dog salivated. After all, he repeatedly rang the bell, pairing it with the meat powder (CS), the animal then associated the bell with the presentation of the meat powder, and began to salivate (CR) when the bell was rung. The dog associated the ranging of the bell with salivation when it was presented alone. Conversely, in the operant conditioning, the animal's behavior changed in response to a comparison between an animal's own behavioral activity and its experiences (Skinner, 1938). Nonetheless, positive experiences tend to enforce a certain behavior, whereas negative experiences tend to suppress an animal's own behavior.

1.2 *Drosophila* as a model organism

Drosophila melanogaster was among the first organisms that were used for genetic analysis. Most organisms share similarities in their genetic make-up, and hence, comprehension of the genetics, transcription and replication of fruit flies will help us in understanding these phenomena in other eukaryotic species, including human. Thomas Hunt Morgan began a pioneering research in fruit flies in his laboratory at Columbia University in 1910. He embarked on this adventure with fruit flies by using bottles to rear the flies and handheld lenses for observing their traits. Thomas Hunt Morgan together with his colleagues further replaced the handheld lenses with microscopes, which enhanced their observations. Also, in succession to Thomas Hunt Morgan, Konopka et al. (1971) published "Clock mutants of *Drosophila* melanogaster", this paper described the first mutations that affected animals' behavior. In addition to this, the first learning mutants i.e. *dunce* and *rutabaga* were isolated in the laboratory of Seymour Benzer. These mutants were investigated to harbor several intracellular signalling pathways involving cAMP, PKA, and a transcriptional factor known as CREB. Certainly, these molecules were shown to be involved in synaptic plasticity in *Aplysia* and mammals.

In *Drosophila*, several critical tools have been developed that pose to be pivotal for the dissection of neural circuits. A noticeable part of these genetic tools includes; GAL4 and Split-GAL4 system (Figure 1). The GAL4 system is a biochemical process that is used to study gene expression in the fruit fly. This system was invented by Hitoshi Kakidani and Mark Ptsahne, (1988). The GAL4 system is made up of two parts; the GAL4 gene which encodes the yeast transcription activator protein and the UAS sequence. The UAS is an enhancer to which the GAL4 binds specifically to activate gene transcription (Figure 1A). Henceforth, a new modern-day technology has been developed which is also based on the GAL4-UAS system. This system allows more spatially defined expression of the desired transgenes. The Split-GAL4 UAS system which is synonymous to the GAL4 phenomenon, with the only exception being the splitting of the GAL4 into two stable domains (Figure 1B). The transgene of each GAL4 protein is placed under the control of the endogenous promoter element. This is observed when the UAS- transgene only occurs in cells in which the DBD and the AD are both present.

In addition to the GAL4 system, other toolsets that enable the stimulation and inhibition of specific neurons using neuron-specific GAL4 drivers are TrpA1 and *Shibire*^{ts1} respectively.

The transgenic expression of the temperature sensitive ion channel TrpA1 activates specific sets of neurons at high temperatures (Hamada et al., 2008).

Conversely, the *Shibire[ts1]* transgene can be used for blocking specific neurons using neuron specific GAL4 drivers at higher temperatures (Kitamoto, 2001). This hinders the release of specific neurotransmitters for a particular function. More specifically, this is normally due to the fact that the transgene encodes a dominant negative, temperature-sensitive *dynamin* which blocks neurotransmitter reuptake, such that the readily releasable pool becomes diminished.
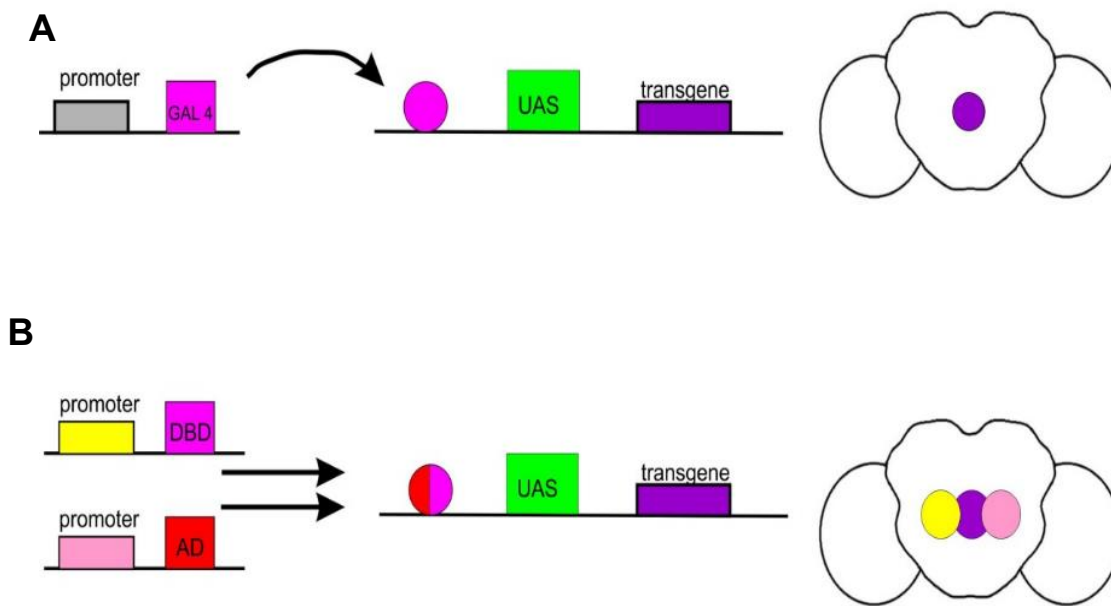
Figure 1. GAL 4–UAS and Split-GAL4 UAS
(A)This shows a GAL4 system which comprises of GAL4 and UAS system. The GAL4 is under the control of an endogenous promoter. In cells in which GAL4 is expressed further binds to the UAS and triggers expression of the downstream transgene. (**B**) The DBD and AD form a functional GAL4 transcription factor in cells in which they are both expressed triggering transgene expression (modified from Lawrence Lewis et al., 2015).

In addition to the above toolsets, the establishment of RNA interference appears to be very beneficial to the modern-day research as shown in Figure 2. The dsRNA in the cell is processed by RNAase III enzyme Dicer (Knight, 2001). This dsRNA possesses a sequence which is compatible to a gene of interest (Cerutti, 2003; Enerly et al., 2003; Giordano et al., 2002; Kalidas and Smith, 2002; Roman, 2004). The dicer then produces 21-23 nucleotides of dsRNA fragments with two nucleotides 3'end overhangs. i.e. siRNAs. These siRNAs interact with the RISC and then cleaved it into ssRNAs that further leads to the degradation of the complementary endogenous mRNA (Bernstein et al., 2001). Thus, gene expression is inactivated specifically at the post-translational level. This posttranscriptional knockdown can

be made very specific by placing the RNAi construct under the control of UAS and driving it at the appropriate GAL4 lines. Although the RNAi technique in fly research serves as an important tool, the problem of off-targets normally arises (Moffat et al., 2007). This problem normally arises when the nucleotide sequence of the introduced RNA matches with the mRNA of other genes. In summary, the availability of many sophisticated toolkits has made the *Drosophila* versatile in performing various forms of research.
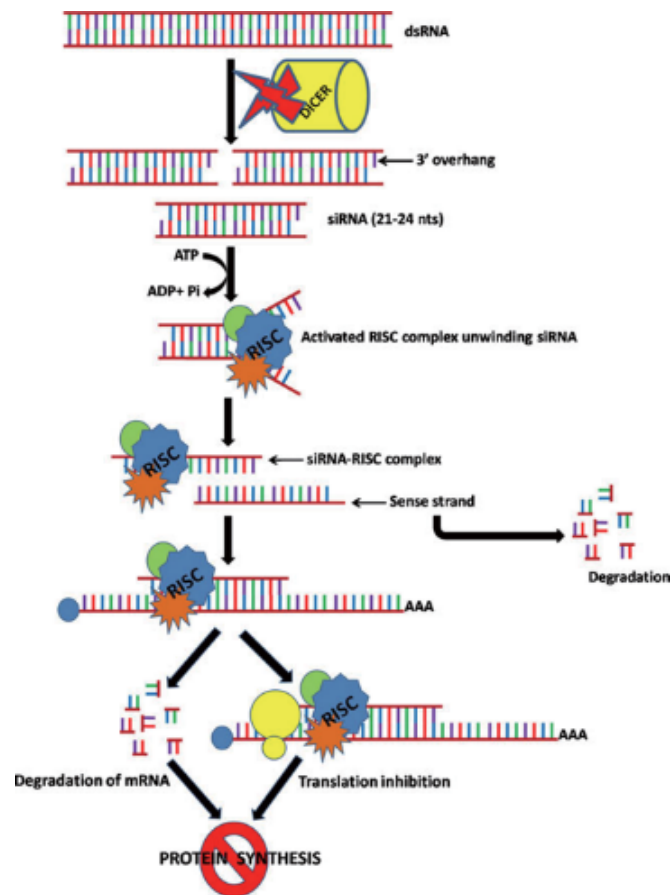
Figure 2. RNAi mechanism (RNA interference). Long dsRNAs are sliced by the dicer into approximately 21-23 nucleotides referred to as siRNA. These siRNAs interact with RISC which is then cleaved to ssRNA. This ultimately yields degradation of the complementary endogenous mRNA (Taken from Japtap et al., 2011).

1.3   Aversive Olfactory Conditioning in the *Drosophila*

The most predominant studied form of learning and memory in *Drosophila* is the olfactory classical conditioning. This is attributed to the ability of the fruit fly to learn odors in a laboratory environment. In addition to this, the olfactory nervous system in insects is homologous to that of vertebrates (Davis, 2005). Olfactory classical conditioning (Pavlovian

Conditioning) requires the fruit flies to associate an odor (CS) to an electric shock (negative stimulus) or a sucrose reward-positive stimulus (US). Classically, this process is performed by alternately subjecting two groups of flies to both CS and CS$^+$, with the latter (CS$^+$) presented simultaneously with the US (Tully et al., 1985; Quinn et al; 1974; Beck et al., 2000) (Figure 3). Thus, the memory of this conditioning is then tested when flies are introduced into a T-maze to make a choice between these two odors (Figure 3). Thus, increasing the time between acquisition and testing, it is then feasible to measure STM, MTM and LTM.
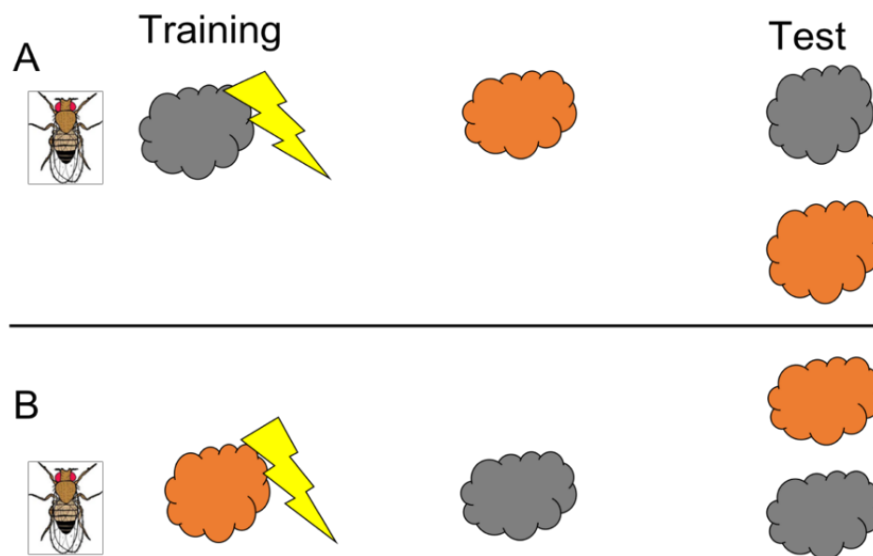
Figure 3. Aversive olfactory learning scheme. This shows the illustration of the olfactory classical conditioning in the *Drosophila.* (A) The conditioned stimulus (CS$^+$)- i.e. when the odor is paired with a reinforcer i.e. an electric shock (US). The fly is then subjected to a different odor (CS$^-$), after a short resting period and then introduced into the T-maze to choose between the two odors (CS$^+$) and (CS$^-$). (B) Alternatively, another group of flies are used for this conditioning. Here, the flies are exposed to the latter odor in A which is paired with electric shock (as shown in the color coding). The flies are then allowed to rest for a short time and then presented with the second odor. The flies are further introduced into the T-maze to make a choice between the two odors.

Several memory phases have been described following an olfactory classical conditioning. These memory phases include STM, MTM which comprises of ASM and ARM and LTM. One of the main objectives of neuroscience is to unravel the dynamics of these memory phases. Although, the investigation of the main dynamics of these forms of memories has proven to be elusive. These memory traces can, however be registered as changes in neuronal excitability, gene or protein expression, or growth or loss of neuronal processes existing between neurons that establish new or remove old connections. Evidence has suggested that both ASM and ARM are regulated at the neuronal and molecular level (Lee et al., 2011; Wu et al., 2013;

Zhang et al., 2013; Bouzaiane et al., 2015; Dudai, 1988; Folkers et al., 1993; Schwaerzel et al., 2007; knapek et al., 2010; Knapek et al., 2011; Scheunemann et al., 2012; Widmann et al., 2016).

1.4 The Molecular Coincidence detector of the CS and US pathway

Most of the molecules involved in the olfactory learning in the *Drosophila* are observed in the MB which serve as the place where memories are formed (Davis,1993; Davis, 1995). One of these molecules is AC which encodes rut. Mutant flies for rut are deficient in olfactory learning and restricted expression in the MB of the wild-type of *rut* restores learning defect (Mao et al., 2004; McGuire et al., 2004; Zars et al., 2000). Additionally, the AC has been postulated to be very critical for CS and US integration (Dudai, 1988). The enzyme is also sensitive to Ca^{2+}/Calmodulin and G-protein stimulation (Levin 1992, Livingstone, 1984). All in all, the association of odor with shock initiated the coincidence detection phenomenon.

The stimulation of the US pathway is linked to the G-protein activation that is coupled with dopaminergic or octopaminergic receptors. Conversely, stimulation of the CS pathway initiates the release of Ca^{2+} in the MB through VGCC.

Furthermore, functional imaging experiments in the cultured *Drosophila* brains revealed that cAMP signals are elevated with the application of DA or OA (Tomchik et al., 2009). The application of Ach to the calyces and dopamine to the lobes together rendered a combined increase in the cAMP signal. This effect on cAMP signalling is reliant on the rut AC; rut *Drosophila* brains fail to show this synergy (Figure 4).

Moreover, a followed-up report further reaffirmed rut AC as a coincidence detector for CS and US by imaging the activity of Protein Kinase A (Gervasi, 2010).
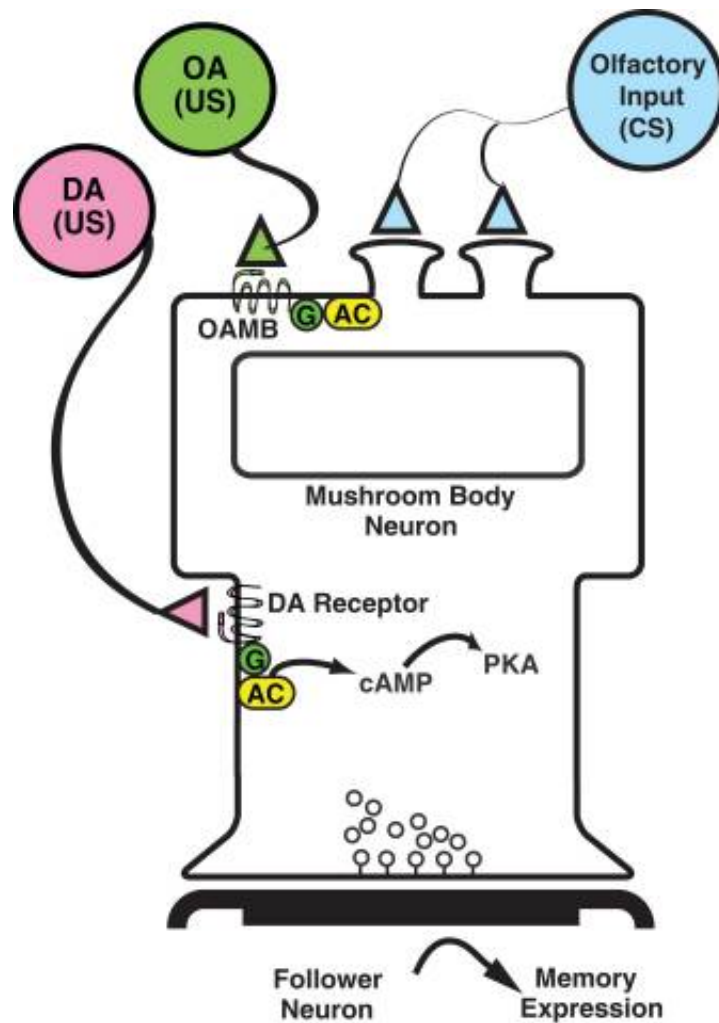
Figure 4. Neural Circuit of CS and US. This model shows the integration of CS and US in the MB after olfactory classical conditioning (Davis, 1993; Han et al., 1996, 1998). The olfactory information (CS) is transmitted into the dendrites of the MB where it is either integrated with information about either positive reinforcers or negative reinforcers. The CS is further modified by the simultaneous activation of the G-protein coupled octopamine receptor which is generated from the octopaminergic inputs to the MB neuron dendrites for appetitive learning. However, information reflecting aversive US stimuli is modified in the MB neurons by dopaminergic neuronal receptors on the axonal tracts of the MB neuron. The dopaminergic inputs adjust the CS information presented simultaneously to the MB neuron through the activation of AC. Thus, the increase in the cAMP and activation of PKA modulates the synaptic output to the downstream mushroom body neurons (Taken from Han et al., 1998).

1.5   Different Memory Phases of Aversive Olfactory Learning

Prior experiments displayed ASM and ARM, after single training session (Tempel, 1983; Quinn, 1976; Tully et al., 1994). Nevertheless, massed training (10 training sessions) produce stronger memory retention and this memory is not sensitive to the protein synthesis inhibitor known as cycloheximide. Thus, the memory produced by massed training can last up to 3 days. Conversely, spaced training i.e. 10 training sessions with 15 minutes resting interval between each cycle form a protein synthesis-dependent memory lasting up to one week (Tully et al. 1994). To sum it up, spaced repetition produces better LTM retention in comparison to massed training which produces ARM. Also, the study of mutant and transgenic flies genetically dissected the olfactory memory phases into four types and these include; STM, ASM, ARM and LTM.

Surprisingly, in flies, dunce and rutabaga mutants identified the cAMP component in STM (Tully 1985; Dudai, 1976; Livingstone, 1984). STM can be disrupted by cold-induced anesthesia directly after training (Quinn and Dudai, 1976; Tully et al., 1994). In addition, several genes have been investigated to be needed for various memory phases, and they are; *latheo, linotte, 14-3-3 (Leonardo), scaborous (volado), fasII and DC0 (PKA)* (Boynton and Tully, 1992; Cheng et al., 2001; Dura et al., 1993; Grotewiel et al., 1998; Skoulakis and Davis, 1996; Skoulakis et al., 1993).

Moreover, ASM which forms the cold sensitive type of memory is impaired in amnesiac mutant gene, which principally encodes the mammalian homologue of PACAP (Feany and Quinn, 1995; Moore et al., 1998).The amnesiac mutant gene, on the other hand, is exclusively expressed in the DPMs of the *Drosophila,* and it is very important in stabilizing both aversive and appetitive memories (Feany and Quinn, 1995; Keene et al., 2006; Keene et al., 2004; Moore et al., 1998; Quinn et al., 1979; Tamura et al., 2003; Waddell et al., 2000; Yu et al., 2005).

Lastly, ARM is referred to as a cold resistant memory form of MTM. In addition, the radish gene is specifically required for ARM (Dudai et al., 1998; Folkers et al., 1993; Isabel et al., 2004; Quinn and Dudai, 1976; Schwaerzel et al., 2007; Tully et al., 1994). ARM is also resistant to anesthetic agents (Quinn and Dudai, 1976) which cause retrograde amnesia in both vertebrates and invertebrates. Indeed, Bouzaiane and colleagues (2015) found that ARM is not a singular memory form, and can be divided into three successive components that are spatially segregated in the Drosophila olfactory network.
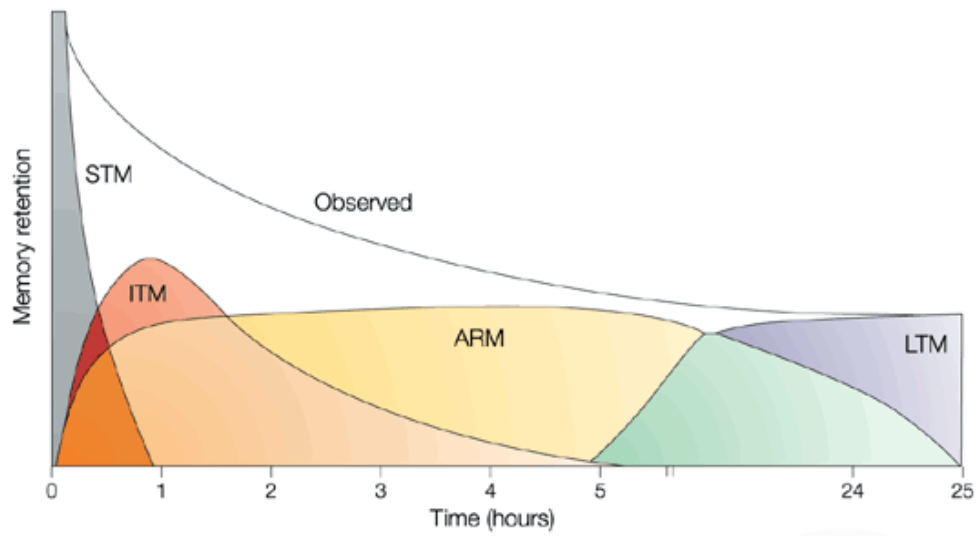
Figure 5. Temporal Phases of Memory. The figure shows the various memory phases that are established when a fruit-fly learned an experience. The distinct memory phases are STM, ITM/MTM, ARM and LTM (Taken from Davis, 2005).

1.6   Olfactory Information Processing in *Drosophila*

Dissecting the neural circuitry of memory acquisition, consolidation and retrieval are pivotal in understanding the fundamental aspects of how animals react to external stimuli that affect its survival, feeding and mating. *Drosophila* melanogaster provides a suitable model for understanding these phenomena. The manageable size of the fly brain that contains approximately 100,000 neurons coupled with the sophisticated molecular genetic techniques for selective visualization and perturbation of specific neurons and recent advances in recording neural activity makes *Drosophila* a powerful system for analyzing the neural circuits of behavior (Olsen and Wilson, 2008).

1.6.1   Peripheral Odor Detection

Despite invertebrates not possessing noses, their olfactory circuit system is apparently analogous to the olfactory system in vertebrates. Across species, odors are detected by ORNs that express ORs (Hallem et al., 2006; Benton et al., 2009; Touhara & Vosshall, 2009). In most cases, ORs work in conjunction with other molecules, e.g. coreceptors (Silbering & Benton, 2010). These neurons bathe their dendrites in a sensillar lymph (Leal, 2013). The lymph possesses several accessory molecules, where olfactory binding proteins are housed (Figure 6). ORNs are located along the insect antennae, and in other appendages in some species (e.g. the maxillary palps in flies and mosquitoes).

The molecular characterization of the receptors has been thoroughly studied in the *Drosophila,* where most antennal and palp receptors belong to the odorant receptor family (Clyne et al., 1999; Gao et al., 1999; Vosshall et al., 1999) which includes 45 receptors expressed in adult olfactory receptors (Couto et al., 2005). These 7 transmembrane receptors appear to form a novel insect-specific protein family, whose membrane topology is inverted compared to the G-protein-coupled receptor superfamily that includes vertebrate odorant receptors (Benton et al., 2006). Nevertheless, in *Drosophila,* Or83b is an example of an odorant receptor which is expressed in most olfactory receptors, where it is required for odor responses (Larsson et al., 2004). It further heterodimerizes with other odorant receptors, and hence required for their trafficking to the dendrites and may act as a co-receptor (Benton et al., 2006; Neuhaus et al., 2005). Current studies (Sato et al., 2008; Wicher et al., 2008) have proposed

that Or83b contributes to an odorant gated or relies on an intermediate cAMP second messenger.

1.6.2 The Antennal Lobe (AL)

Numerous studies have been performed on the AL of the *Drosophila* with major emphasis on the physiological properties and anatomical framework. The AL is also referred to as the first information processing unit of the olfactory circuit. Firstly, AL circuits respond uniquely and reliably to single or combinations of odors, maintain a dynamic range of sensory neurons, and propagate processed olfactory information to higher brain areas. (Bhandawat et al., 2007; Chou et al., 2010; Silbering & Galizia, 2007). Secondly, the functional unit in the AL of the *Drosophila* are the olfactory glomeruli. The glomeruli collect all axons of the respective ORNs that express the same ORs, hence inheriting their odor-response profiles.

Importantly, local interneurons (LNs) which have branches and extensive arborizations in the AL branch within and between glomeruli are involved in gain-control and population coding in the AL, and they are apparently involved in tuning the signal in the AL whereby the refined signal is sent to the higher centers of the brain by the PNs. The PNs have axons that exit the AL and project to the MB and to the LP. The MB and LP are both needed for odor identification and evaluation.
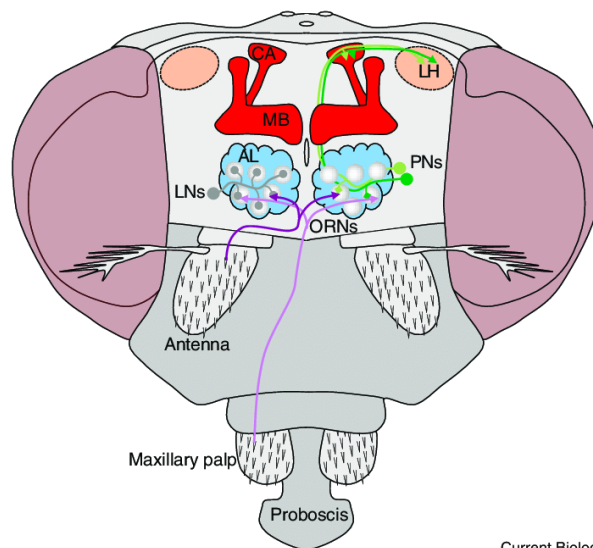
Figure 6. The Drosophila olfactory pathway. ORNs in sensillae on the third antennal segments and the maxillary palps project their axons bilaterally into individual glomeruli in the AL. In these glomeruli, ORN input is integrated and processed by the action of mostly multi-glomerular excitatory and inhibitory LNs.

Processed odor information is then relayed to the CA of the mushroom body (MB) and the lateral horn (LH) by uniglomerular projection neurons (taken from Perisse et al., 2013).

1.6.3 Local Interneurons (LNs)

In insects, GABAergic output within the AL is predominantly known to be provided by LNs (Homberg and Müller, 1999), but little is known about specific functional roles of various classes of interneurons. In order to investigate the functional roles of the different classes of interneurons, Tanaka and colleagues (2009) performed screening of *Drosophila* for *GAL-4* enhancer trap strains and then identified two distinct strains that label GABAergic LNs specifically (*GAL4-LN1 and GAL4-LN2)* (Sachse et al., 2007; Okada et al.,2009). In addition, *GAL4-LN 1* and *GAL4-LN 2* labelled about 18 and 37 LNs respectively (Sachse et al., 2007). Furthermore, anti-GABA antibody staining revealed that 95 % of each population of the LNs were GABAergic (Okada et al., 2009). Although, the functional arrangement of both LNs in the glomeruli appeared to be different, one group of LNs innervated parts of the glomeruli lacking the terminals of receptor neurons (LN 1) (Tanka et al., 2009).

Nonetheless, the LN 2s were widely branched and possessed an extensive arborization within the glomeruli (Tanaka et al., 2009). Henceforth, to test the functional roles of both LN groups, Tanaka and colleagues (2009) used a temperature-sensitive *dynamin* mutant gene known as *shibire* to block the chemical transmission from both LN groups. This manipulation revealed the more widely branching population of LNs i.e. LN2 to be necessary for generating odor-elicited oscillations that are phase-locked to the LFP of the MB.

In order to fully understand the mechanism and the knowledge behind this novelty, a thorough comprehension is needed in deducing the reasons behind the present of oscillatory decoding in some organisms and not the others. In locusts, odors evoke strong network oscillations in the AL, including PNs. These oscillations further synchronise the activity of odor-specific groups of PNs (Wehr et al., 1996).
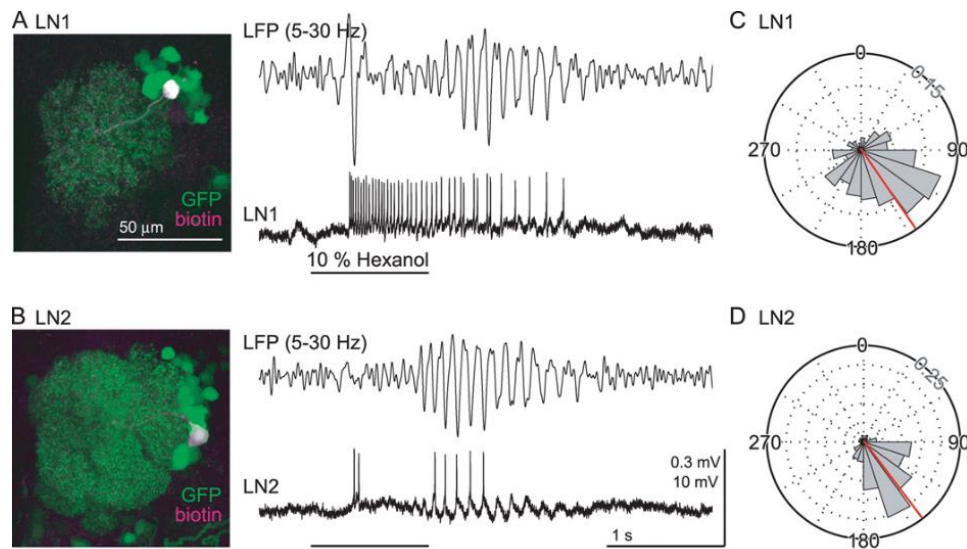
Figure 7. Spikes of LNs locked to the MB (A, B) Representative odor evoked responses in two types of LNs and simultaneously recorded LFPs (top:5 to 30-Hz band- pass). **(C, D)** Phase relationships between spikes in LN 1 (C) or LN 2 (D) and the LFP oscillations (5 to 15- Hz) are consistent (taken from Tanaka et al., 2009)

1.6.4 Projection Neurons (PNs)

Shreds of evidences have proven that PNs do not only convey information to higher centers of the fly brain but, do actively take part in memory formation in the fly brain. Various experiments performed in the PNs have been very thorough in showing the PNs involvement in memory formation. Previous cellular imaging experiments monitoring synaptic transmission from PNs showed that conditioning induces neural plasticity for approximately 5 mins after conditioning by recruiting new synaptic activity into the representation of the newly learned odor (Yu et al., 2004). Secondly, expression of rut cDNA in PNs rescued the appetitive memory deficit of rut mutants but not the aversive memory deficits (Thum et al., 2007). This discovery suggested that neural circuitry for appetitive learning requires some processing by rut encoded AC in the projection neurons that are not needed for aversive learning.

Lastly, RNAi knockdown of polyglutamine tract-binding protein-1 in PNs impaired aversive memory. This effect was potentially attributed to the reducing levels of NMDA receptor subunit 1 (Tamura et al., 2010). More studies are needed to be done in order to unravel the major role of projection neurons in the olfactory memory formation.

1.6.5 Mushroom Body (MB)

MBs are the primary olfactory learning center in the *Drosophila* with approximately 2500 KCs per hemisphere. (Technau et al., 1982; Davis 1993). They integrate olfactory input with punishment or reward and they are referred to be part of the driving force for behavioral response. The MB neurons are further involved in various temporal phases of memory formation. Blocking synaptic transmission from the MB neuron impairs the expression of olfactory memory, and it is consistent with the plastic events underlying the representation of olfactory memories within the MBs themselves or at prior nodes of information flow within the olfactory nervous system (Dubnau et al. 2001; McGuire et al. 2001). MB intrinsic neurons are now divided into three main subtypes, α/β, α'/β' and γ MB neuron with regards to the trajectory and the final destination of their axons into different neuropil. The axons of α/β and α'/β' neurons divide into vertical α and α' lobes, and horizontal β and β' lobes. The γ neurons on the other hand, form only the horizontal lobes (Crittenden et al., 1998). Functional neuroanatomical and physiological studies that use the transient block of various MB neurons, suggest that the MB neuron types perform different roles at different time windows during acquisition, consolidation and retrieval of memory.

1.6.5.1 MB γ neurons

The MB γ lobe neurons have shown clear evidence to be involved in memory acquisition and memory retrieval.

First, blocking of the γ neurons' synaptic transmission specifically during retrieval at 15 minutes after conditioning impairs both aversive and appetitive memory expression (Cervantes-Sandoval et al. 2013). Also, previous experiments revealed the necessity of the γ lobe for the initial formation of aversive memory (Blum et al. 2009; Qin et al. 2012). In addition to this, memory acquisition and expression of STM has been linked to several locations of the olfactory nervous system with mediation largely by the γ MB neurons, possibly by coincidence representation of CS and US. In addition, stimulated conditioning of flies with odor and thermogenetic activation of DA revealed that neuronal plasticity occurs primarily in the γ MB neurons (Boto et al., 2014). This phenomenon was displayed through functional imaging using G-CaMP of subsequent calcium responses to odors.

These above observations are apparent with a clear definition of the γ lobe involvement in the process of acquisition and expression of early memories. Nevertheless, pieces of evidence disclosed the requirement of the synaptic outputs of both the γ and α/β lobe neurons in the retrieval of early aversive and appetitive memories. This discovery may help to rethink how aversive and appetitive memories are processed from memory formation to memory retrieval.

1.6.5.2 MB α'/β' neurons

Blocking neurotransmission from α'/β' during aversive or appetitive training or at any time for up to approximately 90 minutes after conditioning impairs memory performance (Krashes et al. 2007; Cervantes – Scandoval et. 2013). Also, disruption of the synaptic neuronal output activity for up to approximately 90 minutes after aversive conditioning impaired memory expression but didn't affect memory expression drastically (Cervantes- Scandoval et al. 2013). The above experiments of Cervantes-Scandoval and colleagues (2013) indicated that activating communication from α'/β' mushroom body neurons to their postsynaptic partners are absolutely required for the expression of appetitive memories up to 3 hours, but only partially required for the expression of aversive memories up to 90 minutes. These findings show that the appetitive odor memories are present in these neurons for up to 3 hours after conditioning. To add to this, it further reiterates that the synaptic transmission from these neurons is required for memory expression through some other set of neurons. The partial effect from blocking the synaptic output activity of α'/β' lobes reaffirm the existence of parallel neural circuits for this type of memory outside of the α'/β' MB neurons.

1.6.5.3 MB α/β neurons

A vivid function for α/β was clearly shown to be recruited during retrieval of memory. Henceforth, blocking of the synaptic output of these neurons after appetitive conditioning using *shibire* strongly diminishes retrieval of protein synthesis-dependent LTM after 24 hours (Dubnau et al. 2001; McGuire et al. 2001; Cervantes- Sandoval et al. 2013). This finding revealed that the retrieval of 24h memory is solely dependent on α/β neurons.

Strikingly, blocking both α/β and γ MB neurons simultaneously after appetitive conditioning blocks all performance across all time points (Cervantes- Sandoval et al. 2013; Xie et al. 2013).

Indeed, this indicates that there are two separate channels for memory expression up to 24 hours after conditioning, one prominent in α/β mushroom body neurons and the other through the γ mushroom body neuron. In a nutshell, early memories are dependent on α'/β' mushroom body neuron function, while LTM in the same fly are independent.

A similar observation was shown in a unique experiment testing the integrity of LTM for one odor, and the impairment of STM of another after insult to α'/β' mushroom body neurons in flies trained to learn both odors (Cervantes-Sandoval et al. 2013). This shift in overall dependence to different neuron sets for the expression of early vs. late memories has strong similarities with systems consolidation in mammalian systems (Dudai 2004; Cervantes-Sandoval et al. 2013).
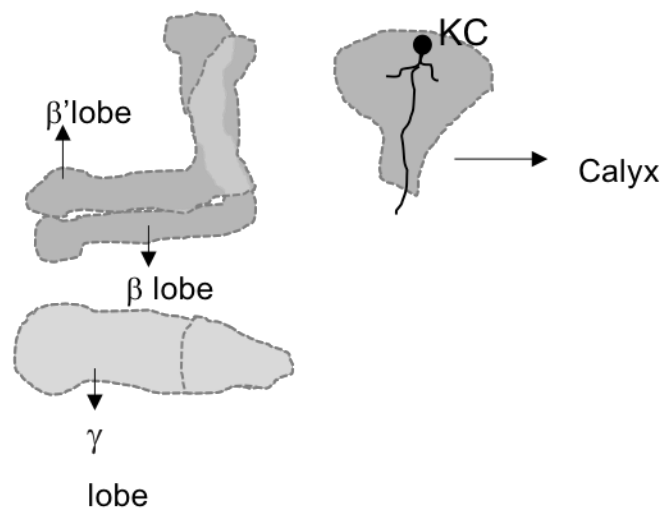
Figure 8. Sub regions within the MB. The various lobe systems of the MB are dismantled to paint a vivid picture of their arrangement. Their anatomical positions within the MB are shown in Figure 1.

1.6.6 Dorsal Paired Medial Neurons (DPM), and Anterior Paired Lateral Neurons

The DPM neurons completely ramify throughout the MB in the adult *Drosophila* brain, and the lobes of the MB are innervated by a pair of neuro-peptidergic amnesiac expressing DPM neurons, which are pivotal for MTM (Waddell et al. 2000). Also, the APL neuron is a GABAergic neuron that broadly innervates the MB. Moreover, reducing GABA synthesis in the APL neuron enhanced olfactory learning, suggesting that APL suppressed learning by releasing the inhibitory neurotransmitter GABA.

A related experiment revealed that the APL and DPM neuron, form heterotypic gap junctions within the MB (Wu et al. 2011). Also, Wu and colleagues (2011) revealed that innexin 7 is required in the APL neuron, and innexin 6 is needed in the DPM neuron to form hemichannels that function in 3 hrs. ASM. Pitman and colleagues (2011) confirmed enriched APL-DPM contact in the KCs prime lobes, where markers of presynaptic APL sites are also highest. The inhibitory neurons were required to sustain ASM in Drosophila MB.

1.6.7 Mushroom Body Output Neurons (MBONs)

The MB lobes are composed of approximately 2500 neurons. They include seven KCs, 21 MBONs and 20 DANs cell types (Aso et al., 2014). Each DAN cell type projects axons to one or at most two of the of the compartments defined by MBONs (Aso et al., 2014). The arrangement of DANs axons with compartmentalized KC-MBON synapses creates an isolated unit for learning that can transform the disordered KC representation into the ordered MBON output.

The MBONs send axonal projections to five discrete neuropils outside of the MB, hence providing loci for the convergence of all the information needed for learned associated responses (Aso et al., 2014). The neuropil regions are medially and laterally located in the vicinity of the vertical lobe of the MB. These neuropils include SIP, SMP and CRE.

MBONs also innervate the lateral horn and several parts of the MBs. Moreover, the MBONs innervating the horizontal lobe of the MB drive aversion and the corresponding MBONs innervating the vertical lobe drive attraction (Aso et al., 2014). The horizontal lobe (β, β' and γ) of the MBONs that drives aversion are glutamatergic. The vertical lobe (α and α') of the MBONs that drives attraction are cholinergic and GABAergic (Aso et al., 2014; Hattori et al., 2014; Sitaraman et al., 2015). A current study revealed that the decorrelated and sparse representations of odors at the level of the Kenyon cells broadly activates MBONs innervating both MB lobes (Hige et al., 2015; Aso et al., 2014).

Thus, it can be considered that the KC-MBON may be the part in the fly brain where olfactory odor identity is largely preserved and generalized into the positive and negative categories that may, in turn, drive attraction or aversive motor programs depending on the make-up of the olfactory sensorium (Hige et al., 2015).
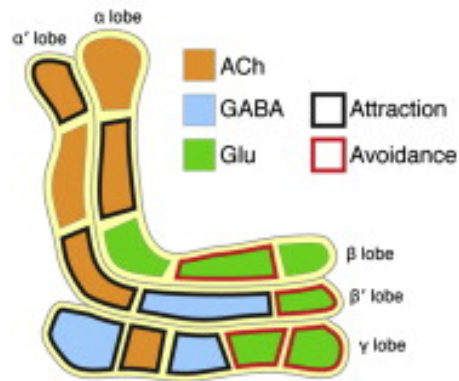
Figure 9. Correlation of MBONs to behavior. MBON compartments define a total of 15 different compartments in the lobes. The colors indicate neurotransmitter released by each MBON. Also, behavioral consequences of MBONs activation are shown by the color of the thick contours around different compartments (Aso et al., 2014)

1.6.8 DANs-MB Input

The DANs are the most prevalent modulatory neurons in the MB and dopamine is thought to act locally to modify KC-MBON synapses (Aso et al., 2010; Waddell, 2013). DANs activity are further required during learning (Schwärzel et al. 2003; Aso et al, 2010, 2012; Burke et al., 2012; Liu et al., 2012), and exogenous activation of DAN subpopulations serve as US in associative learning paradigms (Schroll et al., 2006; Claridge – Chang et al., 2009; Aso et al., 2010, 2012; Burke et al., 2012; Liu et al., 2012). The Drosophila possess four receptors which include dDA1, DAMB, DopEcR and DD2R. Two of the receptors i.e. dDA1 and DAMB were cloned first and appear to be members of the D1-like receptor family. The D1-like receptor family are coupled to the G protein $G_{s\alpha}/G_{olf}$. $G_{s\alpha}$ subsequently activates adenylyl cyclase increasing the intracellular concentration of cAMP (Neve et al., 2004). The D2-like proteins, on the other hand, are coupled to the G protein $G_{i\alpha}$ which directly inhibits the intracellular concentration of cAMP.

Three clusters of dopaminergic neurons (PPL1, PPL2ab and PAM) project their terminals to specific regions within the MB lobes and further transmit information about reward and punishment to the MB to guide learning (Schwaerzel et al., 2013; Claridge – Chang et al., 2009; Mao and Davis, 2009; Aso et al., 2010, 2012; Burke et al., 2012; Liu et al., 2012). Aso and colleagues (2014) identified over 100 DANs of 20 types. Each DAN type contains a small number of neurons: The DAN types from PPL1 clusters contained one or two cells per hemisphere and the corresponding DAN types of PAM cluster contained approximately 20 cells per hemisphere. Nevertheless, in classical conditioning paradigms, different DAN types responded to the US (Riemensperger et al., 2005; Mao and Davis, 2009; Burke et al., 2012;

Liu et al., 2012). The different clusters of the various DANs have a specific section of the MB in which they project.

The PPL1 cluster, made up of 12 neurons, consists of four subtypes that differ in their final projection pattern to the vertical lobes of the MBs. The four regions of the vertical lobe targeted by these neurons are 1) the tip of the α lobe, 2) the tip of the α' lobe, 3) the upper stalk, and 4) the lower stalk and its junction with the horizontal lobe (Figure 5). The PPL2ab cluster extends its axons to the MB calyx, and the PAM neurons innervate the horizontal lobes.
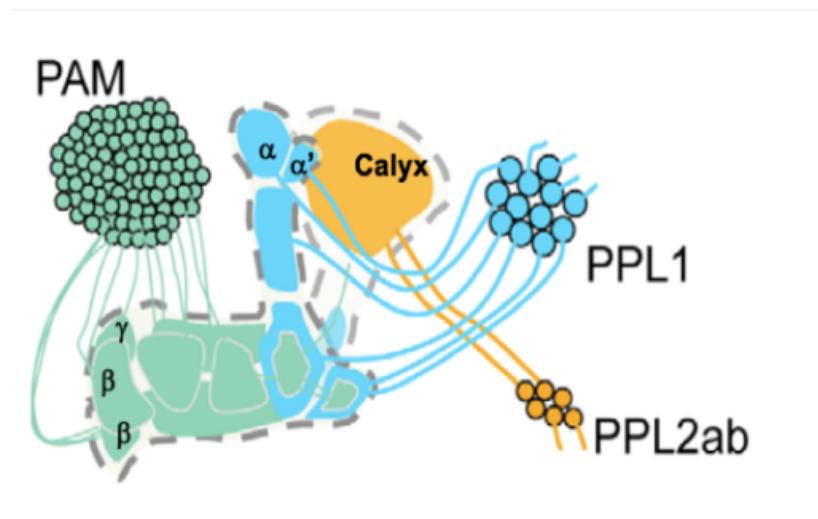

Figure 10. Schematic representation of Dopaminergic neurons
Of the MB. This figure correlates with how the various clusters of Dopaminergic neurons innervate the MB. Thus, the different color coding is synonymous with MB insertions (calyx, α/β, α'/β' and γ). Adapted from Aso et al., 2014

1.7 Presynaptic Active Zone

Active zones are highly specialized microdomains designed to regulate neurotransmitter release on a millisecond timescale. In *Drosophila*, the AZ-specific protein set includes Liprin-α (Fouquet et al., 2009; Kaufmann et al., 2002), Syd-1 (Owald et al., 2010), Unc13 (Aravamudan et al., 1999; Böhme et al., 2016), RIM (Graf et al., 2012; Müller et al., 2012) and Fife [related to mammalian Piccolo; (Bruckner et al., 2012)], RIM-BP ['RIM-binding protein'; (Liu et al., 2011)] and the CAST/ELKS homolog Brp. However, the active zone presents at the Drosophila NMJ is very elaborate as compared to other species (Zhai et al., 2004). Thus, have been given the name of "T bars" due to their morphology of a meshwork on a pedestal (Koenig et al., 1996). Initial studies identified Brp to be a key component in the formation of the T bar. Bruchpilot shows a similar homology to the mammalian active zone protein ELKS/CAST/ERC (Figure 7) which binds RIM1 in a complex with Bassoon and Munc13-1(Wagh et al., 2006). In addition, Brp is very essential in the clustering of Ca^{2+} channels beneath the T-bar at the center of the active zone (Fouquet et al., 2009), which bring the Ca^{2+} source close to the fusion machinery.

1.8 Bruchpilot

Synaptic communication is enhanced by the fusion of neurotransmitter-filled vesicles with the presynaptic membrane at the active zone (AZ); a process triggered by Ca^{2+}- influx through clusters of voltage-gated calcium channels (VGCCs) (Zhai et al., 2004). However, in Drosophila, MAB nc82 specifically labels active zones. Nc82 was previously used to identify Brp which was a previously unknown active zone component. Brp shows homology to the human active zone protein ELKS/CAST/ERC, which further binds RIM1 in a complex with Bassoon and Munc13-1. Notably, pan-neural reduction of brp expression by RNAi in adult Drosophila rendered the loss of T bars at the active zones. Thus, the brp protein provides an entry point to the study of general active-zone formation and function in this species (Wagh, 2006).

Moreover, it is speculated that brp may combine functions of ELKS/CAST/ERC and a cytoskeletal structural protein in a single polypeptide that is highly conserved among insects (Wagh, 2006). Further studies also reveal that brp mutants Ca^{2+} channels are reduced in density; evoked vesicle release is depressed and short-term plasticity is further altered.

In addition, brp-like proteins seem to establish proximity between Ca^{2+} channels and vesicles to allow efficient transmitter release and patterned synaptic plasticity (Kittel, 2006). Drosophila bruchpilot has been shown to be pivotal for the maturation of active zone assembly. Importantly, synaptic vesicles fuse at the AZ membranes where Ca^{2+} channels are clustered and are henceforth decorated by electron-dense projection. Interestingly, mutants of the Drosophila ERC/CAST family protein (Brp) were revealed to lack dense projections (T bars) and to suffer from Ca^{2+} channel-clustering defects (Fouquet, 2009). Brp was also shown to play a role in localizing Unc13A to the active zone and hence co-operated functionally with Unc13A by facilitating synaptic vesicle delivery to the docking sites (Bohme, 2016). A recent study by Fulterer and colleagues (2018) further show that two orthogonal scaffold proteins i.e. Brp and Syd-1 cluster-specific (M)Unc13 release factor isoforms either close or further away from VGCCs respectively across synapses of the Drosophila olfactory system, resulting in different synapse-characteristic forms of short-term plasticity. High Brp/Unc13A levels spear-headed high release probability at the first relay synapse of the olfactory system (ORNs > PNs), and consequently, supported a fast but depressing releasing component (Figure 8).
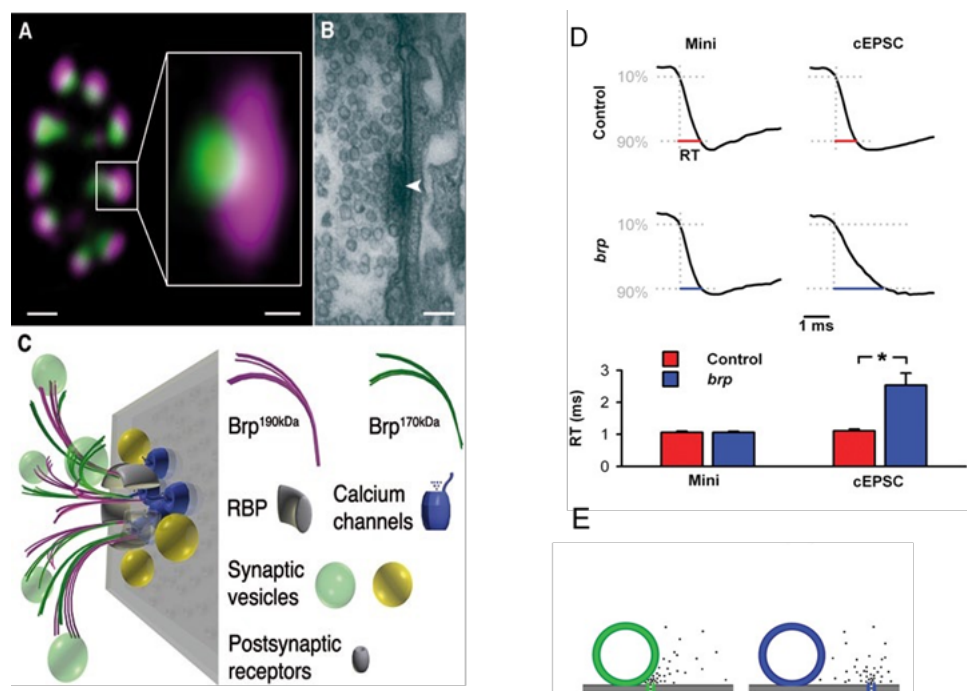
Figure 11. Brp Kinetics. (A) Immunohistochemistry staining showing the bouton of a larval neuromuscular junction which comprised of several synapses and an individual synapse in the lateral view. **(B)** This reveal an ultrastructure of the active zone. The arrow-head pointed at the T-bar. Synaptic vesicles clustered next to it (Andlauer and Sigrist, 2012). (C) Model of the active zone with respective Brp filaments isoforms arranged in an alternating pattern (Matkovic et al., 2013). (D) Average miniature excitatory postsynaptic currents (Mini) and compound excitatory postsynaptic currents from both the control and BRP mutant (*brp*) *Drosophila* NMJ (Kittel,

2006). (E) Shows the interpretation of the difference in the vesicle fusion. This reveal that fast and slow vesicle relate to the average distance between Ca^{2+} channels and vesicles (Modified from Kittel, 2006).

1.9 Synaptic plasticity and NMDA

N-methyl-D-aspartate (NMDA) receptors are part of the three pharmacologically distinct subtypes of ionotropic receptors that mediate a majority of excitatory neurotransmission in the brain via endogenous amino acid, L-glutamate. The Drosophila encodes two homologues of NMDARs and these are dNR1 and dNR2. In addition, dNR1 and dNR2 constitute functional NMDARs with several of the distinguishing molecular properties observed for vertebrate NMDARs, including voltage/Mg^{2+} - dependent activation by glutamate. The NMDAR channel is very permeable to Na^+ and Ca^{2+} channels, and its opening requires simultaneously binding of glutamate and postsynaptic membrane depolarization (figure 9).

Once activated, the NMDAR channel allows calcium to enter the postsynaptic cell where calcium triggers several biochemical cascades (Xia, 2005). Cellular studies have attributed the NMDAR channels to be involved in synaptic plasticity, long-term depression and long-term potentiation. However, NMDAR-mediated Ca^{2+} influx is suppressed at voltages near the resting membrane potential due to Mg^{2+} block (Figure 9), a mechanism in which the pore of the NMDARs is blocked by external Mg^{2+} ions (Mayer et al., 1984; Nowak et al., 1984).

NMDARs have also been proposed to function as "Hebbian coincidence detectors" (Single et al., 2006). Moreover, disruption of NMDARs has also been proven to be essential for associative learning in *Drosophila* (Wu et al., 2007; Xia et al., 2005, Miyashita et al., 2012). In addition to this, NMDARs activity are required for the formation of neural networks (Adesnik et al., 2008; Bellinger et al., 2012; Hirasawa et al., 2003; Lüthi et al., 2001; Tian et al., 2007). In addition, consolidation of LTM (long-term memory) required functional NMDARs (Wu et al., 2007).
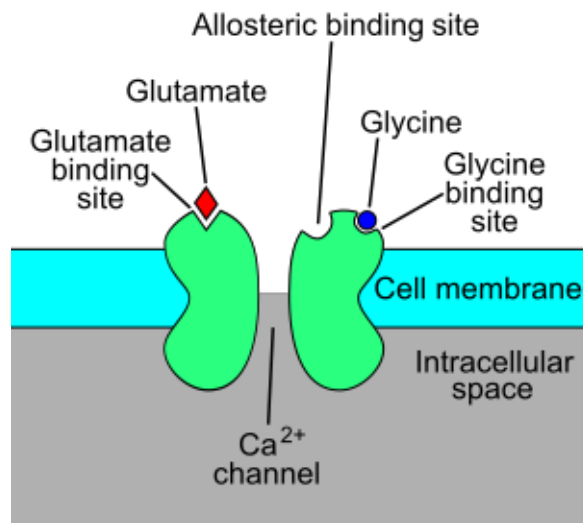
Figure12. Sequential events of NMDARs. Glutamate serve as an excitatory neurotransmitter which binds to the NMDAR receptors. This interaction further activates the NMDAR which then propel the passage of Ca^{2+} through the channel to enhance further biochemical reactions (Mayer et al., 1984)

1.10 Thesis aim

Although various strides have been made to thoroughly understand molecular processes and synaptic mechanisms underlying various memory phases of the Drosophila olfactory memory, hardly anything is known about the dynamics of their neural network circuits. Nonetheless, I use the presynaptic active zone protein Bruchpilot (Knapek et al., 2011), Mg^{2+} blocked of the *Drosophila* NMDA receptors and the functional NMDA receptors *(dsNR1 and dsNR2)* of the *Drosophila* to unravel the mechanism of Anesthesia-Resistant Memory (ARM) neuronal network circuit.

Chapter Two

2 Materials and Methods

2.1 Fly Care and Preparation

Flies were raised at 24°C and 60% relative humidity with a 14:10 h light-dark cycle on cornmeal-based food following the Würzburg recipe (Guo et al., 1996). Genetic crosses were performed according to the standard procedures. The F1 progeny of the various respective crosses, controls and genetic controls were used in the aversive olfactory conditioning.

For the Bruchpilot experiments, homozygous UAS-*bruchpilot*-RNAi lines were used. The combination of *RNAi^{B3}* and *RNAi^{C8}* yielded *w⁻; RNAi$^{B3, C8}$* which was on the III chromosome. The effector line w⁻; RNAi$^{B3, C8}$ as virgin females were crossed to various GAL4, MBONs (Glutamatergic and Cholinergic) and DANs Split-GAL4 which served as males.

However, to ensure the knockdown with *bruchpilot*-RNAi, all the vials were shifted from 24°C to 30°C when the larvae reached late 3rd instar state for these experiments.

The Split-GAL4 driver lines were generated at the Janelia Farm Research Campus by Aso et al. (2014). To ensure the temporal requirements of LN2, *NP2426-GAL4* as males were crossed with *UAS-Shibire^{ts1}* (Kitamoto, 2001) as virgin females and underwent olfactory behavioral experiments.

In relation to the Dopaminergic neuron receptors effect on ARM; *UAS-dNR1*(*wt*), UAS-*dNR2 (wt)* and Mg^{2+} blocked NMDA *UAS-dNR1*(*N631Q*) transgenic lines were used as female virgins and crossed with DANs Split-GAL4 driver lines which included MB087c (PAM β' 2a), MB056B (PAM β'2m, PAM β'2p), MB299B (PAM α1) and MB315c (PAM γ5).

2.1.1 Selected GAL4 lines used

Neuronal Targets	Genotype	References
Olfactory receptor neurons	*white; OR83b; (II)*	Vosshall et al., 2000
Local Interneurons	*white; GH298 (III) LN1*	(Stocker et al., 1997; Tanaka et al., 2009)
	white, NP2426; ;(X)	(Das et al. 2008; Tanaka et al. 2009)
Projection neurons	*white; NP225; (II)*	(Tanaka et al., 2004)
APL neuron	*white; NP2631; (II)*	(Tanaka et al. 2008)
α/β,γ KCs	*white;;mb247 (III)*	(Connolly et al., 1996)
α/β KCs	*white;17d; (II)*	(Zars et al., 2000)
γ KCs	*white; NP1131; (II)*	(Tanaka et al., 2008)
α‘/β‘KCs	*white; c305a; (II)*	(Krashes et al., 2007)
BRP-RNAi	*w⁻; RNAi$^{B3, C8}$* (III)	(Wagh et al., 2006)

Table 1. Selected GAL4 lines used to investigate aversive ARM

2.2 Behavioral Experiments

Flies to be tested in behavioral experiments were transferred to fresh food vials 48 hrs. before the experiments. Behavioral experiments were done in a dim red light at 70% relative humidity and a temperature of 24 °C in a barrel assay (Figure 15).

Conversely, in relation to the *UAS-Shibre*[ts1] (Kitamoto, 2001) behavioral experiments, flies were either trained or tested within a chamber with a temperature of 30 °C. The olfactory cues that were used included ethyl acetate (EA) (1/100 dilution in a mineral oil presented in a 14 mm cup) and 3-octanol (OCT) (1/150 dilution in a 14 mm cup). The US (unconditioned stimulus) used was 120 V DC electric shock with 1.3s duration. Performance of MTM and ARM were determined after 3hrs. of training. Flies were then transferred to neutral containers without food during the resting period. Henceforth, for the separation of consolidated ARM from labile ASM, two groups of flies were trained separately and one group was cooled on an ice at 0 °C for 90 s at the 2.5 hrs. mark after training. These flies were then tested for odor memory after 30 minutes of recovery (Cold + group). Exposing the flies to cold shock totally erases the ASM part of the memory which is labile, and thus the performance of the cold + group is mainly due to ARM. Calculation of behavioral indices was done as shown;

$$PI = (((EA - OCT)/(EA + OCT)) * 100) + ((OCT - EA)/(OCT + EA) * 100))/2$$
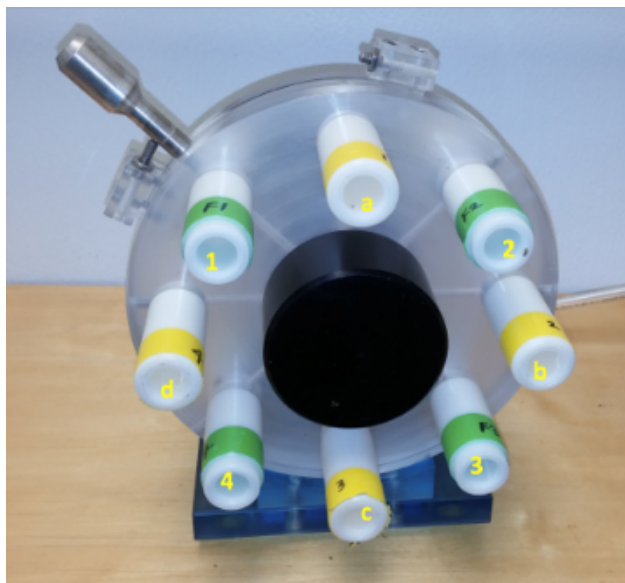
Figure 13. The barrel assay. Flies were trained with shock tubes lined with copper wire gauze either as CS[+] stimulus or CS[-] stimulus. The odor stimulus that were used were 1/100 ethyl acetate (EA) and 1/150 3-octanol (OCT). After training, flies were removed from the machine and placed into a neutral container. Flies were then loaded into the training wheel from the training positions into an empty elevator space. The shock tubes were then

replaced by four testing tubes in front and 4 testing tubes behind the training wheel for the test situation (modified from Schwaerzel et al., 2003).

2.3 Statistical Analysis

All data were analyzed using GraphPad Prism 7. In the case of BRP RNAi effect on ARM and ASM, a non-parametric test was used (*t tests*), and in the case of *UAS-Shibire^{ts1}* effect on LN2 *(NP2426-GAL4)*, Mg^{2+} blocked *(N631Q)* and the knockdown of the relevant functional receptor subunits of NMDA *(dsNR1 and dsNR2)*, one-way ANOVA was used. In the case of statistical differences, Bonferroni *post hoc* comparison was used.

ASM values were calculated from the difference of the performance index (PI) values of MTM and ARM. The error bars (SEM) of the ASM were determined by adding the variances (σ^2) of single PI values of MTM and ARM according to the following formula:

$$\textbf{SEM}_{\textbf{ASM}} = (\sqrt{[1/N * \sigma^2 \textbf{(MTM)} + \sigma^2 \textbf{(ARM)}]})$$ (Scheunemann et al. 2013)

Chapter Three

3   Results

3.1   Brp effect on ARM is required in the antennal lobe

Brp mutant active zones are associated with loss of electron-dense projections referred to as T-bars, reduction of Ca^{2+} channels density, depression of evoked vesicle release and alteration of short-term plasticity (Kittel., 2006; Wagh et al., 2006). Nonetheless, performing brp knockdown at the level of the antennal lobe displayed ARM effect in LN2 (Okada et al., 2009) and PN drivers (Figure14C), whereas ORNs and LN1 showed a normal ARM (Figure14B). These results showed the evidence of brp effects on ARM in the antennal lobe. Kittel et al. (2006) showed that brp is dependent on a low-frequency stimulation to establish a close proximity of Ca^{2+} ion channels with the synaptic vesicles. This type of conformity at the presynaptic active zone enables the precise release of neurotransmitter to the postsynaptic receptors. Thus, tuning the active zone for proper transmission of information (Fulterer et al.,2018). Also, succeeding parts of the *Drosophila* olfactory lobe network were investigated with brp knockdown- and these include; MB, APL, DPM and Th-GAL4.

3.2   Brp is required in the mushroom body

The MB of the *Drosophila* constitute as a primary learning center with approximately 2500 KCs per hemisphere (Technau et al., 1982; Davis, 1993). They integrate olfactory input with punishment or reward and are part of the driving force for the behavioral response. Expression of Brp-RNAi in the MB drivers i.e. *MB247 (α/β* and γ neurons (Zars et al., 2000), *17d* driver (α/β neurons) and lastly, *NP1131* (γ neurons) caused a significant effect on ARM (Fig 14D) (MB*247: t test: $t_{(13)}$, t=2.48, p<0.05, 17d: t test: $t_{(9)}$, t=2.82, p<0.05 and NP1131: t test: $t_{(11)}$, t=2.22, p<0.05*). However, Brp knockdown in the prime lobes (Figure 14D, *C305a*) showed no ARM effect. The outcome of this experiment suggest that ARM requires Brp-dependent mechanism at the level of the mushroom body. This finding is in accordance with previous experiment (Knapek et al., 2011).

3.3 Brp is not required in APL and DPM

The APL and DPM are large and electrically coupled neurons with fibers extending throughout the MBs, providing connections to numerous KCs. APL and DPM neurons possess heterogenous gap junctions between them that are essential in forming recurrent activity in α'/β' KC-DPM and APL-KC loop. The loop created is important in stabilizing ASM formed in the α/β Kenyon cells (Wu et al., 2011). Here, performing brp knockdown in both APL and DPM revealed no ARM effect (Figure14E and Figure14F). Thus, showed that MB-APL/DPM-MB feedback loop which formed part of the circuit required for memory consolidation (Wu et al., 2011), not to be part of brp-dependent ARM neural circuit.

In a nutshell, the above outcome shows the effect of brp on the conditioned stimulus (CS) pathway in the formation of ARM. However, ASM (Figure S2) which forms part of the Middle-Term Memory (MTM) was normal. Kittel et al. (2006) showed that brp null mutant had a decreased quantal content in response to the first arrival of action potential. Moreover, vesicle release after high-frequency action potential spikes was less affected, further revealing the relevance of vesicle release at low-frequency stimulation (Fulterer et al., 2018; Kittel et al., 2006; Wagh et al., 2006). Thus, proved brp-dependent low-frequency stimulation to be necessary for ARM. The next objective was to show whether brp knockdown which is associated with spatiotemporal changes in Ca^{2+} influx (Kittel et al., 2006) would have a profound effect on DANs (US providing signal) in the formation of ARM.

3.4 Brp is required in *TH-GAL4* (DANs)

Dopamine play an important role in associative learning in both vertebrates and invertebrates. In the case of aversive learning, the US reinforcement is carried out by a specific subset of DANs that respond to electric shock (Chang et al., 2009; Mao and Davis, 2009; Aso et al., 2012). Surprisingly, expressing Brp-RNAi in *Th-GAL4* which possess PPL1, PAM and PPL2 ab clusters (Schwaerzel et al., 2003; Mao and Davis, 2009; Aso et al., 2012; Burke et al., 2012) showed a significant ARM effect i.e. *Th-GAL4* ARM (Figure 16G and 16H) *t test: $t_{(14)}$, t=4.02, p<0.05*.Thus, show that brp manipulations at the active zone of dopaminergic neurons are essential for ARM. In conclusion, brp effect on ARM is predominant in both the CS and US (DANs) pathway.
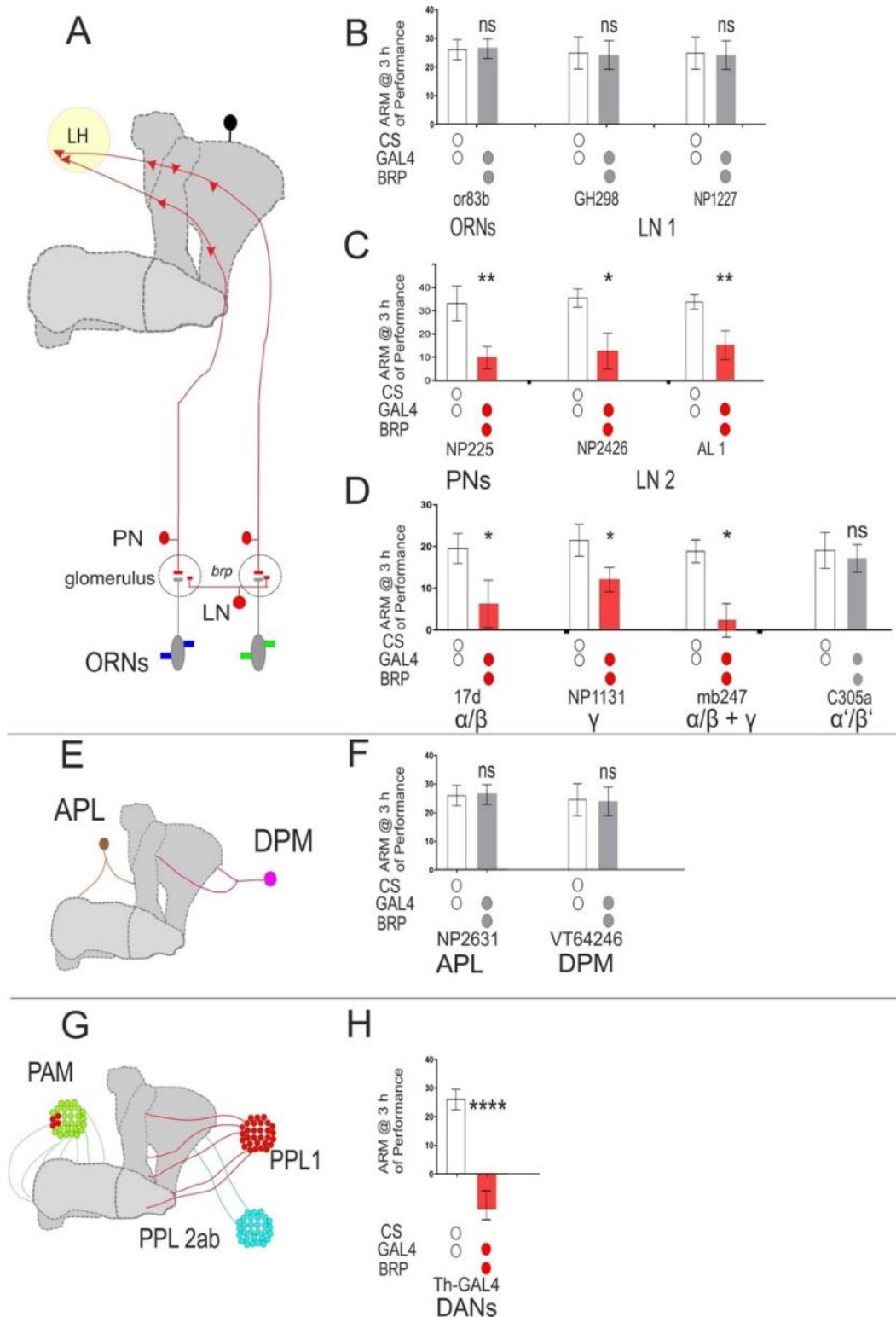
Figure 14. Brp RNAi on ARM

(A) This shows a schematic diagram of the CS pathway of the *Drosophila* olfactory pathway. ORNs = olfactory receptor neurons, PNs = projection neurons, LN = local interneurons MB = mushroom body neurons. (B) Performance indices of *brp* RNAi knockdown in ORNs *(Or83b)* and the two types of LN1s *(NP1227^GAL4 and GH298^GAL4)*. *Or83b* ARM: *test: $t_{(9)}$= 0.06, p=0.10* and for ASM: *test: $t_{(9)}$=0.33 p=0.74.* In the case of *NP1227* ARM: *test: $t_{(12)}$, t=0.60 p=0.59* and for ASM: *test: $t_{(12)}$, t=1.02 p=0.33.* In addition to this, *GH298* ARM: *test: $t_{(11)}$, t=0.45 p=0.79* and for ASM (Fig S2): *test: $t_{(11)}$, t=1.02 p=0.33.* Thus, showed that ORNs and LN1 not to be part of the ARM neural circuit. (C) Brp knockdown in LN 2 and PNs. *NP2426* ARM *test: $t_{(12)}$, t=2.83 p<0.05,* and for ASM (Fig S2) test*: $t_{(10)}$, t=0.50 p=0.62.* In the case of *AL 1* ARM *test: $t_{(13)}$, t=2.80 p<0.05* and for ASM test*: $t_{(13)}$, t = 0.60 p = 0.56. NP225* depicts projection neurons. ARM *test: $t_{(12)}$, t=2.83 p<0.05* and for ASM *test:*

41

$t_{(12)}$, $t=0.57$ $p=0.29$. Thus, also review *brp* knockdown effect in LN2 and projection neurons. (D) *Brp* knockdown effect in the mushroom body Kenyon cells.*17d* ARM t *test:* $t_{(9)}$, *t=2.82, p<0.05* for *ASM t test:* $t_{(9)}$, *t=0.83, p=0.43* and γ neurons i.e. *NP1131* ARM t *test:* $t_{(11)}$, *t=2.22, p<0.05* and for ASM t *test:* $t_{(12)}$, *t=0.35*. For γ and α/β, *mb247* ARM t *test:* $t_{(13)}$, *t = 2.48, p< 0.05* & for ASM t *test:* $t_{(13)}$, *t=0.39, p=0.70*. In the case of α'/β', *C305a* ARM t *test:* $t_{(20)}$, *t=0.30, p=0.77*. E and F show a schematic representation and ARM performance for APL and DPM. *NP2631* ARM t *test:* $t_{(13)}$, *t=0.024, p=0,98;* for ASM t *test:* $t_{(13)}$, *t = 0.87, p=0.398* and for DPM *VT64246* ARM t *test:* $t_{(11)}$, *t =0.77, p = 0.46,* ASM t *test:* $t_{(11)}$, *t =0.12, p = 0.884*. APL and DPM had normal ARM and ASM memory formation. G and H show schematic representation and ARM performance for *Th-GAL4*, ARM t *test:* $t_{(14)}$, *t=4.02, p<0.05* & ASM t *test:* $t_{(14)}$, *t=0.19, p=0.85*. Error bars indicate mean ± SEM of 7-10 biological repetitions. Statistical differences at level of $p \le 0.05$ are denoted by different letters or asterisks. In this and other panels, statistical significance of differences from the control groups is indicated as follows ****p<0.001, **p<0.01, *p<0.05, n.s. p>0.05*.

3.5   LN2 acquisition oscillations are required for ARM

Interestingly, brp knockdown effect in the LN subsets produced contrasting effects on ARM i.e. for LN1 (NP1227 and GH298) and LN2 (NP2426 and AL1). Henceforth, investigating the temporal phase of the aversive learning of LN2 drivers for ARM by performing *shibire* block revealed a significant ARM effect during acquisition phase i.e. one-way ARM ANOVA: F $_{(3,24)}$ = 3.25, *p < 0.05* (Figure 15E). On the contrarily, the retrieval phase displayed a normal ARM i.e. one-way ANOVA: F $_{(3,24)}$ = 0.14, p=*0.94* (Figure 15H).

This outcome disclosed LN2 driver acquisition phase neurotransmission to be required for ARM. Moreover, the LN1 drivers innervated parts of the glomeruli lacking terminals of receptor neurons, whereas the LN2 driver branched more widely, and innervated throughout the glomeruli (Okada et al., 2009). Notably, Tanaka and colleagues (2009) used the temperature-sensitive *dynamin* mutant gene, *shibire* (kitamoto, 2001) to block the chemical transmission from the LN2 driver. The LN2 driver i.e. *NP2426-GAL4* was necessary for generating odor-elicited oscillations. The odor-elicited oscillations generated in the LN2 were in phase-locked with the PNs and the LFP of the MB. This effect was also apparent in locusts (Laurent et al., 1994). These oscillations originated in the fast-GABA-mediated IPSPs induced by the LN.

In conclusion, the phase-locked firing of the LN2 and the PNs may establish a temporal encoding of olfactory information necessary for ARM by establishing binary code for each neuron at each phase peak, i.e. whether the neuron fires or remain silent.
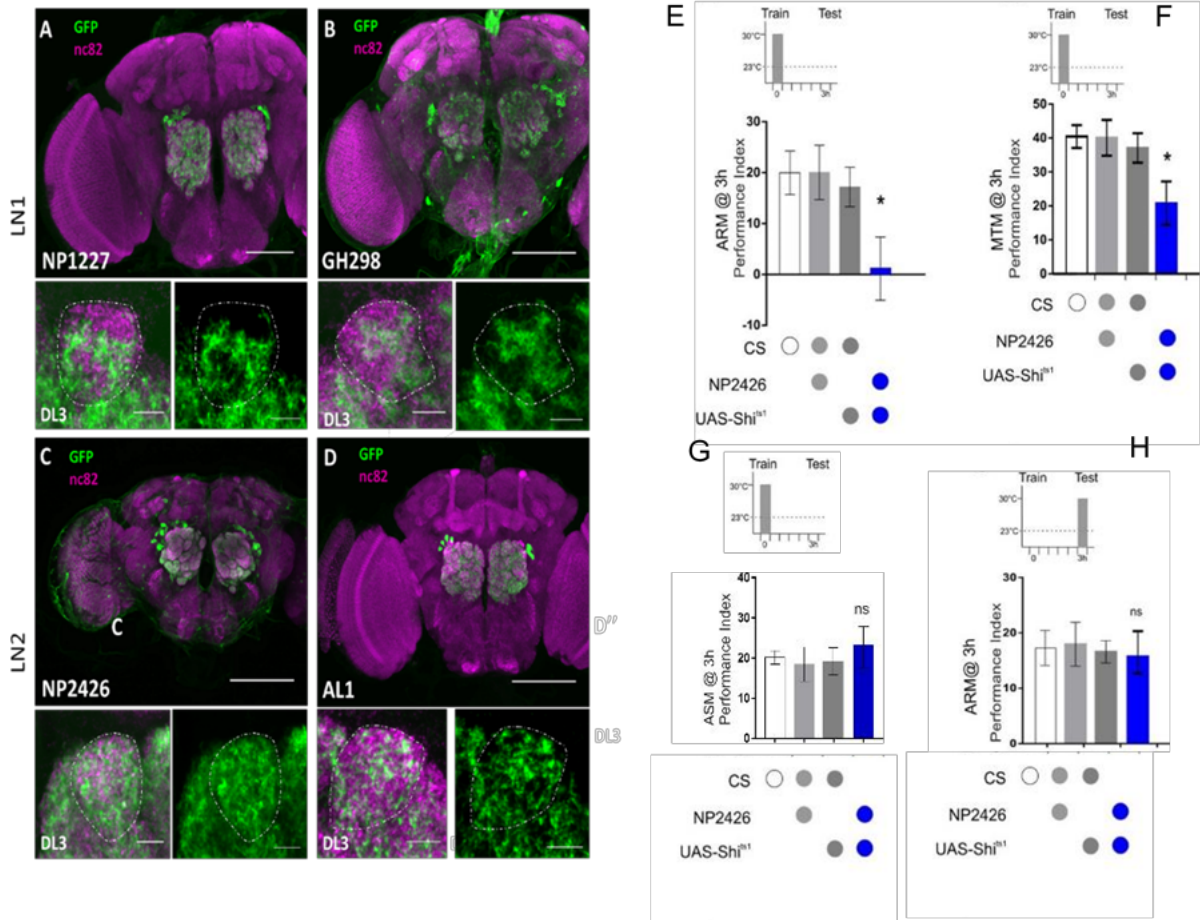
Figure 15. Anatomy of the Local interneurons
(A and B) LN 1 driver lines (A) NP1227 and (B) GH298 which exhibited heterogenous pattern. (C and D) LN 2 driver lines (C) NP2426 and (D)AL 1 exhibited homogenous pattern of the DL3 in the glomerulus. The LN 2 populations overlap with the terminals of ORNs. (E and F) Expressing temperature-sensitive *dynamin* mutant gene *shibire* in *NP2426-GAL4* revealed both ARM and MTM effects during acquisition. (*one-way ANOVA: F(3,24)=3.25, p<0.05 and F(3,24) = 3.19, p < 0.05 for MTM*). Anesthesia-sensitive memory (ASM) on the other-hand displayed no Effect with *shibire* block i.e. $F_{(3,27)}=0.1911$, *p=0.9016* (F) Conversely, expressing temperature – sensitive *dynamin* mutant gene *shibire^{ts1}* to conditionally and reversibly block the *NP2426 GAL4* driver during the retrieval phase showed no ARM effect (*one-way ANOVA: $F_{(3,24)}$ =0.14, p=0.94 for ARM*). Error bars indicate mean ± SEM of 7-10 biological repetitions (i.e., N = 7-10). Statistical differences at the level of $p \leq 0.05$ are denoted by different letters or asterisks. In this and other panels, statistical significance of differences from control groups is indicated as follows: ***p<0.001, **p<0.01, *p<0.05, n.s. p>0.05.* (Immunohistochemistry done by Diana Hilpert)

3.6 Clusters of Dopaminergic neurons

Two clusters of the Dopaminergic neurons (PAM and PPL1) project their axon terminals to specific regions within the MB lobes and transmit information about reward and aversive learning to the MB to guide learning (Schwaerzel et al., 2003: Claridge-Chang et al., 2009; Mao and Davis, 2009; Aso et al., 2010, 2012; Burke et al., 2012; Liu et al., 2012). The tyrosine-hydroxylase Gal4 displayed ARM effect (Fig 14G and 14H). The outcome from this then

43

showed the involvement of the US pathway in the *Brp*-dependent neural circuit for ARM. The two clusters that were investigated included PAM and PPL1 clusters.

The PAM cluster of approximately 100 neurons provide positive reinforcement and they preferentially innervate the β, β' and γ lobes (Burke et al., 2012; Liu et al., 2012). However, MB-M3 which forms part of the subset of PAM clusters, is involved in providing negative reinforcement (Aso et al., 2012). The PPL1 clusters on the other hand, project onto the vertical α, α' lobes, or heel or onto the surface of the peduncle which convey negative reinforcement value during learning (Riemensperger et al., 2005; Aso et al., 2012).

3.7   Bruchpilot is not required in PPL1 neurons for ARM

During learning, dopamine as a neuromodulator, is released to induce plasticity at the synapse between odor-activated Kenyon cells synapse and mushroom body output neurons (Owald et al., 2015; Perisse et al. 2016; Aso et al. 2014). Dopamine released from particular dopaminergic neuron clusters alters the efficacy of the specific KC-MBON connections, which further imposes a skew in the overall drive of the output network, and hence tips the balance of behavior towards approach or avoidance (Owald et al. 2015) as shown below in figure 16A. Notably, the various expression patterns of both PAM and PPL1 cluster neurons are also shown in figure 16B.

Furthermore, the PPL1 split GAL4 drivers included; MB060B and MB058B (Figure17A & Figure17B). The sites of innervation of the mushroom body of MB060B were; PPL1-α'2α2 (MB-V1), PPL1-α3, PPL1-α'3 and PPL1-γ2α'1. However, the MB060B driver displayed a normal ARM i.e. Figure 18A *t test: $t_{(13)}$, $t = 0.60$, $p=0.56$.* Also, the MB058B driver which specifically marks PPL1-α'2α2 (MB-V1) also had normal ARM (Figure 17B) i.e. *t test: $t_{(12)}$, $t=0.87$, $p= 0.40$.* Thus, the outcome of brp knockdown in the PPL1 clusters play no part in the brp-dependent ARM circuit.
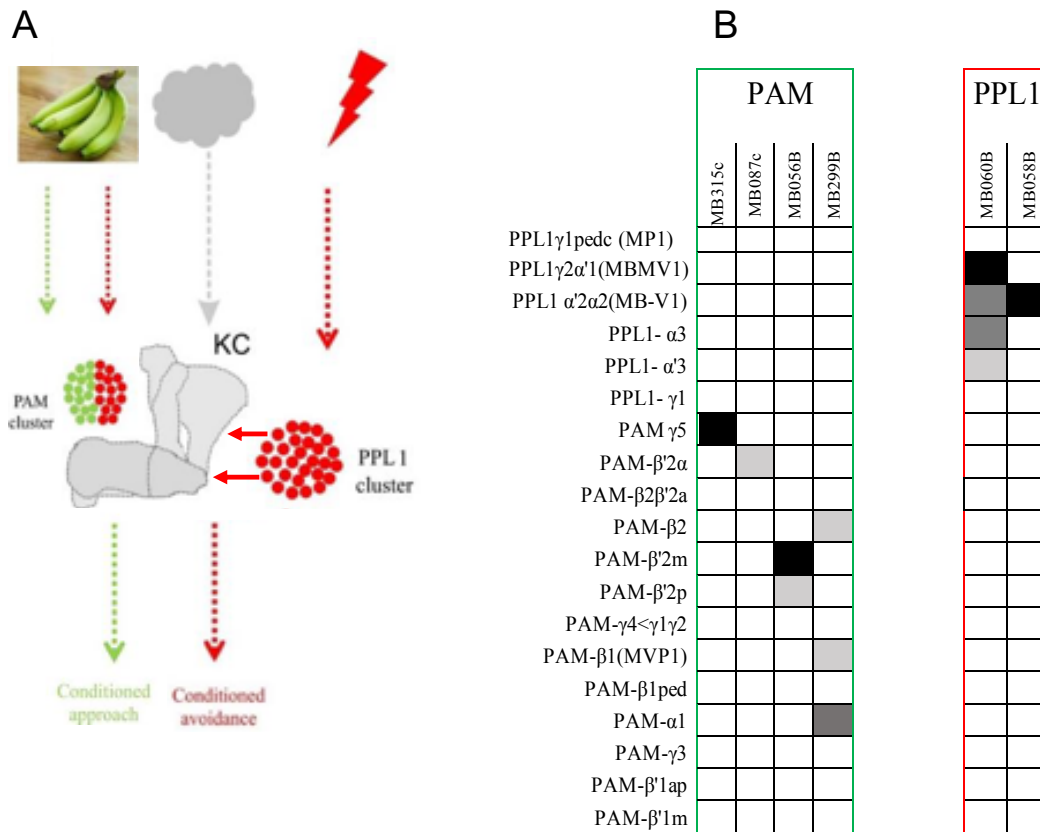
Figure 16. Schematic representation of DANs
(A)This shows the schematic arrangement of various dopaminergic neuron clusters i.e. PAM and PPL 1 and with their innervation sites in the mushroom body (MB). PPL 1 signifies conditioned avoidance during *Drosophila* olfactory conditioning (Modified from Tanaka et al., 2008; Mao and Davis, 2009; Aso et al., 2014). (B) The table 2 shows DAN Split-GAL4 line expression pattern. Each fly line shown with (MB----) targets expression to corresponding cell types as indicated with greyscale rectangles. Black shaded square signifies strongest expression and light grey signifies weakest expression. The Neuronal destinations are indicated on the far left. These anatomical and expressional analysis were carried out by Aso et al. (2014). The names of the DANs in the brackets shows the old MB nomenclature system.
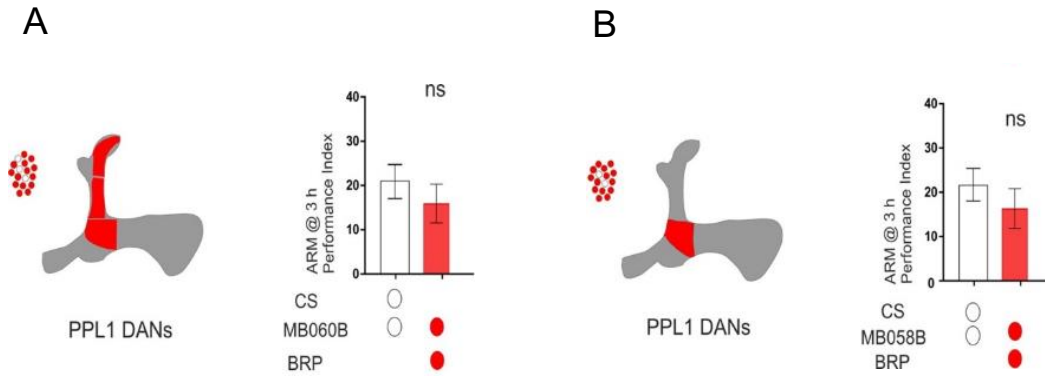
Figure 17. Brp in PPL1 for ARM

(A and B) Shows the innervation of the specific DANs (A) MB060B and (B) MB058B, and the aversive ARM performance indices. ARM performance index of MB060B i.e. *t test: t (13), t = 0.60, p=0.56,* and ARM performance for MB058B i.e. *t test: t(12), t=0.87, p= 0.4* Error bars indicate mean ± SEM of 7-10 biological repetitions (i.e., *N* = 7-10). Statistical differences; ns = Not significant. Statistical significance of differences from control groups is indicated as follows: ****p < 0.001, ** p < 0.01, * p < 0.05, n.s. p > 0.05.*

3.8   Bruchpilot is required in PAM neurons for ARM

Intriguingly, brp knockdown in three PAM neurons innervating the horizontal lobe of the MB displayed ARM effect i.e. MB315c driver with strong expression in γ5 compartment (Figure18A) *t test: t (11), t = 2.728, p<0.05,* MB087c driver with strong expression in the β'2a compartment of the horizontal lobe (Figure 18B) i.e. ARM *t test: t(15), t=3.516, p<0.05* and MB299B driver which possess a strong expression in the α1 compartment of MB (Aso et al., 2014a; Yamagata et al., 2015) (Figure 18D) ARM: *t test: t(15), t = 2.041, p < 0.05*. Interestingly, MB056B driver which specifically marks β'2m and β'2p compartments of the MB displayed normal ARM (Figure 18C) *t test: t(14), t=0.2756, p=0.3934*. Thus, the PAM neurons play a part in the US related plasticity in the brp-dependent ARM circuit.

Prior report revealed that MB-M3 neuron which forms part of the PAM cluster to be essential for aversive labile-ASM (Aso et al., 2012). This shows that several subsets of the PAM cluster neurons function at different vesicle releasing probabilities which may play a fundamental role in dissociating various memory phases.
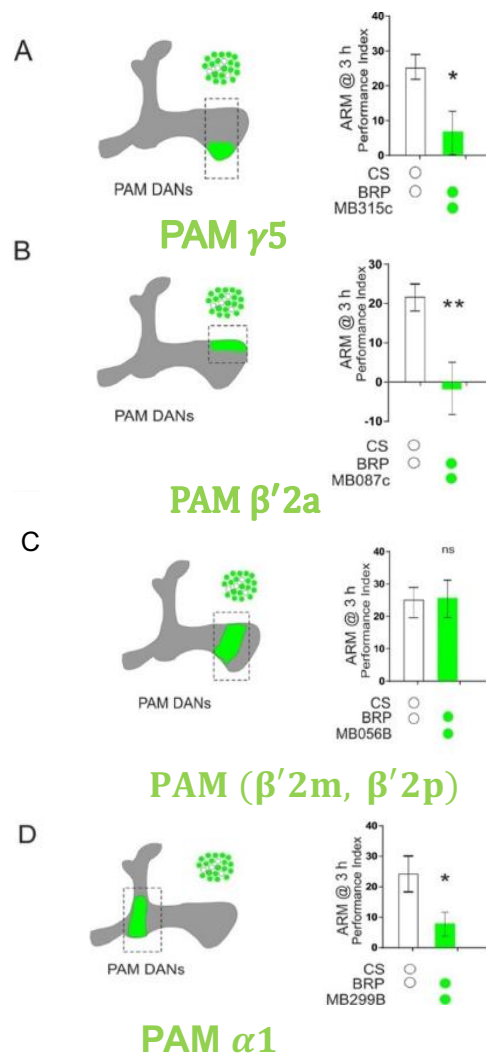
Figure 18. Brp in PAM neurons for ARM.
(A) The sketch reveals the expression pattern of MB315c (PAM γ5). ARM performance: *t test: $t_{(11)}$, t =2.728, p<0.05.* (B) This shows the innervation and expression pattern of MB087c (PAMβ'2a).
(C) The PAM neuron innervates β'2m and β'2p (MB056B) compartment of the horizontal lobe. ARM performance: *t test: $t_{(14)}$, t=0.2756, p=0.3934.* (D) The PAM α1 (MB299B) send input into the α1 MB compartment. ARM performance: *t test: $t_{(15)}$, t = 2.041, p < 0.05.* Error bars indicate mean ± SEM of 7-10 biological repetitions (i.e., *N* = 7-10). **Statistical differences; ($p \leq 0.05$), ns = Not significant.

3.9 DANs-MBONs interactions

During learning, dopamine is released to induce plasticity at the synapses between odor-activated Kenyon cells and the mushroom body output neurons (MBONs) (Owald et al., 2015; Perisse et al., 2016; Cohn et al., 2015; Hige et al., 2015). However, the presynaptic terminals of these dopaminergic neurons i.e. PAM and PPL1 clusters encoding positive or negative valence occupy further non-distinct overlapping partitions of the mushroom body neuropil which are further matched by the dendrites of discrete mushroom body output neurons (Aso et al., 2010; Burke et al., 2012; Claridge-Chang et al., 2009; Liu et al., 2012; Schroll et al., 2006; Aso et al., 2014; Waddell et al., Yamagata et al., 2015).
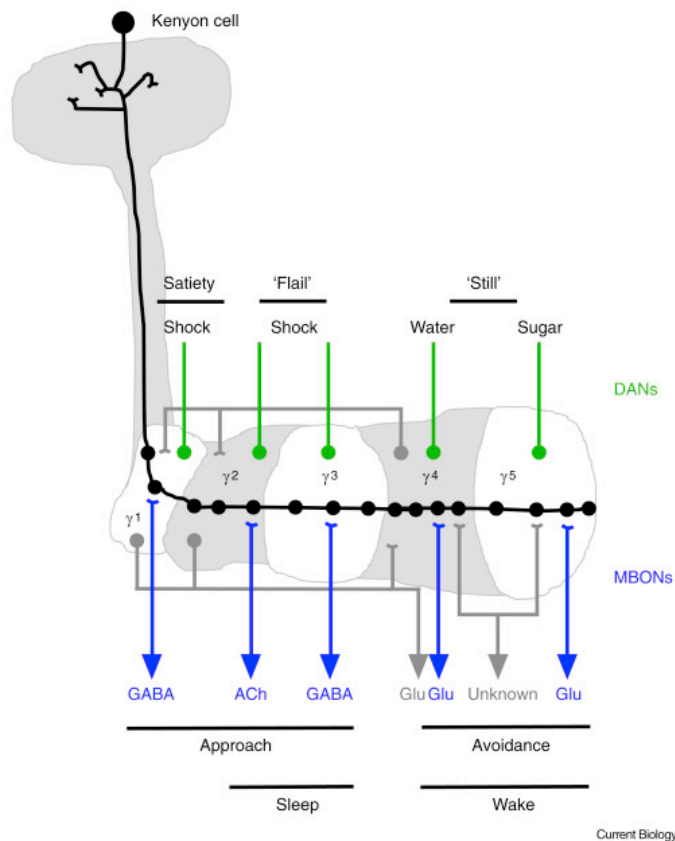
Figure 19. Illustration of DANs modulation of Kenyon cells synapses in MBONs (γ lobe). The γ Kenyon cell form en passant synapses with mushroom body output neurons (blue). The dopaminergic neurons send their presynaptic terminals to various compartments of the MB lobes. The reinforcement stimuli provided by these dopaminergic neurons include water, electric shock, sugar, flailing, satiety. These dopaminergic neurons also inhibit other dopaminergic neurons (Not shown). In addition, the MBONs illustrated in blue color release various neurotransmitters ranging from GABA, Acetylcholine (Ach) and glutamate (Glu). The activation of the individual MBONs enhance approach or avoidance and sleep or wake behaviors. The dopaminergic neurons depress or act on various receptors and channels to skew the MBONs toward a certain behavior (Taken from Scott Waddell et al., 2016)
.

3.10 Glutamatergic MBONs are part of Brp-dependent ARM circuit

To identify MBONs involved in the brp-dependent ARM neural circuit, various Split-GAL4 lines from the collection of MBONs described in Aso et al. (2014) were selected. Here, expressing Brp-RNAi in the glutamatergic MBONs (Figure 19A, 19B, 19C and 19D) which mark the horizontal lobe of the MB displayed ARM effect, whereas there was no ARM effect in the cholinergic MBONs (Figure 19E, 19F and 19G) which mark the vertical lobe of the MB.
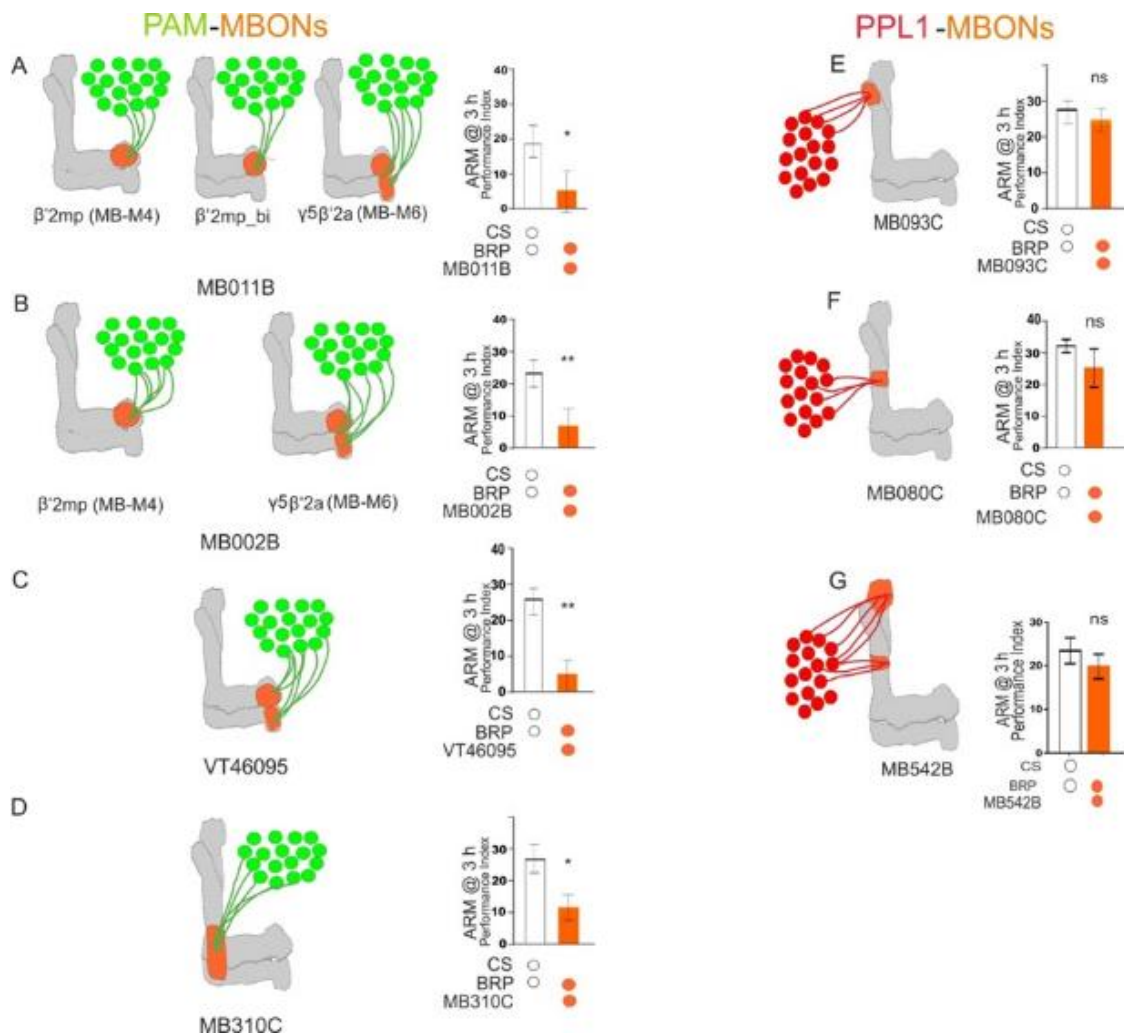
Figure 20. Brp in glutamatergic MBONs Split-GAL4
(A) This shows the expression pattern of MB011B Split-GAL4 i.e. β'2mp_bi, γ5β'2a (M6) and β' 2mp (M4). ARM *t test: $t_{(19)}$, t=2.113, p<0.05*. (B) The MB002B Split-GAL4 included β'2mp (M4) and γ5β'2a (M6). ARM *t test: $t_{(16)}$, t=3.475, p < 0.05*. (C) *Brp* knockdown specifically in M6 neuron i.e. VT46095 ARM *t test: $t_{(19)}$, t=4.721 ***p < 0.0001*. (D) Expressing *brp* in MB310c driver line marked α1 compartment. ARM *t test: $t_{(21)}$, t=3.392, p<0.05*.(E) MB093c ARM *t test:$t_{(17)}$, t=0.09937, p=0.4610*. (F) MB080c ARM: *t test:$t_{(17)}$,t=1.223, p=0.1190*. (G) MB542B driver ARM *t test: $t_{(21)}$, t=0.1632, p= 0.06*. Error bars indicate mean ± SEM of 7-10 biological repetitions (i.e., N = 7-10). Statistical differences; ($p ≤ 0.05$), ns = Not significant. Error bars indicate mean ± SEM of 7-10 biological repetitions (i.e., N = 7-10). Statistical difference; ns = Not significant.

It should be noted that the plastic changes observed at the level of the glutamatergic MBONs are in principle of brp presynaptic origin which possesses an impact on the postsynaptic receptors.

	Horizontal				Vertical		
	MB310c	MB011B	VT46095	MB002B	MB093c	MB542B	MB080c
MBON-γ4>γ1γ2							
MBONβ1>α(MV2)							
MBON-γ5β'2a (M6)		■ (dark grey)	■ (darker grey)	■ (light grey)			
MBON-β'2mp (M4)		■ (light grey)		■ (grey)			
MBONβ'2mpbilateral		■ (light grey)					
MBON-β2β'2a							
MBON-α1	■ (black)						
MBON-γ3							
MBON-γ3β'1							
MBON-β'1							
MBγ1pedc>α/β(MVP2)							
MBON-γ2α'1							
MBON-α'2 (MB-V4)					■ (light grey)		
MBON-α3 (MB-V3)					■ (black)		
MBON-α'1						■ (light grey)	
MBONα2sc (V2α)							■ (grey)
MBON-α2p3p						■ (dark grey)	
MBONα'3ap(V2α'3)							
MBONα'3m (V2α'3)						■ (grey)	
MBON calyx (CP1)							

Table 2. MBON Split-GAL4 line expression patterns Each fly line (MBxxxB) targets expression to the corresponding cells are indicated by grayscale rectangles. The shaded black portion corresponds to the strongest expression whereas, the light grey corresponds to the weakest expression (Aso et al. 2014). The green and orange margins correspond to glutamatergic MBONs cholinergic MBONs respectively

3.11 Crosstalk and Feedback in Dopamine Circuits

Brp knockdown in the ***Th-GAL4*** (Figure 17-18) displayed PAM clusters to be recruited for ARM, and a similar effect on ARM was observed in the corresponding MBONs (Figure 19). Nevertheless, the MBONs axons and the dendrites of the dopaminergic neurons (DANs) form substantial connectivity outside of the MB. Thus, this connectivity forms a feedback and a degree of interconnectivity between these circuits (Aso et al., 2014). Several experiments have shown numerous recurrent loop network existing in the *Drosophila* Olfactory learning (Perisse et al., 2016; Ichinose et al., 201; Owald et al., 2015). The recurrent loop existed between PAMα1 - α1MBONs and PAMγ5, PAMβ'2a – M6 MBON (γ5β'2a).

These microcircuits (Figure 20) provide stimulus re-evaluation functions. The stimulus re-evaluation functions include integration of the MB output neurons and reinforcing stimulus information. Some of the reinforcing stimulus-specific information include; the reliability of the shock and the relative shock value (Perisse et al., 2013). The next questions were to investigate ARM effect by using Mg^{2+} block of the NMDARs (Mayer et al., 1984) of the respective PAM neurons (Figure 20) and the knockdown of the respective NMDARs subunits *(dNR1 and dNR2)* in the PAM neurons (Figure 20). Here, the focus was to observe if the glutamatergic feedback of MBON α1 and MBON γ5β'2a (M6 MBON) further augment the US provided by the PAM neurons (Figure 21).
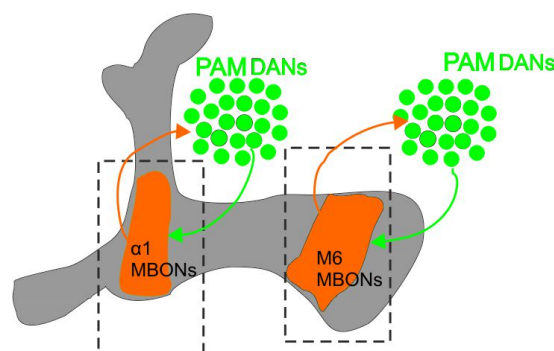

Figure 21. Brp-dependent Feedback Loop for ARM. A closed feedback loop involving the MBON from the γ5β' 2a and α1 compartment, the α/β' Kenyon cells and the DANs innervating the α1 and γ5β'2a compartments.

3.12 NMDA-dependent plasticity is required for ARM

A voltage-dependent Mg^{2+} block of NMDARs allows them to function as Hebbian coincidence detectors (Mayer et al., 1984; Nowak et al., 1984). Binding by glutamate alone is insufficient for channel activation as Mg^{2+} remains bound to a site in the channel pore, effectively blocking ion transport. Eviction of this Mg^{2+} ion additionally requires membrane depolarization. Thus, the coincidence of presynaptic glutamate release and strong depolarizing potential in the postsynaptic neuron is required for the opening of NMDAR channels. Miyashita et al. (2012) showed that Mg^{2+} block mutations do not alter odor specificity of learned associations. Here, they performed olfactory conditioning by pairing a single CS^+ odor with electric shocks (US), and then tested the flies to the CS^+ odor as well as unrelated odors.

Henceforth, the avoidance of the CS^+ odor increases as compared to the nonconditioned odors. Thus, show that odor-specificity during learning remains intact in Mg^{2+} block mutations *(N631Q)*. Subsequent Ca^{2+} influx through the open channel serves as a trigger for synaptic plasticity. Miyashita and colleagues (2012) investigated the role of coincidence detection in *Drosophila* specifically through the Mg^{2+} block mechanism of NMDAR for learning and memory.

Expression of the Mg^{2+} block in the NMDARs of the respective PAM neurons displayed ARM effect (Figure 21, 22 and 23). Thus, Mg^{2+} block mutations in the NMDARs of the PAM neurons may cause further suppression of the NMDA-dependent signaling that exist in the various recurrent loop (Figure 21).

3.13 Functional NMDA Receptors in PAM neurons are required for ARM

NMDA receptors in Drosophila consist of two subunits, i.e. *dNR1* and *dNR2*. These NMDARs are expressed widely in the adult Drosophila brain (Xia et al., 2005). The main objective was to observe whether glutamatergic input to the PAM neurons is required for ARM by downregulating the expression of glutamate receptors in MB299B-GAL4, MB087c-GAL4 and MB315c-GAL4. Intriguingly, knockdown of either *dNR1* or *dNR2* in the above PAM neurons impaired ARM (Figure 21-23) i.e. dsNR1/MB315c; ARM one-way ANOVA: $F_{(3,18)} =$ 3.695, *p<0.05*, dsNR2/MB315c; ARM one-way ANOVA, $F_{(3,26)} = 3.388$, *p<0.05*, dsNR1/MB087c: ARM one-way ANOVA: $F_{(3, 29)} = 3.839$, *p<0.05*, dsNR2/MB087c; ARM:

one-way ANOVA: $F_{(3, 23)} = 0.9669$, *p<0.05* and dsNR2/MB299B ARM: one-way ANOVA: F $_{(3, 24)} = 12.53$, *p < 0.0001*.
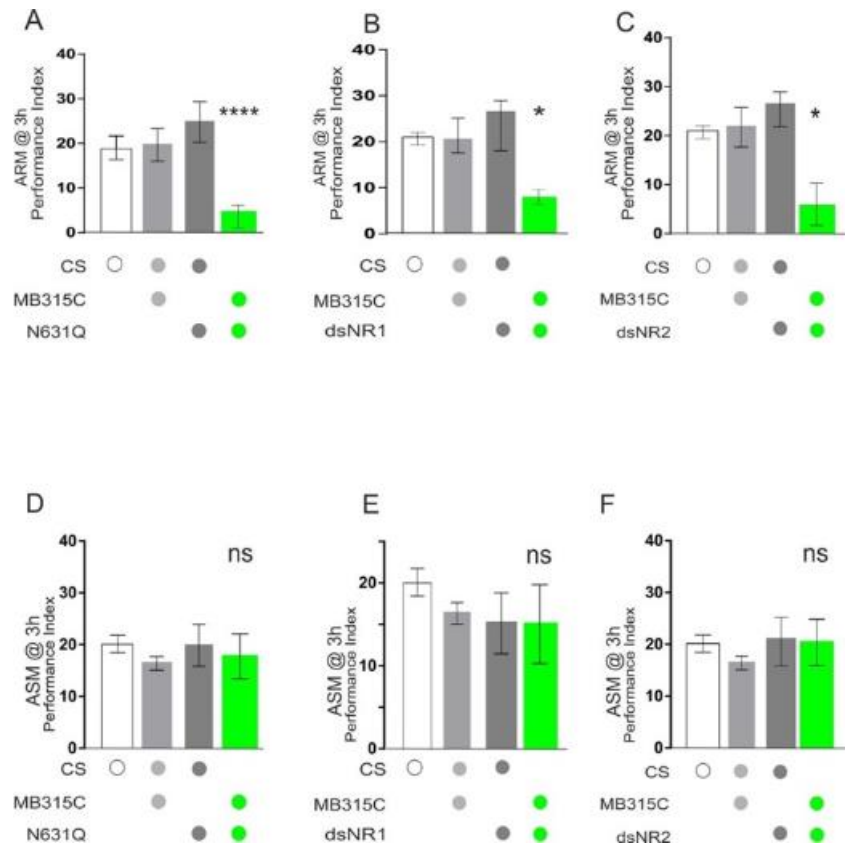
Figure 22. Mg^{2+} and NMDA Receptors in MB315c (PAM γ5) driver for ARM
 (A and D) Expression of Mg^{2+} block in MB315c driver (PAM γ5) had a tremendous effect on ARM formation and had no ASM effect. ARM; one-way ANOVA: F $_{(3,37)} = 10.35$, *p < 0.0001, n=40* and ASM: one – way ANOVA: F $_{(3, 18)} = 1.283\ p = 0.314$. (B and E) Knocking down NMDA functional receptor subunit *(dsNR1)* in MB315c driver (PAM γ5) affected ARM formation and hence no ASM effect. ARM: one-way ANOVA: F$_{(3,18)} = 3.695$, *p < 0.05*. and for ASM: one-way ANOVA: F$_{(3,16)} = 1.232\ p = 0.3306$, *n = 20*. (C and F) Knocking down NMDA functional receptor subunit *(dsNR2)* in MB315c (PAM γ5) displayed an impairment in ARM memory formation with no apparent display of ASM effect. ARM: one – way ANOVA, F$_{(3,26)} = 3.388$, *p < 0.05*, and for ASM: F$_{(3,21)} = 0.2905\ p = 0.8317$, *n = 25*. Error bars indicate mean ± SEM of 7-10 biological repetitions (i.e., *N = 7-10*). ** Statistical difference; *p < 0.05*, ns = Not significant.
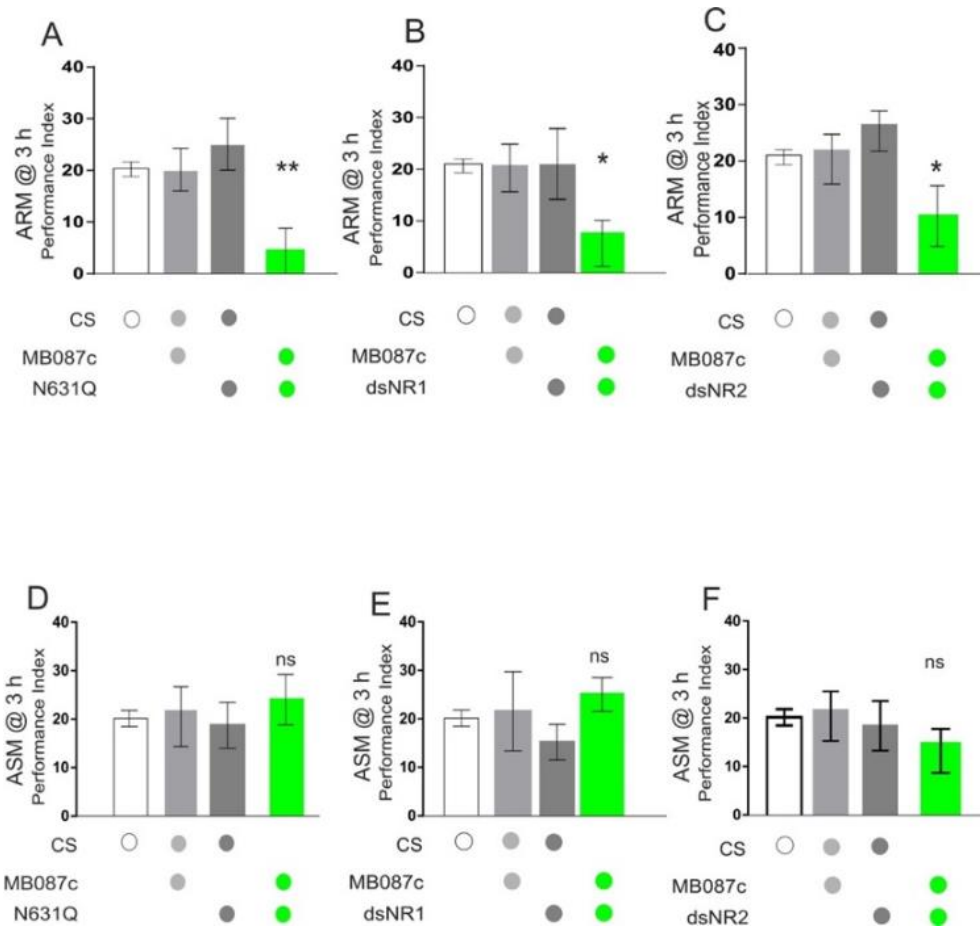
Figure 23. Mg²⁺ and NMDA Receptors in MB087c (PAM β'2a) driver for ARM. (A and D) Mg^{2+} blocked in MB087c driver line which innervates the β'2a compartment of the horizontal lobe proved to be required for ARM formation and had no effect on ASM (Anesthesia sensitive memory) memory. ARM: one-way ANOVA, $F_{(3,28)}$ = 6.029, $p < 0.05$ n = 32. ASM: one-way ANOVA: $F_{(3,22)}$ = 0.2564, p = 0.8559. (B and E) Knocking down of NMDA functional receptor subunit (dsNR1) in MB087c driver (PAM β'2a) displayed ARM impairment and had normal ASM. ARM: one-way ANOVA: $F_{(3,28)}$ = 6.029, $p < 0.05$ n = 32, and ASM: one-way ANOVA: $F_{(3,24)}$ = 2,091, p = 0.1281, n = 28. (C and F) Knocking down NMDA functional receptors subunit (dsNR2) in MB087c driver (PAM β'2a) was essential for ARM memory formation and had no effect on ASM. ARM: one-way ANOVA: $F_{(3,23)}$ = 0.9669, $p < 0.05$. For ASM: one-way ANOVA: $F_{(3,18)}$ = 0.2949 p=0.8286. *Error bars indicate mean ± SEM of 7-10 biological repetitions (i.e., N = 7-10). Statistical difference; p < 0.05, ns = Not significant*

54
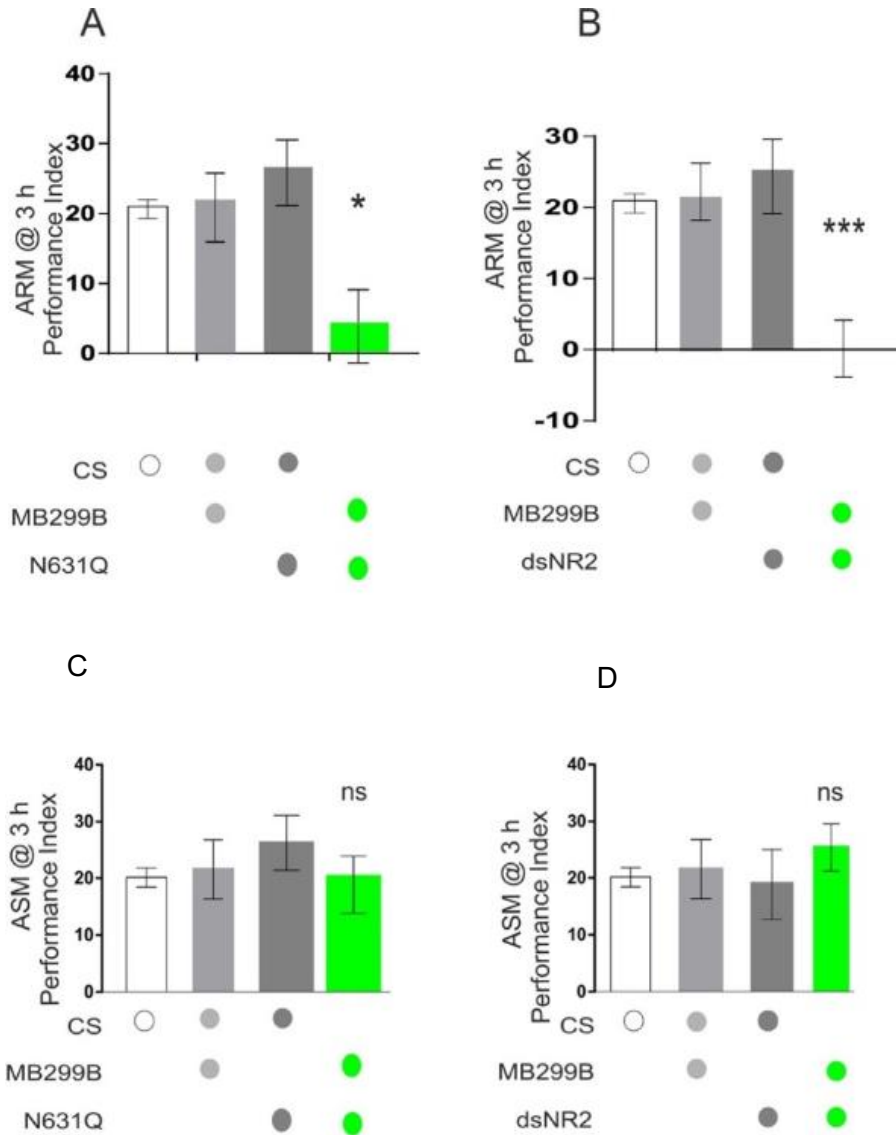
Figure 24. Mg^{2+} and NMDA receptors in PAM α1 (MB299B) for ARM. (A and C) Mg^{2+} blocked in MB299B GAL4 driver displayed ARM memory effect with no effect on ASM memory. ARM: one-way ANOVA: F$_{(3,30)}$ = 4.85, $p < 0.05$, $n = 33$ and ASM: one – way ANOVA; F$_{(3,22)}$ = 0.393, $p = 0.7593$. (B and D) Knocking down NMDA functional receptor subunit *(dsNR2)* in MB299B GAL 4 driver showed an effect on ARM memory formation. The ASM memory which forms a component of 3 h MTM was normal, and one-way *ANOVA*: F$_{(3, 22)}$ = 0.4041 $p = 0.7515$. Error bars indicate mean ± SEM of 7-10 biological repetitions (i.e., N = 7-10). Statistical difference; $p < 0.05$, ns = Not significant.

# Chapter Four

4 Discussion

The MTM of the *Drosophila* aversive olfactory conditioning after a single training cycle is functionally divided into labile ASM and consolidated ARM (Scheunemann et al., 2013; Quinn and Dudai, 1976). Prior reports have shown the impact of presynaptic active zone protein on these memory phases (Knapek et al., 2010). Brp which forms part of the cytomatrix active zone (CAZ) was revealed to have an effect on ARM at the level of Mushroom body Kenyon cells (Knapek et al., 2011). This project however, identified brp to be required in a much broader neural circuit (Figure 14).

Firstly, the antennal lobe brp ratios were apparently noticed to be high in a separate experiment (Fulterer et al., 2018). Thus, tuning their effective coupling distance, and then supporting (Böhme et al. 2016) fast, phasic release probability at ORN > PN synapses. The above phenomenon was present in the LN2 driver (Figure 15) when it's chemical transmission during the training phase was blocked with temperature sensitive dynamin gene. In addition to this, the LN2 driver possess extensive arborizations within the glomeruli, and it may play a part in filtering signals present in the antennal lobe (Bhandawat et al., 2007; Olsen and Wilson, 2008; Okada et al., 2009) using odor-elicited oscillations to determine neurons that would fire or not. Moreover, brp effects on ARM was apparent in the mushroom body γ and α/β neurons (Figure 14D). Indeed, this outcome was in accordance with a separate report (Knapek et al., 2011).

Secondly, brp knockdown in the *Th-GAL4* had an impact on ARM (Figure 14). Here, performing brp knockdown effect on ARM in the various clusters of the *Th-GAL4* proved ARM effect in PAM neurons (Figure 18), whereas PPL1 neurons (Figure 17) showed no ARM effect. Notably, MB-M3 neuron which form part of the PAM clusters had an effect on ASM when blocked with temperature-sensitive *dynamin* gene shibire (Aso et al., 2010). Hence, the above results show the involvement of PAM neurons in the US-related signal in the case of ARM. The subsequent glutamatergic MBONs of the various PAM neurons also had ARM effect when combined with brp (Figure 21). Lastly, Mg^{2+} block and knockdown of Drosophila NMDA

receptors in the PAM neurons displayed ARM effect, and this further identified the importance of NMDA dependent signaling in the formation of ARM.

In a nutshell, brp effect on the Drosophila olfactory network circuit deduced a neural network analysis and mechanism for ARM. Brp effect observed in this large neural confirms that a close proximity of the Ca^{2+} channels to synaptic vesicles and low-frequency dependent release of vesicles are paramount in the formation of ARM. In addition, the proposed model for ARM formation and retrieval is shown below.

4.1 ARM Neuronal Network Circuit Model

4.1.1 Odor specificity of the KCs and MBONs

Odor stimulus during (CS^+) an aversive Drosophila olfactory learning produces spike in some subsets of KCs (Figure 25A). The spikes generated here are due to the endogenous dopaminergic signal produced by the PAMγ5. The endogenous dopaminergic input into the KCs act through the D1 receptor which functions in augmenting the cAMP levels (Nutt et al., 2015). Conversely, the response to the non-reinforced odor (CS^-) is represented by different subsets of KCs, and may act through D2-like receptors which functions in abating the cAMP levels (Doya et al., 2008; Nakano et al., 2010) to maintain a constant homeostasis. Bouzaiane and colleagues (2015) showed that the α/β KC-V2α output neurons (Cholinergic MBONs) response to odor stimulus in a binary manner. Here, training decreased flies respond to CS^+ odorant as compared to CS^-. This V2α output neuron was shown in a separate study to be required for the retrieval of LTM (Sejourne′ et al., 2011; Aso et al., 2014b).

Conversely, the glutamatergic M6 neurons showed a prolonged response to CS^+, and was required for the retrieval of ARM (Bouzaiane et al., 2015). Thus, explained why various distinct memories are not visible in the same KCs and MBONs (Figure 18) (KC-MBON). Notably, much is not known for this spatiotemporal difference, and the possibility of antagonistic effect within the same or different synapses may play a role in this phenomenon. Henceforth the homeostatic balance between D1-like receptors and D2-like receptors at various KC-MBON synapses may a pivotal role (Figure 25B).

4.1.2 Postsynaptic coincident activity of glutamatergic MBONs activity gate US

The aversive reinforcements in the form of electric shocks are provided by MB-MP1 (PPL1-γ1pedc) which innervates the heel and peduncle, and MV1 (PPL1-γ2α'1) (figure 25) neuron which innervates the γ2 compartment (Aso et al., 2014; Owald et al., 2015). It is however apparent that, simultaneous presentation of odor and electric shock would lead to the depression of KC and MBONs synapses, and hence this would render depression of the GABAergic MOBON (MVP2) response to CS$^+$ (Hige et al., 2015; Aso et al., 2014). The GABAergic MBON (MVP2) are feedforward inhibitory interneurons (Figure 25A). Thus, their depression would further lead to the potentiation of the PAM neurons through concurrent activation of the glutamatergic MBONs response to the CS$^+$ (Bouzaiane et al., 2015).

Importantly, the activation of the NMDA receptors of the PAM neurons require concurrent delivery of glutamate and depolarization in order to allow the entry of calcium (Ca^{2+}) (Murphy and Glanzman, 1997; Bao et al., 1998). This phenomenon is dependent on the enhanced activity in the glutamatergic MBONs to CS$^+$ and depolarization by the PAM neuron (Figure 25A). Ueno et al. (2017) proposed the postsynaptic glutamatergic activity in gating the presynaptic dopaminergic neurons plasticity. Indeed, it is apparent to assume that gating of the dopaminergic US signal provides the local activity of DA signal in the recurrent network circuit (Figure 22, 23-24).

The recurrent loop activity generated from the termini of the MBON γ2α'1 and the glutamatergic MBON (M6) together with the dendrites of the PAM γ5 form a gating mechanism that drives the presynaptic activity of the Kenyon cells and the glutamatergic MBONs (M6) in creating a readout for ARM memory (Figure 25A). A similar connection is apparent between the PAM α1 and MBON α1 (Figure 21).

4.1.3 Dopaminergic neuron receptors homeostasis is crucial for ARM

Dopaminergic neuron receptors are G-protein coupled receptors. D1 receptors augment the cAMP activity by activating type 1 Adenylyl cyclase (AC1s), whereas D2 receptors inhibit type 1 adenylyl cyclase (AC1s) by halting the production of cAMP which further activates PKA (Neve et al., 2004; Bonci and Hopf, 2005). The recurrent activity that existed between

the KC-DANs-MBON synapses are kept in the state of homeostasis by the equilibration of the D1 and D2 receptor. D2R inhibits neural circuits activity in order to maintain a state of equilibration (Figure 25B). The knockdown of D2R in the Drosophila olfactory network was shown to have an effect on consolidated ARM (Scholz-Kornehl et al.,2016). Here, the knockdown of D2R in the α/β and γ Kenyon cells of the mushroom body lobes had an effect on ARM. Thus, further show the necessity of having equilibration between the D1 and D2 receptors between the KC-MBONs.

Moreover, it is possible that the disturbance of the homeostasis between the D1 and D2 receptors would have an impact on ARM in the KC-MBONs synapses (Figure 25C). This may be attributed to the hyperexcitability of the KC-MBONs synapses due to the elevation of cAMP signal which then instigate the release of subsequent signaling molecules. This would occur when there is no inhibition from D2R.
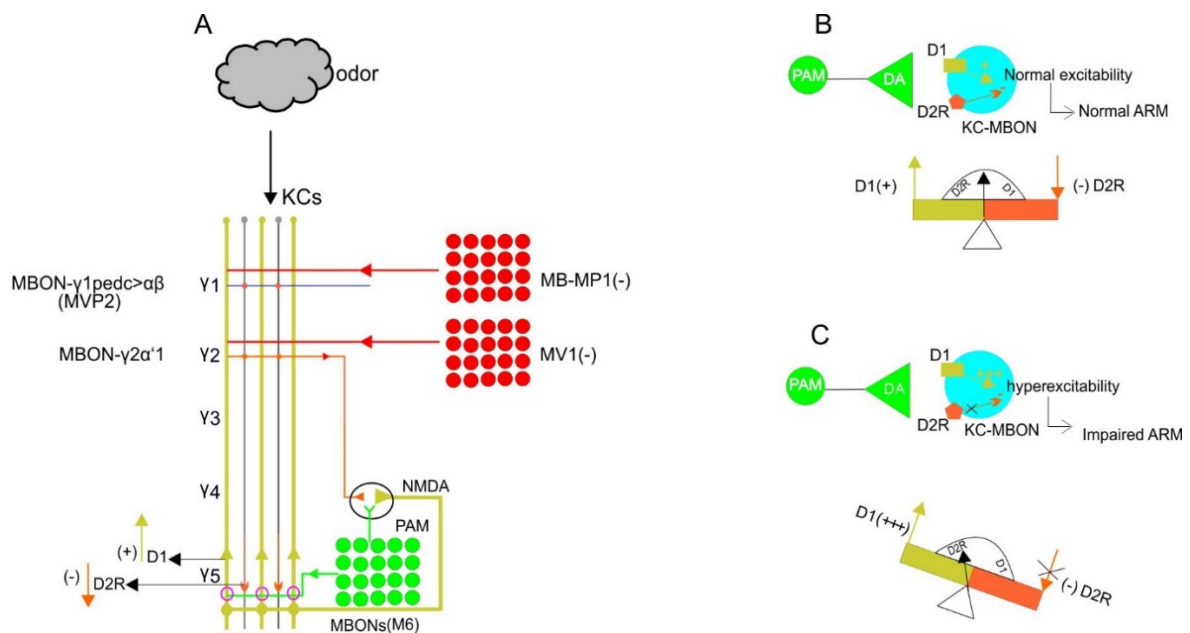

Figure 25. Schematic representation of ARM neural network circuit. (A) Aversive reinforcement is provided by the MP1 and MV1 neuron. The pairing of the odor and the electric shock render the Kenyon cells and the MVP2 sypnases to be depressed. The depression of these synapses further removes the inhibition of the glutamatergic MBON (M6). This then enhances the response of the glutamatergic MBON to the CS+. The enhanced activity in this MBON is enabled by the concurrent activity within the PAM neuron through the D1 receptor. Thus, creates specificity within the M6 neuron. However, in the non-reinforced odors i.e. CS- are represented by different set of KCs and may react through separate dopaminergic receptor i.e. D2R. D2R abates the cAMP activity in order to establish homeostatis. The US signal provided in this recurrent loop depends on the concurrent activity of glutamatergic MBONs that stimulate glutamate coupled with depolarization of the the PAM neurons. (B) D2R inhibits neuronal excitability in the normal state. Henceforth the neural circuits that associate CS+ with US maintain a normal excitability. (C) Here, knockdown of D2R in KC-MBONs synapses further release this inhibition of the D1 receptor activity and further augments cAMP signaling activity that further activates subsequent signaling cascades. This was evident for ARM (Scholz-Kornehl et al., 2016), and may play role in this ARM neural circuit.

Chapter Five

5   Summary and Outlook

Brp which forms part of the CAZ functions in the release of neurotransmitters by establishing a close proximity of Ca^{2+} ion channels with synaptic vesicles and formation of T bars. Reducing Brp levels specifically in KCs via genetically targeted RNA-interference [RNAi; (Wagh et al., 2006) impairs the formation of aversive ARM (Knapek et al., 2011). Furthermore, Histone Deacetylase 6, which influences transmitter release from neuromuscular AZs by shaping the spatial arrangement of Brp also participates in ARM (Perry et al., 2017). This thesis however, performed circuit analysis of brp effect on ARM. Brp effect on Drosophila olfactory aversive ARM learning showed a broader effect than reported earlier on in a separate study (Knapek et al., 2011). Brp effect on the KC-DANs-MBONs synapses showed a recurrent loop activity that existed in the circuits. The recurrent activity in the loop required a concurrent activation of the glutamatergic MBONs and depolarization of the dopaminergic neuron in order to gate the activity of the presynaptic plasticity.

Lastly, the presynaptic activity may involve two dopaminergic receptors i.e. D1 and D2. Equilibration between D1R and D2R are very pivotal in formation of ARM. The thesis laid down the foundation of possible mechanism of ARM. Henceforth, thorough research on the specificity of the Kenyon cells and MBONs synapses coupled with cross-talk between DANs-MBONs connections need to be addressed in relation to their memory valence.

6 Zusammenfassung

Brp, ein Teil der CAZ-Funktion, ist mitverantwortlich für die Freisetzung von Neurotransmittern, indem es eine enge Verbindung mit den Ca^{2+} Ionenkanälen herstellt und zusammen mit synaptischen Vesikeln T-Stäbe erzeugt. Die Reduzierung des Brp-Levels, insbesondere durch genetisch gezielte RNA-Überlagerungen [RNAi; (Wagh et al., 2006), beeinträchtigt die Bildung von aversivem ARM (Knapek et al., 2011). Darüber hinaus beteiligt sich auch Histone Deacetylase 6 am ARM Prozess. Histone Deacetylase 6 verursacht die Freisetzung der Transmitter vom neuromuskulären AZs, indem es die räumliche Anordnung anpasst (Perry et al., 2017).

Im Gegensatz dazu konzentriert sich diese wissenschaftliche Arbeit auf die Schaltkreisanalyse des Brp-Effekt auf das ARM. Der Brp-Effekt auf das olfaktorische aversive ARM-Lernen von Drosophila zeigte eine weitaus größere Wirkung als es zuvor in anderen Studien berichtet wurde (Knapek et al., 2011). Tatsächlich demonstrierte der Brp-Effekt auf die KC-DANs-MBONs eine wiederkehrende Schleifenaktivität innerhalb des Schaltkreises. Dieser wiederkehrende Prozess innerhalb der Schleife erfordert eine gleichzeitige Aktivierung der glutamatergen MBONs und Depolarisation des dopaminergen Neurons, um die Tätigkeiten der präsynaptischen Plastizität zu steuern.

Insgesamt kann die präsynaptische Aktivität zwei dopaminerge Rezeptoren umfassen: D1 und D2. Das Gleichgewicht zwischen D1R und D2R sind entscheidend für die Bildung von ARM. Diese Doktorarbeit legt den Grundstein für einen möglichen Mechanismus des ARM. Zukünftig sollte eine gründlichere Untersuchung der Kenyon-Zellen und MBONs-Synapsen genauso wie den Wechselwirkungen zwischen den DANs und MBONs-Verbindungen im Hinblick auf ihre Gedächtnisvalenz vorgenommen werden.

Chapter Six

7 References

1. **Adesnik H, Li G, During MJ, Pleasure SJ, Nicoll RA**. **(2008):** NMDA receptors inhibit synapse unsilencing during brain development. Proc Natl Acad Sci USA. 2008; 105:5597–5602.

2. **Andreas S. Thum, Arnim Jenett, Kei Ito, Martin Heisenberg, and Hiromu Tanimoto (2007):** Multiple Memory Traces for Olfactory Reward Learning in *Drosophila*. J. Neurosci., October 10, 2007 • 27(41):11132–11138 • 11133

3. **Aravamudan, B., T. Fergestad, W.S. Davis, C.K. Rodesch, and K. Broadie**. **(1999):** *Drosophila* UNC-13 is essential for synaptic transmission. *Nat. Neurosci.* 2:965–971.

4. **Aso, Y., Hattori, D., Yu, Y., Johnston, R. M., Iyer, N. a, Ngo, T.-T., ... Rubin, G. M. (2014):** The neuronal architecture of the mushroom body provides a logic for associative learning. *eLife*, *3*, 1–47.

5. **Aso, Y., Herb, A., Ogueta, M., Siwanowicz, I., Templier, T., Friedrich, A. B., ... Tanimoto, H. (2012):** Three Dopamine Pathways Induce Aversive Odor Memories with Different Stability. *PLoS Genetics*, *8*(7), e1002768.

6. **Aso, Y., Sitaraman, D., Ichinose, T., Kaun, K. R., Vogt, K., Belliart-Guérin, G., ... Rubin, G. M.** (2014): Mushroom body output neurons encode valence and guide memory- based action selection in Drosophila. *eLife*, *3*(3), e04580.

7. **Aso, Y., Siwanowicz, I., Bräcker, L., Ito, K., Kitamoto, T., & Tanimoto, H**. (2010): Specific Dopaminergic Neurons for the Formation of Labile Aversive Memory. *Current Biology*, *20*(16), 1445–1451.

8. **Beck, C.D., Schroeder, B., and Davis, R.L**. **(2000):** Learning performance of normal and mutant Drosophila after repeated conditioning trials with discrete stimuli. J Neurosci *20*, 2944-2953.

9. **Bellinger FP, Wilce PA, Bedi KS, Wilson P**. (2002): Long-lasting synaptic modification in the rat hippocampus resulting from NMDA receptor blockade during development. Synapse. 2002; 43:95–101

10. **Benton R, Vannice KS, Gomez-Diaz C, Vosshall LB. (2009):** Variant ionotropic glutamate receptors as chemosensory receptors in Drosophila. Cell. 2009;136:149–162.

11. **Benton R., Sachse S., Michnick S.W., Vosshall L.B. (2006):** Atypical membrane topology and heteromeric function of Drosophila odorant receptors in vivo. PLoS Biol. 2006;4:e20.

12. **Bernstein E, Caudy AA, Hammond SM, Hannon GJ. (2001):** Role for a bidentate ribonuclease in the initiation step of RNA interference. Nature. 2001; 409:363–366.

13. **Bhandawat, V., Olsen, S. R., Gouwens, N. W., Schlief, M. L., & Wilson, R. I. (2007):** Sensory processing in the Drosophila antennal lobe increases reliability and separability of ensemble odor representations. *Nature Neuroscience*, *10*(11), 1474– 1482.

14. **Blum AL, Li W, Cressy M, Dubnau J (2009):** Short- and long-term memory in *Drosophila* require cAMP signaling in distinct neuron types. Curr Biol 19: 1341–1350

15. **Böhme, M.A., C. Beis, S. Reddy-Alla, E. Reynolds, M.M. Mampell, A.T. Grasskamp, J. Lützkendorf, D.D. Bergeron, J.H. Driller, H. Babikir, (et al. 2016):** Active zone scaffolds differentially accumulate Unc13 isoforms to tune Ca^{2+} channel-vesicle coupling. *Nat. Neurosci.* 19:1311– 1320.

16. **Bouzaiane E., Trannoy S., Scheunemann L., Plaçais P.Y., Preat T. (2015):** Two independent mushroom body output circuits retrieve the six discrete components of Drosophila aversive memory. Cell Rep. 2015;11:1280–1292.

17. **Boto, T., Louis, T., Jindachomthong, K., Jalink, K., Tomchik, S.M. (2014):** Dopaminergic Modulation of cAMP Drives Nonlinear Plasticity across the Drosophila Mushroom Body Lobes. Curr. Biol. 24(8): 822--831.

18. **Boynton, S., Tully, T. (1992):** latheo, a new gene involved in associative learning and memory in Drosophila melanogaster, identified from P-element mutagenesis. *Genetics* **131**: 655--672.

19. **Burke, C.J., Huetteroth, W., Owald, D., Perisse, E., Krashes, M.J., Das, G., Gohl, D., Silies, M., Certel, S., and Waddell, S. (2012):** Layered reward signalling through octopamine and dopamine in Drosophila. *Nature.* 2012; 492: 433–437

20. **Bruckner, J.J., S.J. Gratz, J.K. Slind, R.R. Geske, A.M. Cummings, S.E. Galindo, L.K. Donohue, and K.M. O'Connor-Giles. (2012):** Fife, a *Drosophila* Piccolo-RIM homolog, promotes active zone organization and neurotransmitter release. *J. Neurosci.* 32:17048–17058. http://dx.doi .org/10.1523/JNEUROSCI.3267-12.2012

21. **Cerutti, H. (2003):** RNA interference: traveling in the cell and gaining functions? Trends Genet *19*, 39-46.

22. **Cervantes-Sandoval I, Martin-Pena A, Berry JA, Davis RL (2013):** System-like consolidation of olfactory memories in *Drosophila*. J Neurosci 33: 9846–9854

23. **Cheng, Y., Endo, K., Wu, K.H., Davis, R. (2001):** Fasciclin II is required for the formation of odor memories. *Bellen, Taylor, 2001* : 98.

24. **Chou, Y.H., Spletter, M.L., Yaksi, E., Leong, J.C.S., Wilson, R.I., Luo, L.Q., (2010):** Diversity and wiring variability of olfactory local interneurons in the Drosophila antennal lobe. Nat. Neurosci. 13, 439–449.

25. **Christiansen F, Zube C, Andlauer TFM, Wichmann C, Fouquet W, Owald D, Mertel S, Leiss F, Tavosanis G, Farca Luna AJ, Luna AJ. (2011):** Presynapses in Kenyon cell Dendrites in the mushroom body calyx of Drosophila. The Journal of Neuroscience 31:9696–9707. doi: 10.1523/JNEUROSCI.6542-10.2011.

26. **Claridge-Chang, A., Roorda, R. D., Vrontou, E., Sjulson, L., Li, H., Hirsh, J., & Miesenböck, G. (2009):** Writing Memories with Light-Addressable Reinforcement Circuitry. *Cell*, *139*(2), 405–415.

27. **Clyne P.J., Warr C.G., Freeman M.R., Lessing D., Kim J., Carlson J.R. (1999):** A novel family of divergent seven-transmembrane proteins: Candidate odorant receptors in Drosophila. Neuron. 1999;22:327–38.

28. **Cohn, R., Morantte, I., & Ruta, V. (2015):** Coordinated and Compartmentalized Neuromodulation Shapes Sensory Processing in Drosophila. *Cell*, *163*(7), 1742– 1755.

29. **Connolly, J.B., Roberts, I.J., Armstrong, J.D., Kaiser, K., Forte, M., Tully, T., O'Kane, C.J. (1996):** Associative learning disrupted by impaired Gs signaling in Drosophila mushroom bodies. Science 274(5295): 2104--2107.

30. **Couto A., Alenius M., Dickson B.J. (2005):** Molecular, anatomical, and functional organization of the Drosophila olfactory system. Curr Biol. 2005;15:1535–47

31. **Crittenden JR, Skoulakis EM, Han KA, Kalderon D, Davis RL (1998):** Tripartite mushroom body architecture revealed by antigenic markers. Learn Mem 5: 38–51

32. **Das, A., Sen, S., Lichtneckert, R., Okada, R., Ito, K., Rodrigues, V., Reichert, H. (2008):** Drosophila olfactory local interneurons and projection neurons derive from a common neuroblast lineage specified by the empty spiracles gene. Neural Dev. 3(): 33.

33. **Davis, R.L. (2005):** Olfactory memory formation in Drosophila: from molecular to systems neuroscience. Annu Rev Neurosci *28*, 275-302.

34. **Davis, R.L., Cherry, J., Dauwalder, B., Han, P.L., and Skoulakis, E. (1995):** The cyclic AMP system and Drosophila learning. Mol Cell Biochem *149-150*, 271-278.

35. **Dubnau J, Grady L, Kitamoto T, Tully T (2001):** Disruption of neurotransmission in *Drosophila* mushroom body blocks retrieval but not acquisition of memory. Nature 411: 476–480.

36. **Dudai, Y., Corfas, G., and Hazvi, S. (1988):** What is the possible contribution of Ca2+-stimulated adenylate cyclase to acquisition, consolidation and retention of an associative olfactory memory in Drosophila. J Comp Physiol A *162*, 101-109

37. **Dudai, Y., Jan, Y. N., Byers, D., Quinn, W. G., & Benzer, S. (1976):** Dunce, a mutant of Drosophila deficient in learning. *Proceedings of the National Academy of Sciences of the United States of America*, *73*(5), 1684–8.

38. **Dura, J.M., Preat, T., Tully, T. (1993):** Identification of linotte, a new gene affecting learning and memory in Drosophila melanogaster. J. Neurogenet. 9(1): 1--14.

39. **Enerly, E., Larsson, J., and Lambertsson, A. (2003):.** Silencing the Drosophila ribosomal protein L14 gene using targeted RNA interference causes distinct somatic anomalies. Gene *320*, 41-48.

40. **Feany, M.B., and Quinn, W.G. (1995):** A neuropeptide gene defined by the Drosophila memory mutant amnesiac. Science *268*, 869-873.

41. **Folkers, E., Drain, P., and Quinn, W.G. (1993):** Radish, a Drosophila mutant deficient in consolidated memory. Proc Natl Acad Sci U S A *90*, 8123-8127.

42. **Folkers, E., Waddell, S., and Quinn, W.G. (2006):** The Drosophila radish gene encodes a protein required for anesthesia-resistant memory. Proc Natl Acad Sci U S A *103*, 17496-17500.

43. **Folkers E, Drain P, Quinn WG (1993):** Radish, a *Drosophila* mutant deficient in consolidated memory. Proc Natl Acad Sci 90: 8123–8127

44. **Fouquet, W., Owald, D., Wichmann, C., Mertel, S., Depner, H., Dyba, M., Hallermann, S., Kittel, R.J., Eimer, S., and Sigrist, S.J. (2009):** Maturation of active zone assembly by Drosophila Bruchpilot. J Cell Biol *186*, 129-145.

45. **Fulterer A, Andlauer TFM, Ender A, Maglione M, Eyring K, Woitkuhn J, Lehmann M, Matkovic-Rachid T, Geiger JRP, Walter AM, Nagel KI, Sigrist SJ. (2018):** Cell Rep. 2018 May 1;23(5):1259-1274. doi: 10.1016/j.celrep.2018.03.126.

46. **G. Laurent (2002):** Olfactory network dynamics and the coding of multidimensional signals Nat. Rev. Neurosci., 3 (2002), pp. 884-895

47. **Gao Q., Chess A. (1999):** Identification of candidate Drosophila olfactory receptors from genomic DNA sequence. Genomics. 1999;60:31–39.

48. **Gervasi N, Tchénio P, Preat T. (2010):** PKA dynamics in a *Drosophila* learning center: coincidence detection by rutabaga adenylyl cyclase and spatial regulation by dunce phosphodiesterase. Neuron. 2010; 65:516–529

49. **Giordano, E., Rendina, R., Peluso, I., and Furia, M. (2002):** RNAi triggered by symmetrically transcribed transgenes in Drosophila melanogaster. Genetics *160*, 637-648.

50. **Graf, E.R., V. Valakh, C.M. Wright, C. Wu, Z. Liu, Y.Q. Zhang, and A. DiAntonio. (2012):** RIM promotes calcium channel accumulation at active zones of the *Drosophila* neuromuscular junction. *J. Neurosci.* 32:16586–16596. http://dx.doi.org/10.1523/JNEUROSCI.0965-12.2012

51. **Guo, M., Jan, L.Y., Jan, Y.N. (1996):** Control of daughter cell fates during asymmetric division: Interaction of numb and Notch. Neuron 17(1): 27--41.

52. **Hallem EA, Carlson JR. (2006):** Coding of odors by a receptor repertoire. Cell. 2006;125:143–160.

53. **Hamada F.N., Rosenzweig M., Kang K., Pulver S.R., Ghezzi A., Jegla T.J., Garrity P.A. (2008):** An internal thermal sensor controlling temperature preference in Drosophila.Nature. 454:217–220

54. **Han K, Millar N, Groteweil M, Davis R. (1996):** DAMB, a novel dopamine receptor expressed specifically in *Drosophila* mushroom bodies. Neuron. 1996;16:1127–1135.

55. **Hige, T., Aso, Y., Rubin, G. M., & Turner, G. C. (2015).**:Plasticity-driven individualization of olfactory coding in mushroom body output neurons. *Nature*.

56. **Hige T., Aso Y., Modi M. N., Rubin G. M., Turner G. C. (2015):** Heterosynaptic plasticity underlies aversive olfactory learning in Drosophila. Neuron 88, 985–998. 10.1016/j.neuron.2015.11.00

57. **Hirasawa T, Wada H, Kohsaka S, Uchino S. (2003):** Inhibition of NMDA receptors induces delayed neuronal maturation and sustained proliferation of progenitor cells during neocortical development. J Neurosci Res. 2003;74:676–687.

58. **Homberg U., Müller U. (1999):** Neuroactive substances in the antennal lobe. In: Hansson B.S., editor. Insect Olfaction.Berlin: Springer; 1999. pp. 181–206.

59. **Ichinose, T., Aso, Y., Yamagata, N., Abe, A., Rubin, G. M., & Tanimoto, H. (2015):** Reward signal in a recurrent circuit drives appetitive long-term memory formation. *eLife*, *4*, 1–18.

60. **Isabel, G., Pascual, A., and Preat, T. (2004):** Exclusive consolidated memory phases in Drosophila. Science *304*, 1024-1027.

61. **Jagtap UB, Gurav RG, Bapat VA (2011)**: Role of RNA interference in plant improvement. Naturwissenschaften 98:473–492

62. **Kakidani, Hitoshi; Ptashne, Mark (1988):** "GAL4 activates gene expression in mammalian cells". *Cell*. **52** (2): 161–167. doi:10.1016/0092-8674(88)90504-1. PMID 2830021

63. **Kalidas, S., and Smith, D.P. (2002):** Novel genomic cDNA hybrids produce effective RNA interference in adult Drosophila. Neuron *33*, 177-184.

64. **Kandel ER.** The molecular biology of memory storage: a dialogue between genes and synapses. *Science (New York, N.Y.)*. 294: 1030-8 PMID 11691980 DOI: 10.1126/science.1067020

65. **Kaufmann, N., DeProto, J., Ranjan, R., Wan, H., Van Vactor, D. (2002):** Drosophila liprin-alpha and the receptor phosphatase Dlar control synapse morphogenesis. Neuron 34(1): 27--38.

66. **Kim YC, Lee HG, Han KA (2007):** D1 dopamine receptor dDA1 is required in the mushroom body neurons for aversive and appetitive learning in *Drosophila*. J Neurosci 27: 7640–7647

67. **Kitamoto, T. (2001):** Conditional modification of behavior in Drosophila by targeted expression of a temperature-sensitive *shibire* allele in defined neurons. J. Neurobiol. 47: 81-92.

68. **Knapek, S., Sigrist, S., Tanimoto, H. (2011):** Bruchpilot, a synaptic active zone protein for anesthesia-resistant memory. J. Neurosci. 31(9): 3453--3458.

69. **Knapek S, Gerber B, Tanimoto H (2010):** Synapsin is selectively required for anesthesia-sensitive memory. Learn Mem **17**:76–79.

70. **Knight S.W. and Bass, B.L. (2001):** A role for the RNase III enzyme DCR-1 in RNA interference and germ line development in *C. elegans*. Science, 293, 2269–2271

71. **Koenig, J.H., and Ikeda, K. (1996):** Synaptic vesicles have two distinct recycling pathways. J. Cell Biol. *135*, 797–808.

72. **Krashes, M.J., Keene, A.C., Leung, B., Armstrong, J.D., Waddell, S. (2007):** Sequential use of mushroom body neuron subsets during Drosophila odor memory processing. Neuron 53(1): 103--115.

73. **Larsson M.C., Domingos A.I., Jones W.D., Chiappe M.E., Amrein H., Vosshall L.B. (2004):** Or83b encodes a broadly expressed odorant receptor essential for Drosophila olfaction. Neuron. 2004;43:703–14

74. **Laurent G, Naraghi M.** Odorant-induced oscillations in the mushroom bodies of the locust. J Neurosci 1994;14:2993 – 3004.

75. **Leal WS. (2013):** Odorant reception in insects: roles of receptors, binding proteins, and degrading enzymes. Annual Review of Entomology. 2013;58:373–391. doi: 10.1146/annurev-ento-120811-153635.

76. **Lee, P.T., Lin, H.W., Chang, Y.H., Fu, T.F., Dubnau, J., Hirsh, J., Lee, T., Chiang, A.S. (2011):** Serotonin-mushroom body circuit modulating the formation of anesthesia resistant memory in Drosophila. Proc. Natl. Acad. Sci. U.S.A. 108(33): 13794--13799.

77. **Levin LR, Han P-L, Hwang PM, Feinstein PG, Davis RL, Reed RR. (1992):** The *Drosophila* learning and memory gene *rutabaga* encodes a Ca^{2+}/cadmodulin responsive adenyl cyclase. Cell. 1992; 68:479–489.

78. **Liu, K.S.Y., M. Siebert, S. Mertel, E. Knoche, S. Wegener, C. Wichmann, T. Matkovic, K. Muhammad, H. Depner, C. Mettke, (et al. 2011):** RIM-binding protein, a central part of the active zone, is essential for neurotransmitter release. *Science.* 334:1565–1569.

79. **Liu C., Plaçais P.Y., Yamagata N., Pfeiffer B.D., Aso Y., Friedrich A.B., Siwanowicz I., Rubin G.M., Preat T., Tanimoto H. (2012):** A subset of dopamine neurons signals reward for odour memory in Drosophila. Nature. 2012;488:512–516

80. **Livingstone MS, Sziber PP, Quinn WG. (1984):** Loss of calcium/calmodulin responsiveness in adenylate cyclase of *rutabaga*, a *Drosophila* learning mutant. Cell. 1984; 37:205–215.

81. **Lüthi A, Schwyzer L, Mateos JM, Gähwiler BH, McKinney RA. (2001):** NMDA receptor activation limits the number of synaptic connections during hippocampal development. Nat Neurosci. 2001;4:1102–1107.

82. **Matkovic, T., Siebert, M., Knoche, E., Depner, H., Mertel, S., Owald, D., Schmidt, M., Thomas, U., Sickmann, A., Kamin, D., Hell, S.W., Bürger, J., Hollmann, C., Mielke, T., Wichmann, C., Sigrist, S.J. (2013):** The Bruchpilot cytomatrix determines the size of the readily releasable pool of synaptic vesicles. J. Cell Biol. 202(4): 667--683.

83. **Mao, Z., Roman, G., Zong, L., Davis, R.L. (2004):** Pharmacogenetic rescue in time and space of the rutabaga memory impairment by using Gene-Switch. Proc. Natl. Acad. Sci. U.S.A. 101(1): 198--203.

84. **Mao, Z., and Davis, R.L. (2009):** Eight different types of dopaminergic neurons innervate the Drosophila mushroom body neuropil: anatomical and physiolog- ical heterogeneity. Front. Neural Circuits *3*, 5.

85. **Mayer ML, Westbrook GL, Guthrie PB. (1984):** Voltage-dependent block by Mg2+ of NMDA responses in spinal cord neurones. Nature. 1984;309:261–263.

86. **McGuire, S.E., Le, P.T., Osborn, A.J., Matsumoto, K., and Davis, R.L. (2003):** Spatiotemporal rescue of memory dysfunction in *Drosophila*. Science *302*, 1765–1768.

87. **McGuire SE, Le PT, Davis RL (2001):** The role of *Drosophila* mushroom body signaling in olfactory memory. Science 293: 1330–1333

88. **Moffat J, Reiling JH, Sabatini DM. (2007):** Off-target effects associated with long dsRNAs in Drosophila RNAi screens. Trends Pharmacol Sci. 2007;28:149–151.

89. **M.S. Grotewiel, C.D. Beck, K.H. Wu, X.R. Zhu, R.L. Davis (1998):** Integrin-mediated short-term memory in *Drosophila* Nature, 391 (1998), pp. 455-460

90. **Müller, M., K.S.Y. Liu, S.J. Sigrist, and G.W. Davis. (2012**) RIM controls homeostatic plasticity through modulation of the readily-releasable vesicle pool. *J. Neurosci.* 32:16574–16585. http://dx.doi.org/10.1523/ JNEUROSCI.0981-12.2012

91. **Neuhaus E.M., Gisselmann G., Zhang W., Dooley R., Stortkuhl K., Hatt H. (2005):** Odorant receptor heterodimerization in the olfactory system of Drosophila melanogaster. Nat Neurosci. 2005;8:15–17.

92. **Nowak L, Bregestovski P, Ascher P, Herbet A, Prochiantz A. (1984):** Magnesium gates glutamate-activated channels in mouse central neurones. Nature. 1984;307:462–465.

93. **Okada R, Awasaki T, Ito K. (2009):** g-aminobutyric acid-mediated neural connections in the *Drosophila* antennal lobe. *J Comp Neurol* 514: 74–91, 2009.

94. **Olsen, S.R., and Wilson, R.I. (2008):** Lateral presynaptic inhibition mediates gain control in an olfactory circuit. Nature *452*, 956–960.

95. **Owald D., Fouquet W., Schmidt M., Wichmann C., Mertel S., Depner H., Christiansen F., Zube C., Quentin C., Körner J. A**. **(2010):** Syd-1 homologue regulates pre- and postsynaptic maturation in Drosophila. J. Cell Biol. 2010;188:565–579

96. **Owald, D., Felsenberg, J., Talbot, C. B., Das, G., Perisse, E., Huetteroth, W., & Waddell, S. (2015b):** Activity of Defined Mushroom Body Output Neurons Underlies Learned Olfactory Behavior in Drosophila. *Neuron, 86*(2), 417–427.

97. **Owald, D., Felsenberg, J., Talbot, C. B., Das, G., Perisse, E., Huetteroth, W., & Waddell, S. (2015a):** Activity of Defined Mushroom Body Output Neurons Underlies Learned Olfactory Behavior in Drosophila. *Neuron*, 1–11.

98. **Pavlov, I.P. (1927).**:Conditioned Reflexes (London: Oxford University Press).

99. **Perez-Orive J, Mazor O, Turner GC, Cassenaer S, Wilson RI, Laurent G. (2002):** Oscillations and sparsening of odor representations in the mushroom body. *Science* 297: 359–365, 2002.

100. **Perisse, E., Owald, D., Barnstedt, O., Talbot, C. B., Huetteroth, W., and Waddell, S. (2016):** Aversive learning and appetitive motivation toggle feed-forward inhibition in the Drosophila mushroom body. *Neuron* 90, 1086–1099. doi: 10.1016/j.neuron.2016.04.034

101. **Perisse, E., Yin, Y., Lin, A., Lin, S., Huetteroth, W., & Waddell, S. (2013):** Different Kenyon Cell Populations Drive Learned Approach and Avoidance in Drosophila. *Neuron, 79*(5), 945–956.

102. **Pitman JL, Huetteroth W, Burke CJ, Krashes MJ, Lai SL, Lee T, Waddell S (2011):** A pair of inhibitory neurons are required to sustain labile memory in the *Drosophila* mushroom body. Curr Biol 21: 855–861

103. **Qin H, Cressy M, Li W, Coravos JS, Izzi SA, Dubnau J (2012):**Gamma neurons mediate dopaminergic input during aversive olfactory memory formation in *Drosophila*. Curr Biol 22: 608–614

104. **Quinn, W.G., Harris, W.A., and Benzer, S. (1974):** Conditioned behavior in Drosophila melanogaster. Proc Natl Acad Sci U S A *71*, 708-712.

105. **R.J. Kittel, C. Wichmann, T.M. Rasse, W. Fouquet, M. Schmidt, A. Schmid, D.A. Wag h, Pawlu, R.R.Kellner, K.I. Willig, (et al. 2006):** Bruchpilot promotes active zone assembly, Ca2+ channel clustering, and vesicle release. Science. 312:1051–1054

106. **R.L. Davis (1993):** Mushroom bodies and Drosophila learning Neuron, 11 (1993), pp. 1-14

107. **Riemensperger, T., Voʹller, T., Stock, P., Buchner, E., and Fiala, A. (2005):** Punishment prediction by dopaminergic neurons in Drosophila. Curr. Biol. *15*, 1953–1960.

108. **Roman, G. (2004):** The genetics of Drosophila transgenics. Bioessays *26*, 1243-1253.

109. **Sachse S, Rueckert E, Keller A, Okada R, Tanaka NK, Ito K, Vosshall LB. (2007):** Activity-dependent plasticity in an olfactory circuit. *Neuron* 56: 838 – 850, 2007.

110. **Sato K., Pellegrino M., Nakagawa T., Vosshall L.B., Touhara K. (2008):** Insect olfactory receptors are heteromeric ligand-gated ion channels. Nature. 2008;452:1002–6.

111. **Scheunemann, L., Jost, E., Richlitzki, A., Day, J.P., Sebastian, S., Thum, A.S., Efetova, M., Davies, S.A., Schwärzel, M. (2012):** Consolidated and Labile Odor Memory Are Separately Encoded within the Drosophila Brain. J. Neurosci. 32(48): 17163--17171.

112. **Scholz-Kornehl S, Schwärzel M (2016):** Circuit analysis of a *Drosophila* dopamine type 2 receptor that supports anesthesia-resistant memory. J Neurosci **36**:7936– 7945. doi:10.1523/JNEUROSCI.4475-15.2016pmid:27466338

113. **Schroll, C., Riemensperger, T., Bucher, D., Ehmer, J., Völler, T., Erbguth, K., ... Fiala, A. (2006):** Light-Induced Activation of Distinct Modulatory Neurons Triggers Appetitive or Aversive Learning in Drosophila Larvae. *Current Biology*, *16*(17), 1741–1747.

114. **Schwaerzel M, Heisenberg M, Zars T (2002)**: Extinction antagonizes olfactory memory at the subcellular level. Neuron **35**:951–960.

115. **Schwaerzel M, Jaeckel A, Mueller U (2007):** Signaling at A-kinase anchoring proteins organizes anesthesia-sensitive memory in *Drosophila*. J Neurosci 27: 1229–1233

116. **Schwaerzel, M., Monastirioti, M., Scholz, H., Friggi-Grelin, F., Birman, S., & Heisenberg, M. (2003):** Dopamine and octopamine differentiate between aversive and appetitive olfactory memories in Drosophila. *The Journal of neuroscience : the official journal of the Society for Neuroscience*, *23*(33), 10495–502.

117. **Silbering, A. F., and Benton, R. (2010):** Ionotropic and metabotropic mechanisms in chemoreception: 'chance or design'? *EMBO Rep.* 11, 173–179. doi: 10.1038/embor.2010.8

118. **Silbering, a. F., & Galizia, C. G. (2007):** Processing of Odor Mixtures in the Drosophila Antennal Lobe Reveals both Global Inhibition and Glomerulus-Specific Interactions. *Journal of Neuroscience*, *27*(44), 11966–11977.

119. **Silbering, A.F., Galizia, C.G., (2007):** Processing of odor mixtures in the Drosophila antennal lobe reveals both global inhibition and glomerulus-specific interac- tions. J. Neurosci. 27, 11966–11977.

120. **Single FN, Rozov A, Burnashev N, Zimmermann F, Hanley DF, Forrest D, Curran T, Jensen V, Hvalby O, Sprengel R, Seeburg PH. (2000):** Dysfunctions in mice by NMDA receptor point mutations NR1(N598Q) and NR1(N598R) J Neurosci. 2000;20:2558–2566.

121. **Skoulakis E, Kalderon D, Davis R. (1993):** Preferential expression in mushroom bodies of the catalytic subunit of protein kinase A and its role in learning and memory. Neuron. 1993; 11:197–208.

122. **Skoulakis, E.M., Davis, R.L. (1996).:**Olfactory learning deficits in mutants for leonardo, a Drosophila gene encoding a 14-3-3 protein. Neuron 17(5): 931--944.

123. **Stocker, R. F., Heimbeck, G., Gendre, N., & de Belle, J. S. (1997):** Neuroblast ablation in Drosophila P[GAL4] lines reveals origins of olfactory interneurons. *Journal of Neurobiology*, *32*(5), 443–56.

124. **Stopfer, M., Bhagavan, S., Smith, B.H., Laurent, G., (1997):** Impaired odour discrimi- nation on desynchronization of odour-encoding neural assemblies. Nature 390, 70–74.

125. **Tamura, T., Horiuchi, D., Chen, Y.C., Sone, M., Miyashita, T., Saitoe, M., Yoshimura, N., Chiang, A.S., Okazawa, H. (2010):** Drosophila PQBP1 regulates learning acquisition at projection neurons in aversive olfactory conditioning. J. Neurosci. 30(42): 14091--14101.

126. **Tanaka, N. K., Tanimoto, H., & Ito, K. (2008):** Neuronal assemblies of the Drosophila mushroom body. *The Journal of comparative neurology*, *508*(5), 711–55.

127. **Tanaka NK, Ito K, Stopfer M. (2009):** Odor-evoked neural oscillations in *Drosophila* are mediated by widely branching interneurons. *J Neurosci* 29: 8595–8603, 2009.

128. **Tanaka, N.K., Awasaki, T., Shimada, T., Ito, K. (2004):** Integration of chemosensory pathways in the Drosophila second-order olfactory centers. Curr. Biol. 14(6): 449--457.

129. **Tanaka, N.K., Tanimoto, H., Ito, K. (2008):** Neuronal assemblies of the Drosophila mushroom body. J. Comp. Neurol. 508(5): 711--755.

130. **Tanaka, N. K., Ito, K., & Stopfer, M. (2009):** Odor-Evoked Neural Oscillations in Drosophila Are Mediated by Widely Branching Interneurons. *Journal of Neuroscience*, *29*(26), 8595–8603.

131. **Technau G, Heisenberg M (1982):** Neural reorganization during metamorphosis of the corpora pedunculata in *Drosophila melanogaster*. Nature 295: 405–407

132. **Tempel B, Livingstone M, Quinn W. (1984):** Mutations in the dopa decarboxylase gene affect learning in *Drosophila.* Proc Natl Acad Sci. 1984;81:3577–3581.

133. **Tian L, Stefanidakis M, Ning L, Van Lint P, Nyman-Huttunen H, Libert C, Itohara S, Mishina M, Rauvala H, Gahmberg CG (2007):** Activation of NMDA receptors promotes dendritic spine development through MMP-mediated ICAM-5 cleavage. J Cell Biol. 2007;178:687–700.

134. **Till F M Andlauer, Stephan J. Sigrist (2012):** In vivo imaging of Drosophila larval neuromuscular junctions to study synapse assembly cold spring harbor protocols

135. **Tomchik, S. M. (2013):** Dopaminergic neurons encode a distributed, asymmetric representation of temperature in Drosophila. *The Journal of neuroscience : the official journal of the Society for Neuroscience*, *33*(5), 2166–76a.

136. **Tomchik SM, Davis RL (2009)**: Dynamics of learning-related cAMP signaling and stimulus integration in the *Drosophila* olfactory pathway. Neuron **64**:510–521.

137. **Touhara K, Vosshall LB. (2009):** Sensing odorants and pheromones with chemosensory receptors. Annu Rev Physiol. 2009;71:307–332.

138. **Tully, T., and Quinn, W.G. (1985):** Classical conditioning and retention in normal and mutant Drosophila melanogaster. J Comp Physiol A *157*, 263-277.

139. **Vosshall L.B., Amrein H., Morozov P.S., Rzhetsky A., Axel R. (1999):** A spatial map of olfactory receptor expression in the Drosophila antenna. Cell. 1999;96:725–36

140. **Vosshall, L.B., Wong, A.M., Axel, R. (2000):** An olfactory sensory map in the fly brain. Cell 102(2): 147--159.

141. **Waddell S, Armstrong JD, Kitamoto T, Kaiser K, Quinn WG (2000):** The amnesiac gene product is expressed in two neurons in the *Drosophila* brain that are critical for memory. Cell 103: 805–813

142. **Waddell S. (2013):** Reinforcement signalling in Drosophila; dopamine does it all after all. Curr. Opin. Neurobiol. 2013;23:324–329

143. **Wagh, D.A., T.M. Rasse, E. Asan, A. Hofbauer, I. Schwenkert, H. Dürrbeck, S. Buchner, M.-C. Dabauvalle, M. Schmidt, G. Qin, (et al. 2006.**): Bruchpilot, a protein with homology to ELKS/CAST, is required for structural integrity and function of synaptic active zones in *Drosophila. Neuron.* 49:833–844.

144. **Wehr M., Laurent G. (1996):** Odour encoding by temporal sequences of firing in oscillating neural assemblies. Nature 384, 162–166 10.1038/384162a0

145. **Wicher D., Schafer R., Bauernfeind R., Stensmyr M.C., Heller R., (et al. 2008):** Drosophila odorant receptors are both ligand-gated and cyclic-nucleotide-activated cation channels. Nature. 2008;452:1007–11.

146. **Widmann A, Artinger M, Biesinger L, Boepple K, Peters C, Schlechter J, Selcho M, Thum AS. (2016):** Genetic Dissection of Aversive Associative Olfactory Learning and Memory in Drosophila Larvae. PLOS Genetics 12: e1006378. DOI: https://doi.org/10.1371/journal.pgen.1006378, PMID: 27768692

147. **Wu CL, Shih MF, Lee PT, Chiang AS (2013):** An octopamine-mushroom body circuit modulates the formation of anesthesia-resistant memory in *Drosophila*. Curr Biol 23: 2346–2354

148. **Wu CL, Shih MF, Lai JS, Yang HT, Turner GC, Chen L, Chiang AS (2011):** Heterotypic gap junctions between two neurons in the *Drosophila* brain are critical for memory. Curr Biol 21: 848–854

149. **Wu CL, Xia S, Fu TF, Wang H, Chen YH, Leong D, Chiang AS, Tully T. (2007):** Specific requirement of NMDA receptors for long-term memory consolidation in Drosophila ellipsoid body. Nat Neurosci. 2007;10:1578–1586.

150. **W.W. Liu, R.I. Wilson (2013):** Glutamate is an inhibitory neurotransmitter in the Drosophila olfactory system Proc. Natl. Acad. Sci. USA, 110 (2013), pp. 10294-10299

151. **Xia S, Miyashita T, Fu TF, Lin WY, Wu CL, Pyzocha L, Lin IR, Saitoe M, Tully T, Chiang AS. (2005):** NMDA receptors mediate olfactory learning and memory in Drosophila. Curr Biol. 2005;15:603–615.

152. **Xiaoliang Zhao, Daniela Lenek, Ugur Dag, Barry J Dickson Krystyna Keleman (2018):** Persistent activity in a recurrent circuit underlies courtship memory in *Drosophil* eLife. 2018; 7: e31425.

153. **Xie Z, Huang C, Ci B, Wang L, Zhong Y (2013):** Requirement of the combination of mushroom body gamma lobe and α/β lobes for the retrieval of both aversive and appetitive early memories in *Drosophila*. Learn Mem 20: 474–481

154. **Yamagata, N., Ichinose, T., Aso, Y., Placais, P. Y., Friedrich, A. B., Sima, R. J., et al. (2015):** Distinct dopamine neurons mediate reward signals for short- and long-term memories. *Proc. Natl. Acad. Sci. U.S.A.* 112, 578–583. doi: 10.1073/pnas.1421930112

155. **Yu, J., Fleming, S.L., Williams, B., Williams, E.V., Li, Z., Somma, P., Rieder, C.L., Goldberg, M.L. (2004):** Greatwall kinase: a nuclear protein required for proper chromosome condensation and mitotic progression in Drosophila. J. Cell Biol. 164(4): 487--492.

156. **Zars, T., Fischer, M., Schulz, R., and Heisenberg, M. (2000):** Localization of a short-term memory in *Drosophila*. Science *288*, 672–675.

157. **Zhai, R.G., and H.J. Bellen. (2004):** The architecture of the active zone in the presynaptic nerve terminal. *Physiology (Bethesda).* 19:262–270. http://dx .doi.org/10.1152/physiol.00014.2004

158. **Zhang S, Roman G (2013):** Presynaptic inhibition of gamma lobe neurons is required for olfactory learning in *Drosophila*. Curr Biol 23: 2519–2527

7.1 Curriculum Vitae

7.2 List of Publications

1. **ChristianKönig, EmmanuelAntwi-Adjei, MathangiGanesan, Kasyoka Kilonzo, Vignesh Viswanathan, Archana Durairaja, Anne Voigt, Ayse Yarali**. (2017) Aversive olfactory associative memory loses odor specificity over time. Journal of Experimental Biology 2017 220: 1548-1553; doi: 10.1242/jeb.155317.

2. **VarunK.Gupta, UlrikePech, AnuradhaBhukel, AndreasFulterer, Anatoli Ender, StephanF.Mauermann,TillF.M.Andlauer EmmanuelAntwi-Adjei, ChristineBeuschel, KerstinThriene, MartaMaglioneQuentin René Bushow, Martin Schwärzel, ThorstenMielke, Frank Madeo, Joern Dengjel,Andre Fiala , and Stephan J. Sigrist** .2016 Spermidine Suppresses Age-Associated Memory Impairment by Preventing Adverse Increase of Presynaptic Active Zone Size and Release. PLoS Biol. 2016 Sep; 14(9): e1002563. doi: 10.1371/journal.pbio.1002563

3. **Appel M, Scholz CJ, Müller T, Dittrich M, König C, Bockstaller M, Oguz T, Khalili A, Antwi-Adjei E, Schauer T, Margulies C, Tanimoto H, Yarali** A. Genome-Wide Association Analyses Point to Candidate Genes for Electric Shock Avoidance in Drosophila melanogaster. *PLoS One. 2015 May 18;10(5)*:e0126986.

8 Appendix
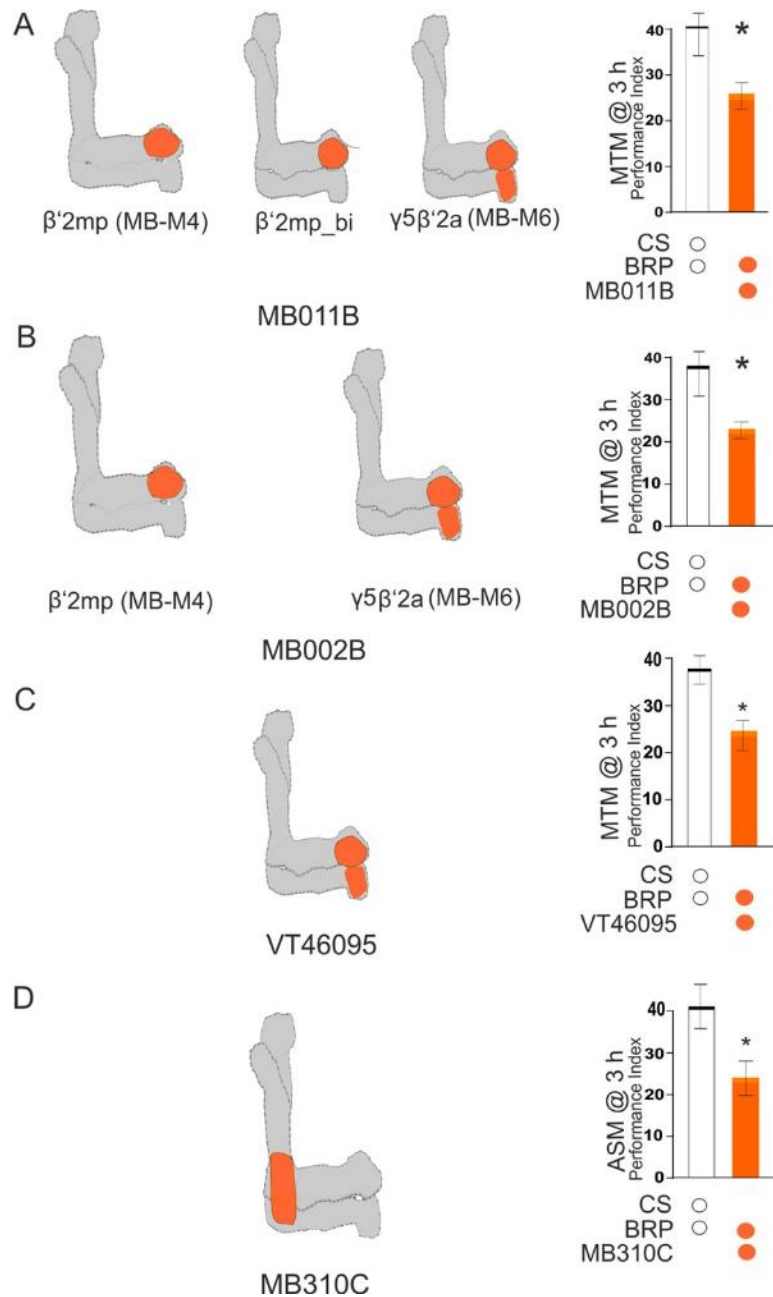
8.1 Supplementary Data
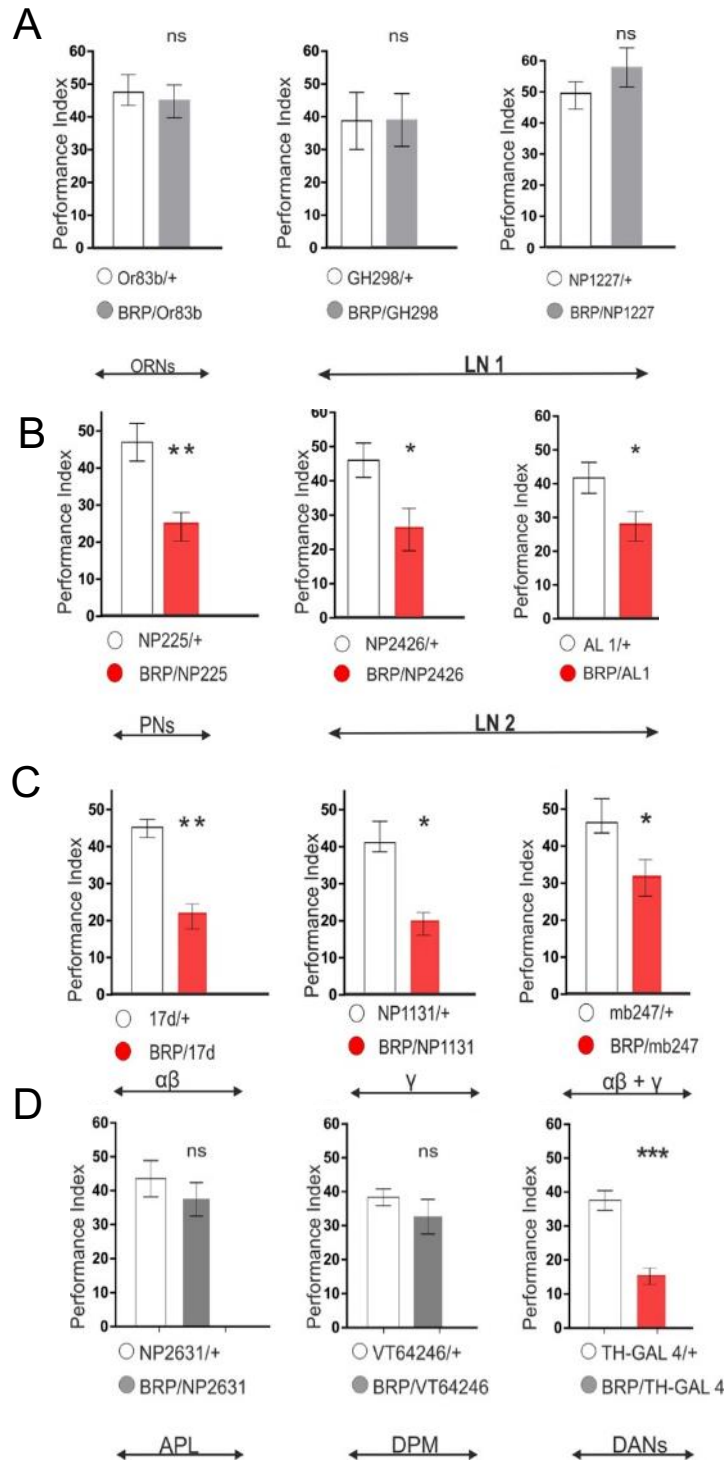
Supplementary figure 1. Brp knockdown effects on MTM. The figure above shows the effect on the *brp* knockdown on MTM after aversive olfactory memory as explained in the material and methods section. (A) *brp* knockdown in ORNs (or83b^{GAL4}), LN1s (GH298^{GAL4} and NP1227^{GAL4}). MTM for or83b^{GAL4}: *test; t$_{(9)}$, t =0.4143 p = 0.3442. MTM for GH298^{GAL4}: t$_{(11)}$, t =0.01104 p = 0.9914. MTM for NP1227^{GAL4}: t $_{(12)}$, t=1.064 p = 0.3082.*

The results here display that these neural circuits in the *Drosophila* olfactory circuit pose no effect on aversive 3 h MTM. (B) The driver lines used here were NP225^{GAL4} (PNs), and NP2426^{GAL4} (LN2) and AL 1^{GAL4}(LN2). NP225^{GAL4} MTM: $t_{(12)}, t = 4.998\ p<0.05$. NP2426^{GAL4} (LN2) MTM: $t_{(12)}, t = 2.415\ p<0.05$. AL 1^{GAL4}(LN2): $t_{(13)}, t = 2.928\ p<0.05$, *brp* knockdown in LN2s and PNs proved pivotal in the formation of MTM. (C) *brp* knockdown in the mushroom body Kenyon cells proved to be important in the formation of ARM memory in a previous experiment (Knapek et al. 2011). However, in the case of MTM, (α/β) 17d^{GAL4}: *test: $t_{(9)}, t = 4.213\ p<0.05$*. Also, in the case of NP1131^{GAL4} MTM: *test: $t_{(10)}, t = 3.326\ p<0.05$* , and in the scenario of mb247^{GAL4}: *test: $t_{(11)}, t = 2.719\ p<0.05$*. This reaffirms the effect that was seen in the Knapek et al. (2011) publication. (D) Conversely, a different outcome was observed in APL, DPM. There was no effect on Middle term memory in these driver lines for APL (NP2631^{GAL4}, MTM: *$t_{(13)}, t = 0.8274\ \ p = 0.4229$;* VT64246^{GAL4} MTM: *test: $t_{(11)}, t = 1.069\ p =0.3081$* and in the case of *Th-GAL4,* MTM effect was observed. This then signifies the involvement of the US pathway; MTM *test: $t_{(15)}, t = 3.767\ p <0.05$*. Error bars indicate mean ± SEM of 7-10 biological repetitions (i.e., *N* = 7-10). **Statistical differences; ($p ≤ 0.05$), ns = Not significant.
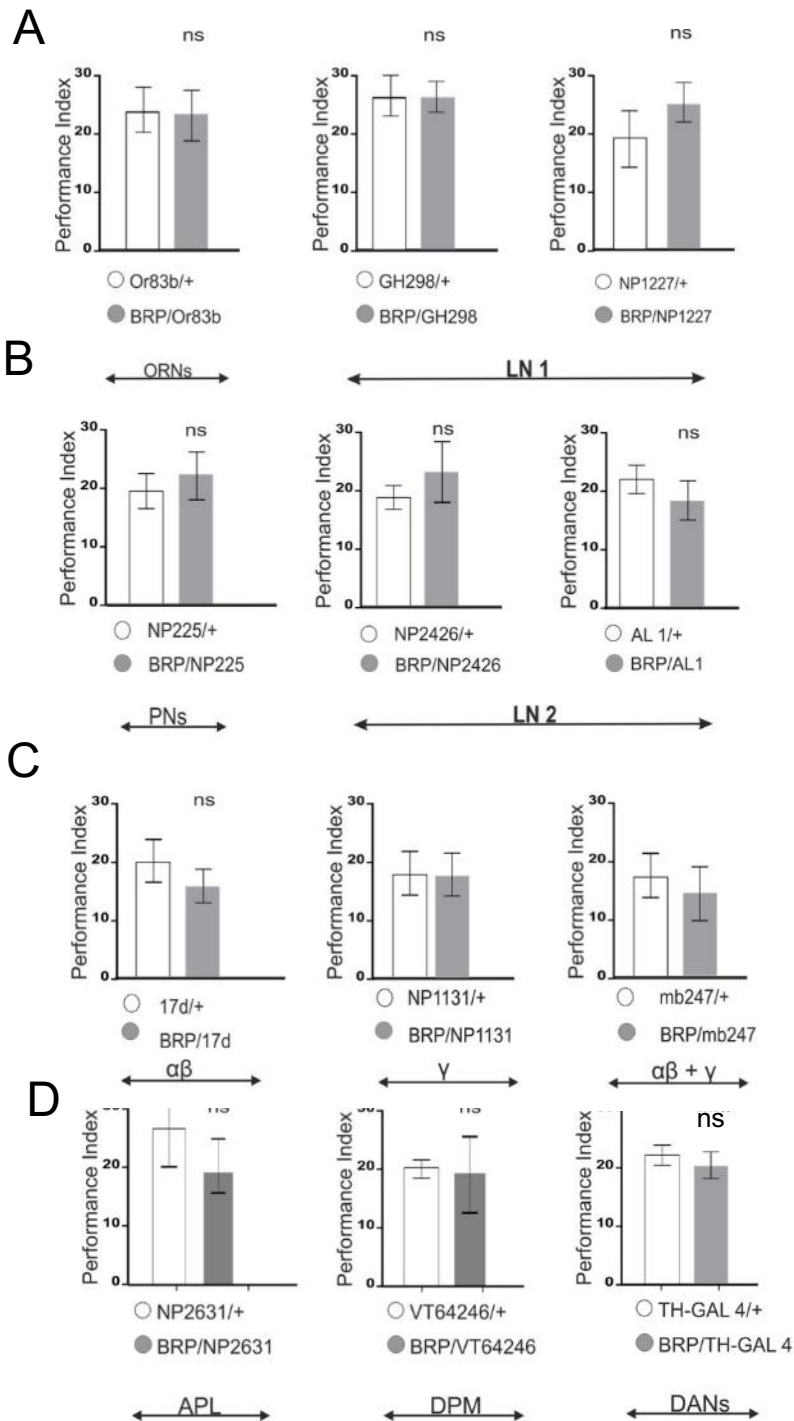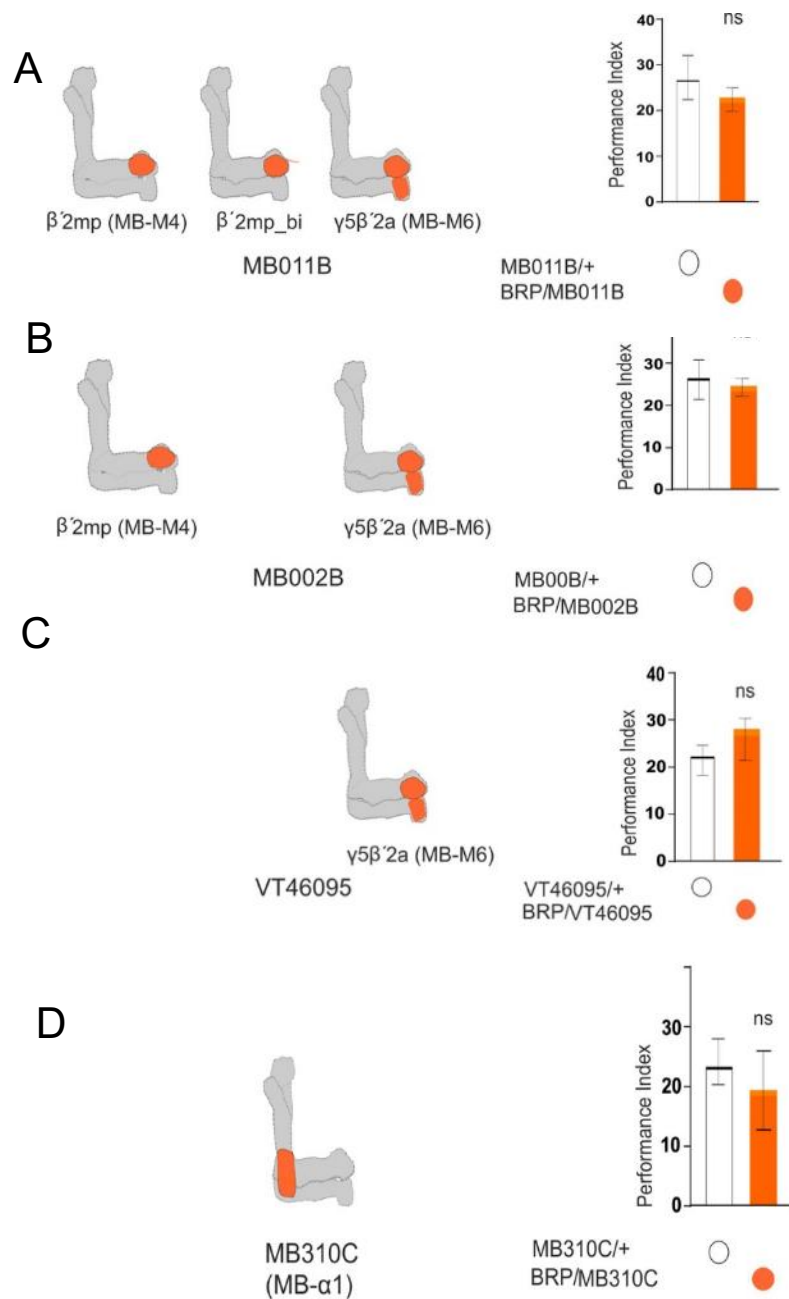
Supplementary figure 2. brp effect on ASM memory formation. Anesthesia-sensitive memory (ASM) forms part of the Middle-term memory as shown in the methods section. It's deduced by subtracting the performance index of ARM from MTM i.e. $PI^{MTM} - PI^{ARM}$. *brp* impairment revealed no apparent effect on ASM. Thus, shows a specific effect only on Anesthesia-resistant memory (ARM). (A) ASM effect had no effect on ORNs (Or83b), NP1227 (LN1) and GH298 (LN1). i.e. Or83b, ASM: $t_{(9)}= 0.33$ $p = 0.74$. ASM for NP1227: *test: t $_{(12)}$, t = 1.02 p = 0.33*. In addition to this, GH298[GAL4], ASM: *test: t $_{(11)}$, t = 1.02 p = 0.33*. (B) The ASM for LN2s and PNs were normal apparently. ASM for NP2426[GAL4]: *test, t$_{(10)}$ t = 0.50, p = 0.62* and for AL1[GAL4], ASM: *test, t$_{(13)}$ t = 0.60, p = 0.56*. Also, ASM for NP225[GAL4]: *test, t$_{(12)}$ t = 0.57, p = 0.29*.(C) ASM for 17d (α/β) and NP1131(γ) displayed no effect. ASM for 17d (α/β): *test, t$_{(9)}$ t = 0.83, p = 0.43* and in the case of NP1131(γ): *test, t$_{(12)}$ t = 0.35,*

$p = 0.72$. ASM for mb247^{GAL4} (γ + α/β) proved to be normal memory: *test, $t_{(13)}$ t = 0.39, p = 0.70.*(D) For VT64246^{GAL4}, ASM(DPM): *test, $t_{(11)}$ t = 0.12, p = 0.884,* and for NP2631^{GAL4}, ASM (APL): *test, $t_{(13)}$ t = 0.87, p = 0.398.* Hence, ASM formation in APL, DPM and *Th-GAL4* proved normal.In the case of *Th-GAL4*; ASM: *test, $t_{(14)}$ t = 0.19, p = 0.85.*Error bars indicate mean $\pm$ SEM of 7-10 biological repetitions (i.e., N = 7-10). **Statistical differences; ($p \leq 0.05$), ns = Not significant.

Supplementary Figure S3. Brp effect on MBON Split-GAL4 MTM. The figure showed here display the schematic representations of various MBONs in the lobes and the corresponding performance indices. (A) MB011B Split-GAL4 driver line is composed of three expression patterns and they are; MB-M4, MB-M6 and β'2mp_bilateral. The MTM performance index of MB011B: *t test, t $_{(15)}$, t = 2.1 p < 0.05.*(B) MB002B Split-GAL4 driver line included both M4 MBON and M6 MBON. MTM for the performance index: *t test, t $_{(16)}$, t = 3.28 p < 0.05.*(C) In the case of VT46095 driver line which was specifically for M6 MBON driver line, MTM for the performance index included: *t test, t $_{(12)}$, t = 3.032 p < 0.05.*(D) In the case of MBON α1 i.e. MB310c, MTM of the performance index was; *t test, t $_{(17)}$, t = 2.054 p < 0.05.* Error bars indicate mean ± SEM of 7-10 biological repetitions (i.e., *N* = 7-10). **Statistical differences; (*p* ≤ 0.05), ns = Not significant.
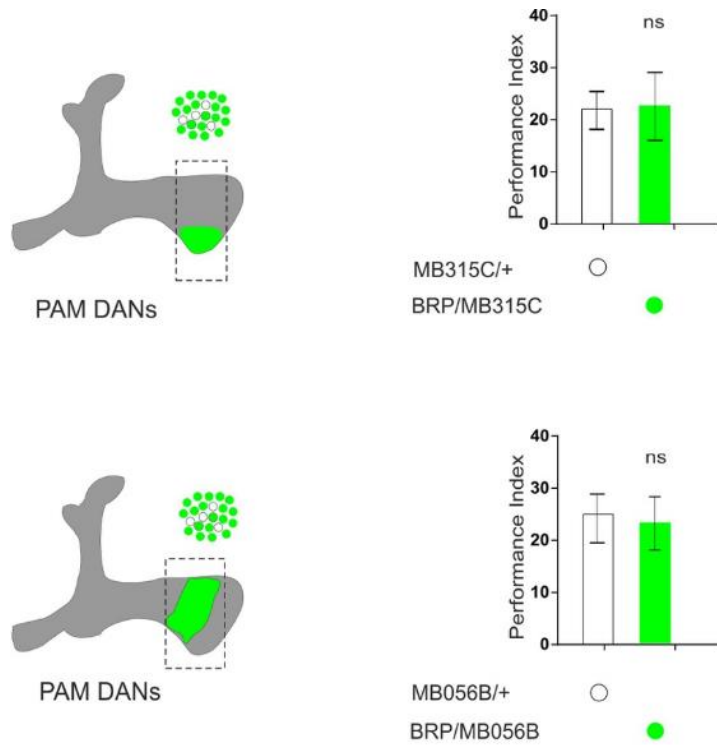
Supplementary Figure S4: brp effect on ASM formation in MBONs Split-GAL4 drivers. The above figure shows a schematic representation of various MBONs and their performance indices. (A) MB011B Split-GAL4 driver lines are made up of M4, M6 and β'2mp bilateral. ASM formation was normal during the aversive olfactory conditioning i.e.MB011B[GAL4]: ASM *t test*: $t_{(8)}, t = 0.718, p = 0.25$.(B) ASM Formation in MB002B Split-GAL4 driver line was apparently not affected.ASM for MB002B: *t test*: $t_{(11)}, t = 0.2569, p = 0.8020$.(C) The same ASM scenario observed in A and B was also seen in C.Hence, the VT46095 driver line which specifically marks the M6 MBON had a normal ASM.VT46095 ASM: *t test*: $t_{(11)}, t = 1.596, p = 0.1389$.(D) ASM formation in the case of MBON α1 was also normal. MB310c, ASM: *t test*: $t_{(14)}, t = 0.1696, p = 0.4339$.
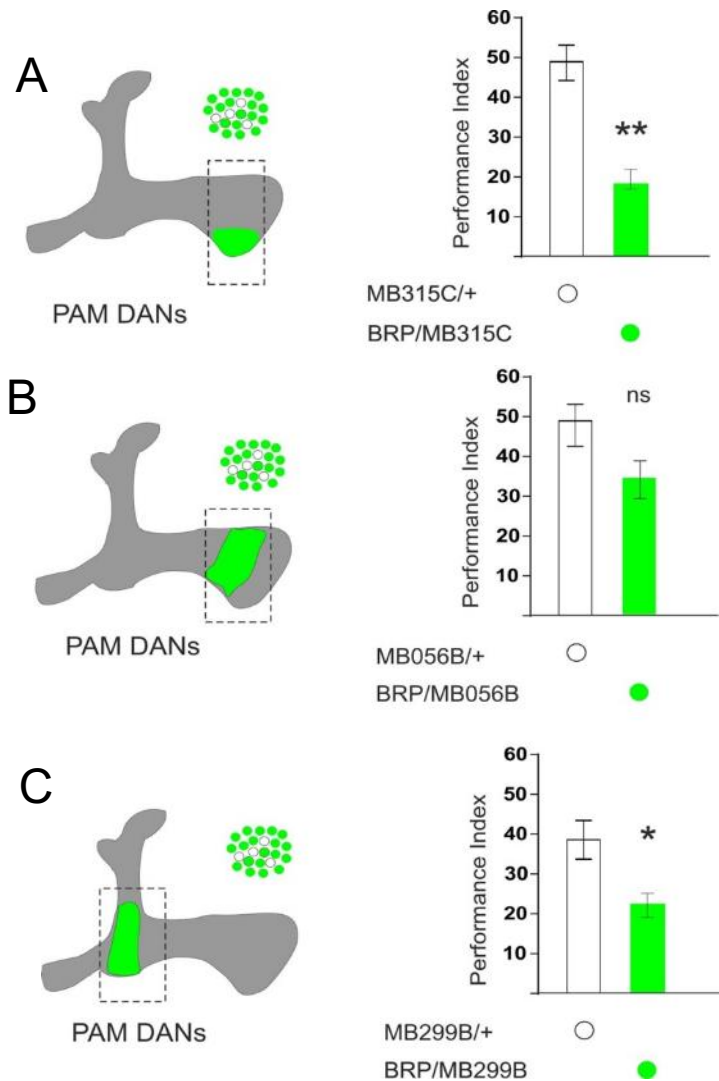
**Supplementary Figure S5. PAM cluster DANs are required for the formation of MTM.**
Above figures show the insertion pattern of PAM γ5 (MB315c), PAM β'2m, PAM β'2p (MB056B) and PAM α1(MB299B).(A) This reveals the schematic insertion and performance index of PAM γ5. *brp* knockdown in the PAM γ5 proved to be essential for 3 h MTM formation. MTM: *t test: $t_{(11)}$, t = 2.195 p < 0.05*.(B) In the case of MB056B, MTM: *t test: $t_{(11)}$, t = 0.03659 p=0.4857*. The MTM performance in the MB056B which marks the β'2m, PAM β'2p of the horizontal lobe was normal. (C) The MB299B driver line marks the α1 component of the mushroom body (MB).*brp* knockdown in this line proved essential for the formation of MTM. Error bars indicate mean ± SEM of 7-10 biological repetitions (i.e., N = 7-10). Statistical differences; ($p \leq 0.05$), ns = Not significant.

Supplementary Figure S6. Brp knockdown effect on PAM DANs ASM formation. *brp* knockdown had no effect on aversive ASM formation in PAM DANs cluster.(A) As shown in Figure S5, PAM γ5 had a tremendous effect on both ARM and MTM formation without influencing ASM component. ASM for MB315c: *t test; t $_{(11)}$, t = 0.0519, p = 0.4798.*(B) *brp* effect on ASM of the MB056B was normal. ASM: *t test; t $_{(11)}$, t = 0.1685, p = 0.4346.* Error bars indicate mean ± SEM of 7-10 biological repetitions (i.e., N = 7-10). Statistical differences; ($p \leq 0.05$), ns = Not significant.
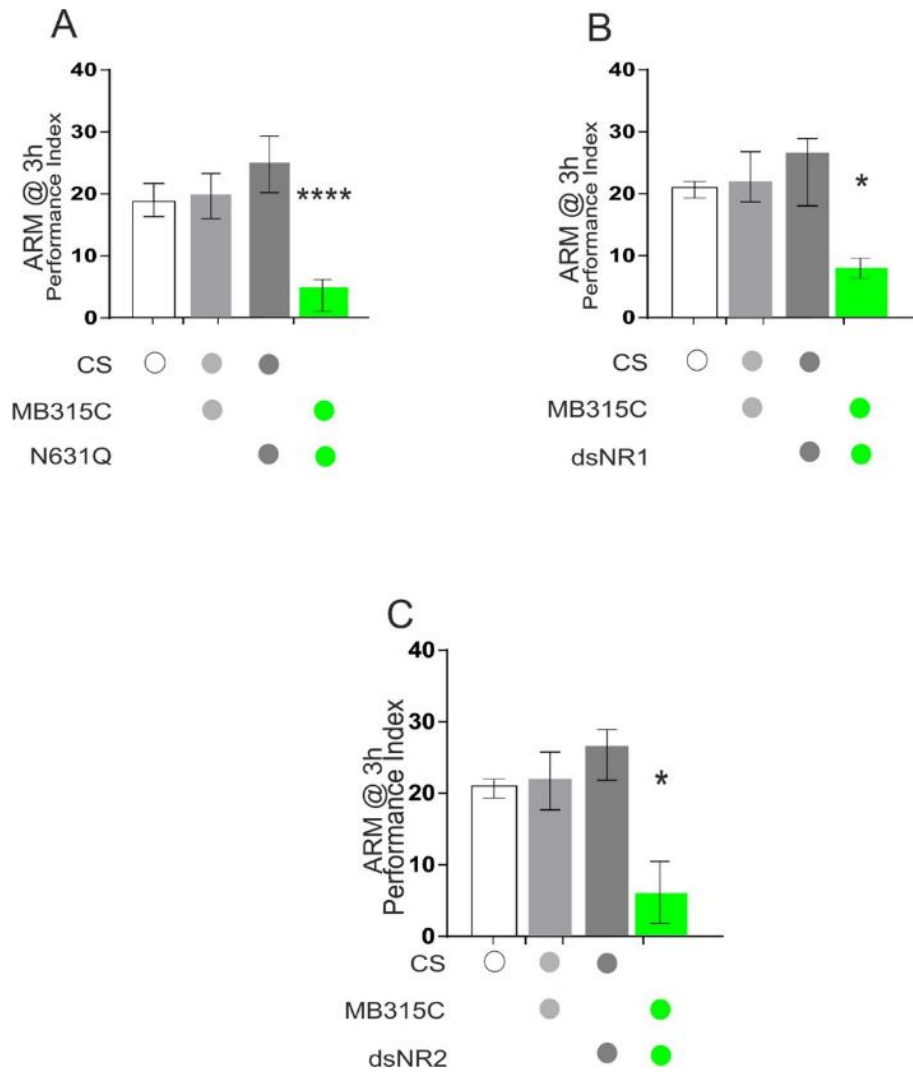
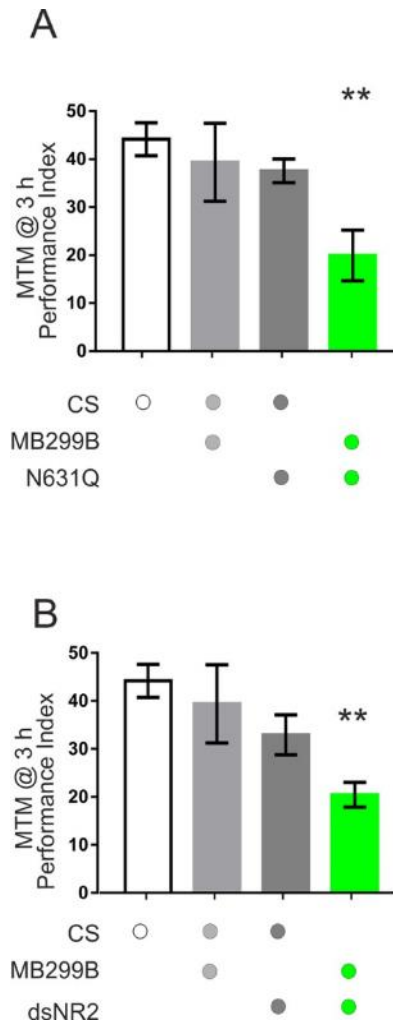**Supplementary Figure S7. Mg^{2+} and NMDA Receptors in MB315c driver (PAM γ5) are required for MTM.** (A) Mg^{2+} blocked in PAM γ5 (MB315c) *(N631Q)* was essential for the formation of MTM. MTM of MB315c (PAM γ5): *one-way ANOVA, $F_{(3,35)}$ = 5.203, p < 0.05.* (B) Knocking down the functional NMDA receptor *(dsNR1)* in PAM γ5 (MB315c) was also essential in the formation of MTM. MTM: *one-way ANOVA, $F_{(3,26)}$ = 4.334, p < 0.05.*(C) Knocking down the functional NMDA receptor *(dsNR2)* in PAM γ5 was also essential for the formation of MTM. MTM: *one-way ANOVA, $F_{(3,28)}$ = 5.67, p < 0.05.* Error bars indicate mean ± SEM of 7-10 biological repetitions (i.e., N = 7-10). Statistical differences; ($p ≤ 0.05$), ns = Not significant.
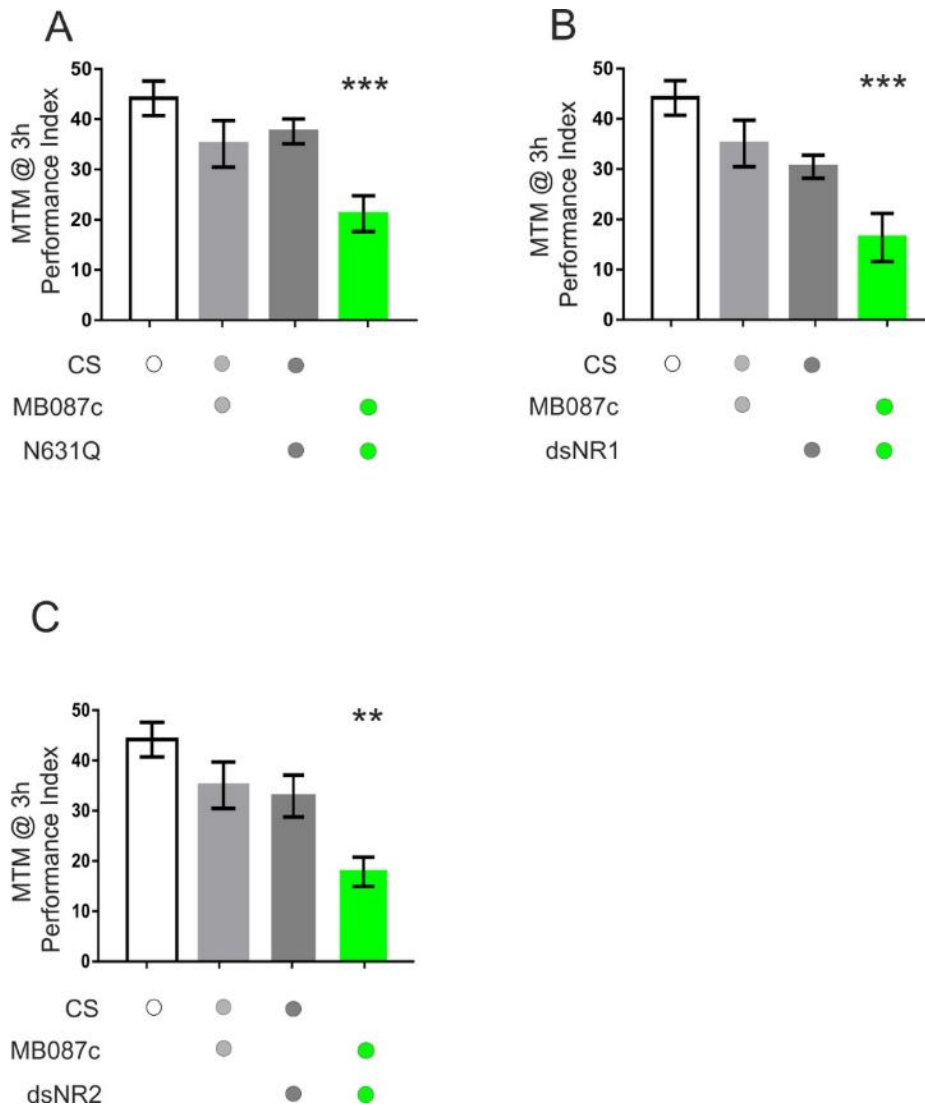
Supplementary figure S8. Mg^{2+} and NMDA Receptors in PAM β'2m and 2p (MB087c) are required for MTM. (A) Mg^{2+} blocked in MB087c also proved to be needed for MTM formation. MTM: *one-way ANOVA,* MTM: one-way ANOVA: F$_{(3,39)}$ = 7.856, *p < ***0.001*. (B) Knocking down the functional NMDA receptor (dsNR1) in MB087c displayed impairment of MTM formation. MTM: one-way ANOVA: F$_{(3,28)}$ = 8.031 *p < 0.05*. (C) knocking down the functional NMDA receptor in MB087c displayed impairment of MTM formation. MTM: one-way ANOVA: F$_{(3, 29)}$ = 6.721 *p < 0.05*.Error bars indicate mean ± SEM of 7-10 biological repetitions (i.e., *N* = 7-10). Statistical differences; (*p* ≤ 0.05), ns = Not significant.

Supplementary figure S9. Mg^{2+} and knockdown of NMDA Receptors in MB299B driver (PAM α1).
(A) Mg^{2+} block in PAM α1 (MB299B) affected MTM formation. MTM: *one-way ANOVA: F $_{(3,31)}$ = 4.703; p < 0.05*(B) functional knockdown of dsNR2 in PAM α1 affected MTM formation. MTM: *one-way ANOVA; F $_{(3, 27)}$ = 5.227; p < 0.05.* Error bars indicate mean ± SEM of 7-10 biological repetitions (i.e., *N* = 7-10). Statistical differences; (p ≤ 0.05), ns = Not significant.